universität wien

DIPLOMARBEIT

Titel der Diplomarbeit

„**Phytochemical analysis of *Ligularia sp.* collected in Yunnan and Sichuan Provinces of China**“

Verfasserin

Sin-Yeung Yoo

angestrebter akademischer Grad

Magistra der Pharmazie (Mag.pharm.)

Wien, im Februar 2012

Studienkennzahl lt. Studienblatt: A 449

Studienrichtung lt. Studienblatt: Diplomstudium Pharmazie

Betreuerin / Betreuer: Univ. Prof. Mag. Dr. Gerhard Buchbauer

I, Sin-Yeung Yoo, declare that the work presented in this thesis is, to the best of knowledge and belief, original, except as acknowledged in the text, and that the material has not been submitted, either in whole or in part, for a degree at this or any other university.

Acknowledgement

First of all I wish to thank my two supervisors, Prof. Gerhard Buchbauer and Prof. Motoo Tori for the opportunity to work on this thesis. I owe my deepest gratitude to Prof. Tori for his kindness and support during and after the work with his patience and knowledge. I would like to thank Prof. Buchbauer for his excellent guidance and kindness before and after the work and throughout my studies. Most of all, I offer my regard and blessings to both supervisors who supported me in any respect during the completion of the thesis.

I would like to offer my special thanks to the members of the Faculty of Pharmaceutical Sciences, Tokushima Bunri University, Japan for giving me the opportunity to work on my thesis.

I am deeply indebted to Prof. Tori's working group for their warm welcome, kindness and support in the lab and outside the work. I would like to thank Yoshinori Saito for his encouragement and effort for helping me out to run my experiments and I am very grateful to Miss Yasuko Okamoto and Prof. Katsuyuki Nakashima for their technical guidance.

My special thanks are extended to Mr. Maeda from Agilent Technologies for his kindness and effort for the LC-MS runs of my samples.

In my daily work I was blessed with a friendly and cheerful group of fellow students, with whom I loved to spend my time during lunch breaks. Thank you all for your kindness and funny conversations.

Finally, I would like to express my special thanks to my family and friends for the support, encouragement and patience throughout my studies.

Abstract

Root chemicals of the genus *Ligularia*, belonging to the family of Asteraceae, tribe Senecioneae were analyzed by phytochemical methods. The inter- and intraspecific variation on the basis of the chemical composition were examined by GC-MS, because this work focuses on the volatile part of the extract. For this purpose plant material were collected in Yunnan and Sichuan provinces of China and extracted with EtOH or AcOEt. The results of nine different species suggest that the members of this genus produce sesquiterpenoids of the eremophilane type as major components. Furanoeremophilanes were used as chemical index to explore the diversity of this genus. In addition, extracts of fresh roots contained monoterpene components, which might be responsible for the characteristic fragrance of the plant roots.

Intraspecific diversity was present for the species *L. virgaurea*, *subspicata*, *vellerea*, *pleurocaulis*, *dictyoneura* and *tongolensis* with different degrees of diversity. In contrast *L. cyathiceps*, *przewalskii* and *sagitta* were assigned to be uniform. Furthermore, it can be said that *L. virgaurea* and *pleurocaulis* contained chemically distinct populations, while *L. subspicata* and *dictyoneura* were rather continuous, being in an early stage of differentiation.

The correlation between chemical composition and geographical distribution was confirmed for *L. virgaurea*. In addition, the presence of a third type was reported. Samples of *L. virgaurea* type 1 contained 6-oxygenated furanoeremophil-1(10)-en-2-ones and their lactones, while type 2 contained ligularol (**16**) as major compounds. In contrast, benzofuranosesquiterpenes were detected for *L. virgaurea* type 3.

Benzofuranosesquiterpene derivatives were also found in *L. przewalskii*, while *L. subspicata* and *dictyoneura* contained furanoeremophilanes and eremophilan-8-one derivatives. *L. cyathiceps* produced 6β-(acyloxy)-furanoeremophilan-9-ones and cacalol (**15**) as major components. By comparison 6β-(angeloyloxy)- and 6β-(tigloyloxy)-furanoeremophil-1(10)-en-3β-ol (**50** and **51**) was found in *L. pleurocaulis* as major compounds. Two types of *L. pleurocaulis* could be distinguished for a subset of samples. The first one containing 3β-(angeloyloxy)-furanoeremophil-1(10)-en-6β-ol (**52**) and the second one contain-

ing furanoligularenone (**40**). In the majority of cases the classification of these two types was consistent with the geographical distribution of the samples.

In general, account must be taken of the fact that the chemical composition is dependent on the plant material (fresh or dried roots), environment, soil condition, genotype, climate and method of extraction. In addition, furanocomponents are known to be unstable under acidic conditions, high temperature and oxygen.

Zusammenfassung

Die Inhaltsstoffe der Gattung *Ligularia* aus der Familie der Asteraceae, Tribus Senecioneae wurden mit Hilfe phytochemischer Methoden untersucht. Für die Bestimmung der inter- und intraspezifischen Vielfalt dieser Gattung wurde das Pflanzenmaterial aus den Provinzen Yunnan und Sichuan (China) gesammelt, deren Wurzeln mit EtOH oder AcOEt extrahiert und anschließend mittels GC-MS untersucht, wobei das Hauptinteresse auf die flüchtigen Verbindungen der Extrakte gelegt wurde. Die charakteristischen Inhaltsstoffe von *Ligularia sp.* sind Sesquiterpene vom Eremophilan-Typ, wobei insbesonders Furanoeremophilane zur Bestimmung der Artenvielfalt herangezogen wurden. Neben diesen Furanosesquiterpenen wurden auch Monoterpene, die vermutlich für den Geruch der Wurzeln mitverantwortlich sind, als Inhaltsstoffe ermittelt. Die Ergebnisse aus neun verschiedenen Arten zeigten das Vorhandensein von intraspezifischer Variabilität. Während die chemische Zusammensetzung von *L. virgaurea*, *subspicata*, *vellerea*, *pleurocaulis*, *dictyoneura* und *tongolensis* komplex zu sein schienen, waren die von *L. cyathiceps*, *przewalskii* und *sagitta* einheitlich. Außerdem wurde beobachtet, dass eindeutig abgrenzbare Chemotypen von *L. virgaurea* und *pleurocaulis* existierten, während die Entwicklung bestimmter Chemotypen bei *L. subspicata* und *dictyoneura* noch nicht vollständig abgeschlossen war. Der Zusammenhang zwischen chemischer Zusammensetzung und geographischer Verteilung für *L. virgaurea* wurde bestätigt und drei verschiedene Gruppen ermittelt. Die Hauptinhaltsstoffe der ersten Gruppe waren Furanoeremophil-1(10)-en-2-one und deren Laktone, Typ 2 enthielt Ligularol (**16**) und Typ 3 Benzofuranosesquiterpen Derivate. Diese waren auch in *L. przewalskii* zu finden. Die Ergebnisse zeigten das Vorhandensein von Furanoeremophilan Derivaten und Eremophilan-8-one für *L. subspicata* und *dictyoneura*. Die Hauptinhaltsstoffe für *L. cyathiceps* waren 6β-(Acyloxy)-furanoeremophilan-9-one und Cacalol (**15**). Im Vergleich dazu enthielt *L. pleurocaulis* 6β-(Angeloyloxy)- und 6β-(Tigloyloxy)-furanoeremophil-1(10)-en-3β-ole (**50** and **51**) als Hauptinhaltstoffe. Zwei Chemotypen wurden bei *L. pleurocaulis* unterschieden. Die erste Gruppe enthielt 3β-(Angeloyloxy)-furanoeremophil-1(10)-en-6β-ol (**52**) und die zweite Furanoligularenon (**40**) zusätzlich zu den Hauptinhaltsstof-

fen. In den meisten Fällen korrelierte diese Einteilung auch mit der geographischen Verteilung beider Gruppen.

Die chemische Zusammensetzung des Extraktes ist abhängig vom Pfanzenmaterial (frische oder getrocknete Wurzeln), Umwelt, Bodenbeschaffenheit, Genotyp, Klima und Gewinnungsmethode. Zusätzlich sollte auf die Empfindlichkeit und die daraus resultierenden Zersetzungsprodukte der Furanosesquiterpene geachtet werden.

.

List of contents

List of figures

List of tables

Abbreviations

syn.	synonym
L.	Ligularia
sp.	species
var.	variety
lat.	Latin
No.	number
m	meter
mm	millimeter
µm	micrometer
nm	nanometer
° C	degree Celsius
amu	atomar mass unit
psig	pounds per square inch gauge
V	Volt
l/min	liter per minute
ml/min	milliliter per minute
MeOH	methanol
EtOH	ethanol
AcOEt	ethyl acetate
HCl	hydrochloric acid
TLC	thin layer chromatography
GC	gas chromatography
LC	liquid chromatography
MS	mass spectrometry
EI	electron impact, electron ionization
APCI	atmospheric pressure chemical ionization
µl	microliter
TIC	total ion current
RT	retention time
min	minutes
FE	furanoeremophil-, furanoeremophilan(e)
OAng	angeloyloxy
OTig	tigloyloxy
OMeAcr	methylacryloyloxy

OiBu	isobutanoyloxy
OMeBu	2-methylbutanoyloxy
$Ce(SO_4)_2$	Cerium (IV) sulfate
H_2SO_4	sulfuric acid
RDA	retro Diels Alder
MW	molecular weight

1. Introduction

1.1. Background

The Flora of Asia has drawn attention since decades, not only to gain an advantage in the field of traditional folk medicine, but also to analyze its morphological, genetic and chemical diversity. The focus of this work lies on the Flora of the Hengduan Mountains, which is geographically located in the south-central and southwestern region of China (Figure 1). More precisely it lies on the southeastern part of the Tibetan plateau, ranging from the Sichuan Basin to Xizang (Tibet) and to the Yunnan plateau southwards [17].

The Hengduan area is characterized through an extremely complex topography as a result of a wide range of climate conditions and is rich in temperate and tropical river systems [18]. Because of these conditions the area has a high degree of biodiversity, which ranges from vascular plants to fungi.

Using the example of *Ligularia* species belonging to the family of Asteraceae (syn. Compositae), this work is trying to explore its diversity in plant chemicals.

Figure 1. Map of China [16]

1.2. *Ligularia* sp.

The genus *Ligularia* (lat.: ligula = small tongue), belonging to the family of Asteraceae, tribe Senecioneae, has many common names, for example golden ray, leopard plant, golden groundsel or summer ragwort. The members of this genus are distributed in the Hengduan Mountains of China with more than 100 species [6], which are assigned to different series and sections. In general, the roots of approximately 40 species have been used in the traditional Chinese medicine for the treatment of stomach ache and nausea [19], relieving internal heat or fever, reducing phlegm, relieving cough and asthma, invigorating the circulation of blood, and for stopping pain and inflammation [20].

The *Ligularia* sp., located in the southeastern edge of the Tibetan plateau, is diverse in their morphological appearance and grows in a great variety of habitats including forests, grassy slopes, swamps and alpine meadows ranging from 1000 to 4500m in altitude [2, 9].

The plant itself can be characterized as a perennial herb with leaves basal and alternate on stems. Basal leaves (rosulate and lower stem leaves) are well developed and palmately or pinnately veined. Their petioles are longer and the base is broadly sheathed in comparison with the smaller stem leaves. The erect stem is arising from the outer axil of rosulate leaves and ends with yellow or orange flowers, which usually bloom in the mid to late summer. The heads of the flowers, numerous in corymbs, racemes or solitary, have yellow ray and disc florets with few or numerous supplementary bracts. Branches of style are slender, apex obtuse or rounded. The roots are stout or slender, glabrous or hairy [21, 27, 28]. An example of the plant is shown in Figure 2.

Figure 2. *L. subspicata*, plant and dried roots (Sample No. 07 95)

1.3. Phytochemicals of *Ligularia* sp.

Chemical constituents of the genus *Ligularia* have been studied since 1960s [2]. Former phytochemical analysis of various *Ligularia* sp. showed, that sesquiterpenoids, first of all those of the eremophilane type including the furanoeremophilanes are the major components. Other sesquiterpenoids occurring in this genus are those of the bisabolane type, oplopane type, guaiane and pseudoguaiane types and eudesmane type. Besides all this the presence of monoterpenoids, diterpenoids and triterpenoids has been reported [29].

In addition other chemical constituents like pyrrolizidine alkaloids, flavonoids and lignans were detected [5, 29].

Although the compounds of the *Ligularia* plant and related genera have been investigated intensively during the last decades, there are less studies regarding to the diversity in plant chemicals generated through evolution [2].

Hence the aim of this work is to analyze inter- and intraspecific differences between *Ligularia* sp. according to their compounds with focus on the volatile part of the plant.

Therefore, furanoeremophilane derivatives were used as the chemical index to explore the plant diversity as it was easy to detect by Ehrlich's Test (see chapter 2.2). The basic skeleton of eremophilane (**1**) and furanoeremophilane (**2**) with corresponding numbering are shown in figure 3.

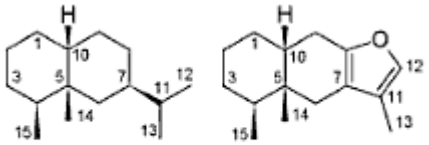

1 **2**

Figure 3. Numbering of eremophilane (**1**) and furanoeremophilane (**2**) [25].

2. Experimental

2.1. Plant materials

Plant collection and identification was previously done in August by the members of the Kunming Institute of Botany, Chinese Academy of Science from 2003 to 2009 at several locations.

2.2. Ehrlich's Test

Ehrlich's Test, a color reaction of pyrroles or furans with p-dimethylaminobenzaldhyde (*Ehrlich*'s reagent) in aqueous HCl, is an easy and rapid method to detect the presence or absence of furanoeremophilane components prior to isolation [3]. Therefore, the ethanol (EtOH) extract of fresh roots of each plant (about 10g) was used after several days of extraction at room temperature and separation of the solid plant material [6].

The thin layer chromatography (Kieselgel 60 F254, layer thickness 0,2mm) was carried out by the members of the Department of Chemistry from the Rikkyo University in Tokyo using hexane-ethyl acetate (7:3) as the solvent. The TLC plate was dipped into a 1% solution of p-dimethylaminobenzaldehyde in EtOH, dried and dipped in a 1M solution of hydrochloric acid in aqueous EtOH [6]. Ehrlich positive samples showed colored spots due to the presence of furanosesquiterpenes, *Ehrlich* negative samples otherwise. The result of each plate was photographed.

2.3. Extraction

Fresh roots or dried roots were cut into small pieces and extracted with EtOH, methanol (MeOH) or ethyl acetate (AcOEt) at room temperature for three month. After the separation of the solid plant material, the extract was either directly used for further phytochemical analysis or processed for storage purposes prior to purification. Therefore, the solvent was evaporated to afford an

oily residue. To recover the organic layer the extract was partitioned between diethyl ether and water. The ether solution was dried over anhydrous sodium sulfate, filtrated and the solvent evaporated to yield an oily extract [11, 7].

2.4. Gas chromatography (GC) – Mass Spectrometry (MS)

To get an overview of the diversity of the *Ligularia* sp. crude extracts were analyzed to its components, focusing on the volatile part of the extracts. Hence gas chromatography was applied to separate those constituents followed by a mass spectrometer.

The gas chromatography is a kind of a column chromatography, at which the mobile phase is a gas. This method is used for separation and for qualitative and quantitative analysis of substances [23]. Given that only volatile or volatilized compounds without decomposition or conversion at high temperatures can be used, the application of the GC is limited [24]. Two types of GC can be distinguished, according to the different stationary phase, gas-liquid (GLC) and gas-solid chromatography (GSC), respectively [23, 24].

The EtOH or AcOEt soluble fraction of each extract was filtrated and 1µl of each solution was injected into the pre-heated sample inlet (injector) of the GLC. After immediate vaporization of the solution, the molecules were transported with the carrier gas (helium) through a liquid coated capillary column. Due to different distribution coefficients of the molecules between the mobile and stationary phase, the separation could be carried out and registered as peaks in a chromatogram with retention times (Figure 4).

The gas chromatography is often coupled with a mass spectrometer. At the end of the column the compounds eluted were passing through a heated transfer line to an ion source, where compounds were ionized via Electron Impact (EI).

The parameters for GC-MS are shown in table 1. The results appear as a total ion chromatogram (TIC) with information about mass spectra and retention times.

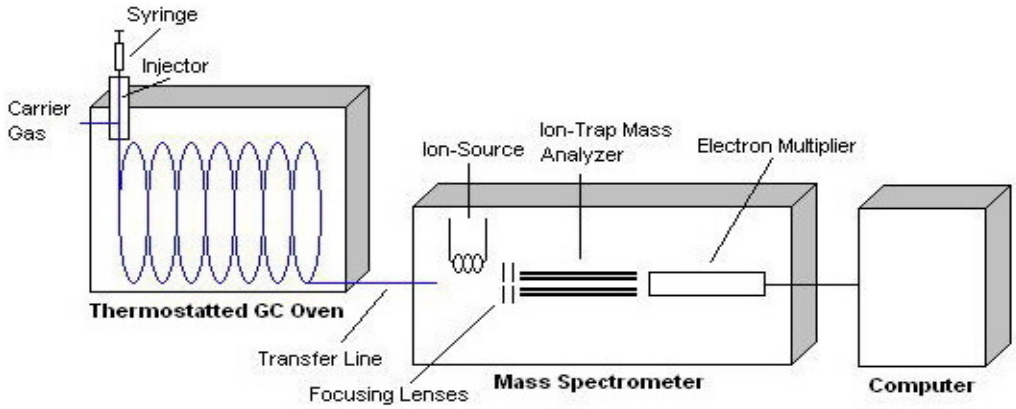

Figure 4. Schematic GC-MS System [22]

Device	HP 6890 Series GC System HP 5973 MSD (Mass Selective Detector)
Column	**5% Phenyl Methyl Siloxane** 30m x 250µm x 0,25µm film thickness
Carrier gas	Helium, constant flow (1ml/min)
Ion source	**EI**, 70,1V, 230° C
Oven temperature	50° C (1min) - 250° C (10min), rate: 20° C/min
Injection	1µl, split (50:1), 260° C
Libraries	MassFinder, Wiley

Table 1. Parameters of GC-MS

2.5. Liquid Chromatography (LC) – Mass Spectrometry (MS)[1]

To obtain more information about the extracts LC-MS analysis was carried out. The advantage of this method compared to GC-MS is that it is capable of analyzing a wider range of components with non-volatile and thermally unstable properties. One requirement for this method is that the sample can be solved to interact with the available mobile phase. Hence 1µl of the EtOH soluble fraction of each sample was injected after filtration and separated on a reversed phase

[1] LC-MS was carried out by Mr. Maeda from Agilent Technologies

column to its components. The resulting molecules were ionized via APCI mode subsequently. The parameters of the LC-MS and the solvent gradient are shown in table 2 and 3.

Device	Agilent 6100 Series Single Quadrupole LC/MS Systems
Column	**COSMOSIL 5C_{18}- MS II** 4,6 x 150mm, 40° C
Solvent	**A**: H_2O, **B**: MeOH
Injection volume	1µl
Detection	**DAD** 210nm, 254nm **MSD** (APCI positive, Fragmentator: 100)

Table 2. Parameters of LC-MS

Time (min)	Solvent A (%)	Solvent B (%)	Flow (ml/min)
0 - 20	30	70	1
20 - 23	0	100	1
23,1 - 28	0	100	1,5
28,1 - 40	30	70	1,5

Table 3. Solvent gradient for LC

2.6. Mass Spectrometry direct measurement

MS direct measurement was carried out to obtain rapid information about the sample composition. In contrast to *Ehrlich*'s Test, which indicates the presence or absence of furanoeremophilanes, this method is able to deduce the chemical components via assignment of different mass spectra.

Therefore, EtOH soluble fractions of different samples were directly injected in the Mass spectrometer after filtration of the solution to obtain chemical patterns of the whole sample. The corresponding parameters are shown in table 4.

Device	HP 1100 series MSD
Injection volume	1-5 µl
Ionisation mode	**APCI** positive, Fragmentator: 60
Mass range	100 – 1000 amu, scan mode
Drying gas flow (l/min)	8.0
Nebulizer pressure (psig)	40
Drying gas temperature (° C)	300
Vaporizer temperature (° C)	329
Capillary Voltage (V)	2500

Table 4. Parameters of MS direct measurement

2.7. Generating a library

Given that the available libraries were not able to match the volatile compounds of the *Ligularia* sp. in the majority of cases, a new library was created in addition to the existing one. As it was known that the members of the genus *Ligularia* contain sesquiterpenes of the eremophilane type, isolated pure compounds[2] were solved with AcOEt and injected in the GC device. For this purpose a program called MassFinder 4 was used to visualize and interpret the results of GC-MS. It is a software system originally developed in combination of essential oil analysis with focus on the terpenoid composition [30].

The mass spectral data of the extended library are shown in chapter 6.3.

[2] Isolated and identified by the members of the Faculty of Pharmaceutical Sciences, Tokushima Bunri University

3. Results and Discussion

3.1. Ligularia sp.

3.1.1. L. virgaurea

L.virgaurea, belonging to the section Senecillis, inhabits alpine meadows of more than 4000m in altitude and is widely distributed in Yunnan, Sichuan, Qinghai, and Gansu provinces of China, and in Nepal and Bhutan. Three varieties, *virgaurea*, *pilosa*, and *oligocephala* have been proposed, due to the large morphological variation within the species [6].

Thirty samples of *L. virgaurea var. virgaurea* were collected in 2009 in the southwestern Sichuan province of China, extracted with EtOH and examined by GC-MS and LC-MS (see chapter 6.4.1).

Based on *Ehrlich*'s test *L. virgaurea* can be separated into three groups. All types showed positive *Ehrlich* coloring spots, which indicate the presence of furanoeremophilanes. Type 1 showed two major components with yellow spots at R_f = 0.45 and 0.53 (hexane-AcOEt 7:3), whereas type 2 showed several pink spots with major components at R_f = 0.54 and 0.59 [6]. The presence of a third type, already reported by Jia and co-workers [26], was confirmed as the *Ehrlich*'s test of sample 1 showed one dark blue spot at R_f = 0.60 after several hours of coloring reaction. The different colors on the TLC suggest furanoeremophilanes with different substituents. The effect may occur due to the fact that oxygenated functionalities are given at position 6 and 9 of the furanoeremophilane skeleton [3].

No.	Sample	Place	Altitude (m)	Ehrlich Type	Major compound
1	09 56	Laima	3746	3	**15**
2	09 60	Anbalashan	3933	1	**8**
3	09 66	Shiqu	4419	1	**9**
4	09 71	Qiwu	4295	1	**9**
5	09 97	Maerkang/Xianjin	4018	1	**9**
6	09 512	Maanshan	4146	2	**16**
7	09 513	Maanshan	4145	2	unknown, m/z = 262
8	09 514	Maanshan	4148	2	**16**
9	09 515	Maanshan	4161	2	**41**
10	09 516	Maanshan	4164	2	**41**
11	09 517	Maanshan	4164	2	**41**
12	09 518	Wumingshan	4196	1	**9**
13	09 519	Wumingshan	4189	1	**111**
14	09 520	Wumingshan	4192	1	**111**
15	09 521	Wumingshan	4191	1	**111**
16	09 522	Wumingshan	4198	1	**109**
17	09 523	Wumingshan	4185	1	**109**
18	09 524	Wumingshan	4288	2	**16**
19	09 525	Wumingshan	4293	1	**111**
20	09 526	Wumingshan	4288	1	**109**
21	09 527	Wumingshan	4614	2	**16**
22	09 528	Wumingshan	2627	2	**16**
23	09 529	Wumingshan	4654	1	**111**
24	09 530	Wumingshan	4647	2	**16**
25	09 531	Wumingshan	4674	2	**16**
26	09 532	Wumingshan	4616	2	**17**
27	09 533	Wumingshan	4625	2	**16**
28	09 534	Wumingshan	4450	1	**9**
29	09 535	Wumingshan	4309	1	**9**
30	09 536	Wumingshan	4169	1	**9**

Table 5. Samples of *L.virgaurea* var. *virgaurea*. Samples 6 to 30 were EtOH extracts of fresh roots, while samples 1 to 6 were AcOEt extracts of dried roots.

Similar to TLC analysis MS direct measurements of each extract can be applied prior to separation, to obtain useful information about the chemical patterns. In contrast to *Ehrlich*'s test, this method yields more information, given that the spectrum shows the quasi-molecular ion peak as well as fragment ion peaks of different constituents [7]. The mass spectra of each type of *L. virgaurea* can be compared in chapter 6.4.1.

Given that this work focuses on the volatile part of the extracts GC-MS analysis was applied. The grouping of each sample based on *Ehrlich*'s test and the corresponding major compounds found via GC-MS analysis are shown in table 5. The TIC profile and their corresponding matches with the library and literature are listed in chapter 6.3.1.

In general, the major compounds of *L. virgaurea* type 1 are virgaurenone A (**8**, Figure 14, m/z = 328 $[M]^+$, 228 [M-AngOH]$^+$, 213 $[C_{15}H_{16}O_2\text{-}CH_3]^+$, 186, 83 = base $[C_4H_7CO]^+$, 55 $[C_4H_7]^+$), virgaurenone B (**9**, Figure 13, m/z = 288 $[M]^+$, 246 $[C_{15}H_{18}O_3]^+$, 228 [M-AcOH]$^+$, 213 $[C_{15}H_{16}O_2\text{-}CH_3]^+$, 186 = base, 123 $[C_7H_7O_2]^+$ *retro*-Diels-Alder (RDA) fragment, 43 $[C_2H_3O]^+$), cis-ocimene (**111**) and β-pinene (**109**) at retention times 13.74, 11.86, 4.66 and 4.20 minutes, respectively (Table 5). Furthermore characteristic peaks could be observed at retention times 3.82, 4.47, 5.11, 8.01, 11.50, 12.69, 12.74, 14.58 and 18.77 minutes, which corresponds to α-pinene (**108**), 3-carene (**110**), α-terpinolene (**116**), eremophilene (**67**), virgaurenone C (**10**, Figure 21, m/z = 246 $[M]^+$, 228 $[M\text{-}H_2O]^+$, 213 $[C_{14}H_{13}O_2]^+$, 186, 123 = base $[C_7H_7O_2]^+$ RDA), 6β-(isobutanoyloxy)-furanoeremophil-1(10)-en-2-one (**11**, Figure 17, m/z = 316 $[M]^+$, 246 $[C_{15}H_{18}O_3]^+$, 228 $[M\text{-}C_4H_8O_2]^+$, 213 $[C_{14}H_{13}O_2]^+$, 186 = base, 123 $[C_7H_7O_2]^+$ RDA, 71 $[C_4H_7O]^+$, 43 $[C_3H_7]^+$), 6β-(2'-methylacryloyl)-oxy-furanoeremophil-1(10)-en-2-one (**12**, Figure 18, m/z = 314 $[M]^+$, 228 $[M\text{-}C_4H_8O_2]^+$, 186 = base, 69 $[C_3H_5CO]^+$, 41 $[C_3H_5]^+$), virgaurenolide B (**14**) and virgaurenolide A (**13**, Figure 15, m/z = 342 $[M]^+$, 83 = base $[C_4H_7CO]^+$, 55 $[C_4H_7]^+$), respectively. The peak at retention time 11.32 minutes is unknown (Figure 11, m/z = 228), although it is known that the EI mass spectrum has the same pattern as the assumed profile of **8** and **9**. Because of this assumption, it is most likely that these compounds share the same carbon skeleton.

In contrast, *L. virgaurea* type 2 indicates a different GC-MS profile. The major compounds found are ligularol (**16**), its derivative ligularol ethyl ether (**17**, Figure

25, m/z = 262 $[M]^+$, 152 = base $[C_9H_{12}O_2]^+$ RDA, 123 $[C_7H_7O_2]^+$) and 6-hydroxy-3-(2'-methylacryloyl)oxy-furanoeremophilane (**41**, Figure 28, m/z = 318 $[M]^+$, 124 = base $[C_7H_8O_2]^+$ RDA, 109 $[C_7H_9O]^+$, 69 $[C_3H_5CO]^+$, 41 $[C_3H_5]^+$) at retention times 9.99, 9.85 and 12.89 minutes, respectively. Characteristic peaks of this type are at retention times 3.82, 4.16, 4.20, 4.42, 4.47, 8.01, 9.69, 10.74 and 13.83 minutes, which corresponds to α-pinene (**108**), sabinene (**118**), β-pinene (**109**), α-phellandrene (**112**), 3-carene (**110**), eremophilene (**58**), 8-oxo-12-noreremophil-6-en-11-one (**78**, Figure 35, m/z = 220 $[M]^+$, 205 = base $[M-CH_3]^+$, 178 $[M\text{-ketene}(C_2H_2O)]^+$, 43 $[C_2H_3O]^+$), furanoeremophilan-6β,10β-diol (**22**, Figure 27, m/z = 250 $[M]^+$, 232 $[M-H_2O]^+$, 124 = base $[C_7H_8O_2]^+$ RDA) and 6-hydroxy-3-angeloyloxy-furanoermemophilane (**42**, Figure 29, m/z = 332 $[M]^+$, 124 = base $[C_7H_8O_2]^+$ RDA, 109 $[C_7H_9O]^+$, 83 $[C_4H_7CO]^+$, 55 $[C_4H_7]^+$), respectively. The peak at retention time 9.90 minutes is unknown (Figure 26, m/z = 262).

The third type of *L. virgaurea* (sample 1) contained cacalol (**15**) at retention time 11.30 minutes as the major component, followed by 1-Hydroxy-2-(3'-pentenyl)-3,7-dimethylbenzofuran (**94**, Figure 37, m/z 230 $[M]^+$, 175 = base, $[230-C_4H_7]^+$, 55 $[C_4H_7]^+$) at retention time 10.28 minutes with 53.23% and 19.35% of relative distribution, respectively (Table 27).

The results suggest the presence of intra-specific variations. *L. virgaurea* type 1 contained 6-oxygenated furanoeremophil-1(10)-en-2-ones as the major constituents and their corresponding lactones (= 2-oxoeremophil-1(10),7(11),8-triene-12,8-olide), which were probably produced by oxidation in the plant [6], while type 2 contained ligularol (**16**) and its derivative ligularol ethyl ether (**17**) as major compounds. **17** might be an artifact due to extraction procedure. Moreover, it is possible that *L. virgaurea* type 2 contained 6-hydroxy-3-(2'-methylacryloyl-oxy)-furanoeremophilane (**41**), which might be oxidized to eremofarfugin B (**59**), the compound already isolated and reported by Tori and co-workers [6]. Other common constituents found in samples of *L. virgaurea* type 2, were eremophilene (**67**), **22**, **42** and 8-oxo-12-noreremophil-6-en-11-one (**78**), which could be the decarboxylated product of **79** [6].

In addition to the proposed two types, a third type was found as the chemical profile of sample 1 was different (Figure 37 and Table 27). Cacalol (**15**), followed by a benzofuranosesquiterpene derivative (**94**) were the major compo-

nents found in the extract. This result confirmed the previous phytochemical analysis of *L. virgaurea* from Gansu province of China reported by Jia and co-workers [26].

Besides all this monoterpenes of the plant essential oil were found for all types of *L. virgaurea*. While type 1 contained β-pinene (**109**) and cis-ocimene (**111**) as major components, type 2 showed a high amount of 3-carene (**110**). Furthermore, the monoterpene composition of *L. virgaurea* type 1 consisted of α-pinene (**108**), 3-carene (**110**), β-myrcene (**107**), α-phellandrene (**112**), p-cymene (**114**), α-terpinolene (**116**), o-cymene (**115**) and α-limonene (**117**), compared to type 2, which contained sabinene (**118**), α-pinene (**108**), β-pinene (**109**), α-phellandrene (**112**) and β-phellandrene (**113**). For the third type of *L. virgaurea* 3-carene (**110**) was the only monoterpene component found in the extract, which could have several reasons, for example a short extraction time followed by a low concentration of the components or the loss of the volatile compounds through the drying process of the roots.

A further difference between *L. virgaurea* type 1 and type 2 were that some samples of type 1 (Tables 17, 18 and 20) contained a small amount of β-caryophyllene (**98**).

At last it is interesting, that the geographical distribution of all three types does not coincide with the intraspecific classifications due to different chemical composition of each sample.

3.1.2. L. subspicata

L. subspicata, belonging to the section Ligularia, series Ligularia, is located in northwestern Yunnan and southwestern Sichuan provinces of China and can be found at swamps, scrubs and forest understories, ranging from 3000 to 5000m in altitude [5].

Seven samples of *L. subspicata* were collected in Yunnan and Sichuan provinces of China from 2007 to 2009 and analyzed by GC-MS. The results are listed in chapter 6.2.2.

No.	Sample	Place	Altitude (m)	Type
1	08 32	Tianchi	3888	A + L
2	07 95	Haizishan (Batang County)	4180	F
3	07 113	Wumingshan	4100	decomposed
4	07 123	Daxueshan	4124	F
5	09 34	Haizishan	4488	F
6	09 44	Litang	4236	B + L
7	09 45	Litang	4236	L

Table 6. Samples of *L. subspicata.* F = Fukinone (**69**), A = Subspicatin A (**27**), B = Subspicatin B (**28**), L = Ligularol (**16**). Samples 5 to 7 were MeOH extracts of dried roots (several days of extraction), whereas samples 1 to 4 were concentrated by the standard method and solved with AcOEt prior to separation.

Samples 2, 4 and 5 contained fukinone (**69**) as the major component with 100.00, 86.61 and 87.64% of relative distribution, respectively. Whereas sample 2 showed a single peak at retention time 9.56 minutes, samples 4 and 5 contained a small amount of dehydrofukinone (**70**) in addition to the major component (Tables 28 and 29). Furthermore 8-hydroxyeremophil-7(11)-en-12,8-olide (**60**) was found in sample 4 and a small amount of β-myrcene (**107**) in sample 5. On the contrary, samples 1 and 3 showed complex TIC profiles. The major components of sample 1 were subspicatin A (**27**), followed by ligularol (**16**) at retention times 13.84 and 9.99 minutes. Other compounds found in this sample were β-myrcene (**107**), 3-carene (**110**), cis-ocimene (**111**), eremophila-1(10),11-diene (**67**), 6-acetoxy-furanoeremophilan-10-ol (**23**, Figure 41, m/z = 292 $[M]^+$,

232 $[M\text{-}AcOH]^+$, 124 = base $[C_7H_8O_2]^+$ RDA, 43 $[C_2H_3O]^+$), 6-isobutanoyloxy-furanoeremophilane (**21**, Figure 42, m/z = 304 $[M]^+$, 234 $[C_{15}H_{22}O_2]^+$, 216 $[M\text{-}C_4H_8O_2]^+$, 159 = base $[C_{11}H_{11}O]^+$, 145 $[C_{10}H_9O]^+$, 124 $[C_7H_8O_2]^+$ RDA, 71 $[C_4H_7O]^+$, 43 $[C_3H_7]^+$), eremofarfugin C (**58**), 6-(2'-methylbutanoyloxy)-furanoeremophilane (**20**, Figure 43, m/z = 318 $[M]^+$, 216 $[M\text{-}C_5H_{10}O_2]^+$, 159 = base $[C_{11}H_{11}O]^+$, 145 $[C_{10}H_9O]^+$, 86 $[C_5H_{10}O]^+$, 57 $[C_4H_{10}]^+$), 6-isobutanoyloxy-furanoeremophilan-10-ol (**26**), 6-(2'-methylbutanoyloxy)-furanoeremophilan-10-ol (**25**), 6-(angeloyloxy)-furanoeremophilan-10-ol (**24**), 6-isobutanoyloxy-furano-eremophilan-9-one (**31**), 6-angeloyloxy-furanoeremophilan-9-one (**30**) and subspicatin B (**28**) at retention times 4.28, 4.48, 4.66, 8.01, 10.84, 10.92, 11.12, 11.36, 11.39, 11.89, 12.11, 12.17, 13.09 and 13.15 minutes, respectively (Table 30).

Sample 3 showed peaks at retention times 8.01, 9.95, 10.74, 10.86, 12.33 and 12.37 minutes. They correspond to eremophila-1(10),11-diene (**67**), bakkenolide A (**66**), subspicatolide (**5**), 8-oxoeremophil-6(7)-en-12-oic acid (**79**), 6-hydroxy-8H-eremophil-7(11)-en-12,8-olide (**61**) and 6,8-dihydroxy-eremophil-7(11)-en-12,8-olide (**62**, Figure 55, m/z = 266 $[M]^+$, 248 $[M\text{-}H_2O]^+$, 140, 109 = base), respectively. The major peak, observed at 11.34 minutes (Figure 54, m/z = 304) is unknown.

The major compounds of sample 6 were ligularol (**16**) and subspicatin B (**28**) at retention times 9.98 and 13.15 minutes (Table 31). The peak, observed at 4.28 minutes, corresponds to β-myrcene (**107**).

Similar to sample 6, sample 7 showed a major peak at retention time 9.98 minutes with 47.54% of relative distribution. Furthermore a small amount of β-myrcene (**107**) and an unknown compound at retention times 10.44 minutes (Figure 49, m/z = 232) were found in the extract.

Samples 5, 6 and 7 were measured again one month after the first measurement. Samples 6 and 7 were different with respect to their chemical composition. By comparison sample 6 contained β-myrcene (**107**), eremofarfugin C (**58**) and 6-hydroxy-eremophil-7(11)-en-12,8-olide (**61**), respectively. The major compounds at retention times 12.08 (Figure 47, m/z = 262) and 11.48 minutes (Figure 46, m/z = 248) are unknown (Table 32). These results indicate that major compounds (**16** and **28**) measured earlier have decomposed to their corresponding lactones (**61** and **58**).

For sample 7, the TIC of the second measurement showed peaks at retention times 4.27, 9.73, 9.98 and 12.32 minutes, respectively (Table 34). They correspond to β-myrcene (**107**), ligularol methyl ether (**18**, Figure 51, m/z = 248 $[M]^+$, 138 = base $[C_8H_{10}O_2]^+$ RDA), ligularol (**16**) and 6-hydroxy-eremophil-7(11)-en-12,8-olide (**61**). The major compound at retention time 10.44 minutes is unknown (Figure 52, m/z = 264). Compound **18** is most likely to be an artifact of **16**. In addition, **61** might be the oxidation product of **16**.

The presence of intraspecific diversity of *L. subspicata* is known from previous reports [5, 32]. The classification within the species was done according to their major compounds (Table 6).

The samples analyzed by GC-MS showed sesquiterpenoids of furano- and non-furanoeremophilane type. Whereas samples 1, 6 and 7 showed C_1 and C_6 (**27** and **28**) and/or C_6 (**16**) oxygenated furanoeremophilanes, samples 2, 4 and 5 contained eremophilan-8-one derivatives as the major component. Previous publications stated that the chemical composition of *L. subspicata* appear rather continuous, which implies the assumption that the species is still developing from a type producing eremophilan-8-ones to a type producing furanoeremophilanes [5, 32].

As mentioned before, samples 1 and 3 showed complex chemical profiles. Sample 1 contained furanoeremophilane derivatives oxygenated at different positions, C_6 and C_{10} (**23**, **24**, **25** and **26**), C_6 and C_9 (**30** and **31**), C_1 and C_6 (**27** and **28**) and C_6 (**16**, **20** and **21**), respectively.

However, furanoeremophilanes possessing an oxygen-function, such as hydroxyl, acyloxyl, and alkoxyl on ring B, showed similar EI fragmentation patterns [8]. In cases where *retro*-Diels-Alder fragmentation was not predominant, the spectra of the compounds measured, showed peaks at either m/z 159 or m/z 159 and 145, containing the furan moiety [8]. The plausible fragmentation mechanism, proposed by Nagano and co-workers [8] is shown in figure 5.

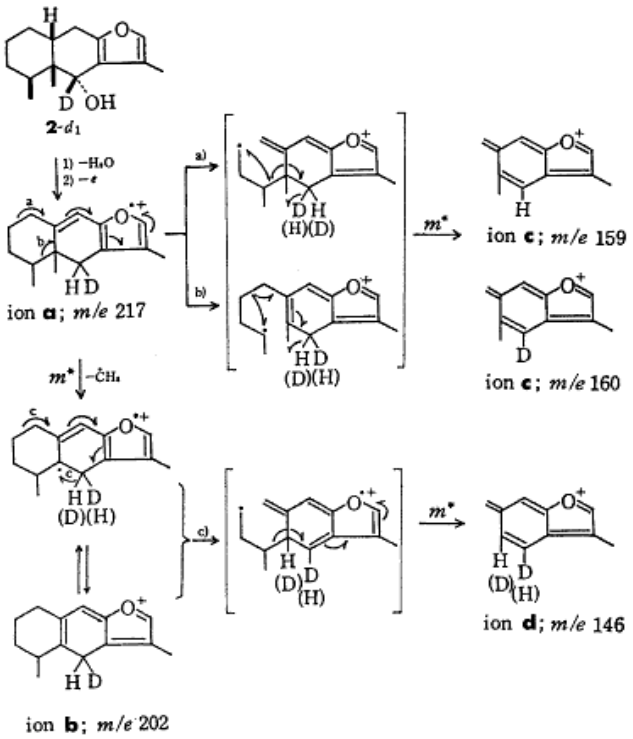

Figure 5. EI fragmentation mechanism of oxygenated furanoeremophilanes on ring B [8]

Furthermore, it has been reported that thermal dehydration of furano-eremophilan-6β,10β-ol (**22**) results in benzofuran derivatives, farfugin A (**95**) and B (**96**). This conclusion was made as farfugin B showed a fragmentation pattern due to benzylic cleavage, which results in a peak at m/z 159. In contrast the main peaks of farfugin A could be observed at m/z 214 and at m/z 199. These findings lead to the assumption that furanoeremophilane-6β,10β-ol (**22**) and its derivatives follow an aromatization by elimination of the oxygen functions at C_6 and C_{10} [8, 34].

In contrast to sample 1, sample 3 showed a different chemical profile. The main compounds, identified by searching in the available libraries and literature, were lactones (**61**, **62**, **66** and **5**) and sesquiterpenoids of the eremophilane type (**67** and **79**). The presence of lactones indicates that oxidation of furanoeremo-philanes has occurred. Hence the conclusion was drawn, that sample 3 has decomposed eventually.

The biogenetic pathway of subspicatolide (**5**) proposed by Tori and co-workers is shown in figure 6.

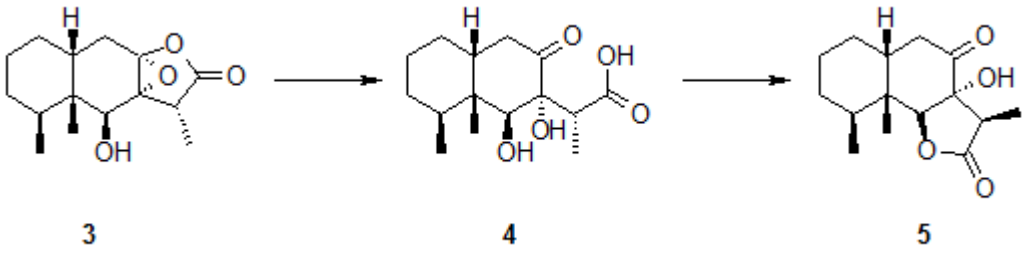

Figure 6. Biogenetic pathway of subspicatolide (**5**) [5]

In addition, *L. lamarum*, a taxonomically closely related species to *L. subspicata* can be compared to explore the interspecific diversity of this genus. The main morphological difference between *L. subspicata* and *L. lamarum* is the absence and presence of ligulate florets, respectively and the color of the pappi. Furthermore, the two species occupy similar habitats, whereas *L. lamarum* is more widely distributed [32]. Previous publications investigated the chemical composition of these two species and their intra- and interspecific diversity [5, 32].

During this work root chemicals of *L. lamarum* collected in 2009 (Maerkang/Xianjin, 3939m) were extracted with AcOEt and have been analyzed by GC-MS. The results indicate 6β-(2'-methylbutanoyl)oxy-furanoeremophilan-10β-ol (**25**) as the major component followed by α-phellandrene (**112**) with 49.96% and 18.24% of relative distribution, respectively. Further compounds, detected in the extract, are 6β-isobutanoyloxy-furanoeremophilan-10β-ol (**26**), ligularol (**16**) and o-cymene (**115**).

These findings suggest similarities in the chemical composition with *L. subspicata* as it is known, that both species have types producing furanoeremophilan-6β,10β-ol derivatives and ligularol (**16**). Hence, it is difficult to distinguish these two species with respect to their chemical composition as it is also known that they occupy similar habitats and are often intermingled at some locations, which leads to the conclusion that similar processes of adaption to alpine environment is going on [32].

3.1.3. L. vellerea

L. vellerea, belonging to the section Scapicaulis, is located in northwestern Yunnan and southwestern Sichuan provinces of China and inhabits alpine meadows ranging from 2500 to 4000m in altitude. The main morphological characteristic of this plant is the presence of dense white lanate hair at the base of its stem and petioles [1].

Three samples of *L. vellerea* were collected in 2007 in the Sichuan and Gansu provinces of China and analyzed by GC-MS. Previous reports suggested the presence of 3 types for the samples collected in the Yunnan province of China based on their chemical composition. The major components of type A (Jianchuan, Lijian and Zhogdian areas), B (Luguhu area) and C (Kunming area) were 6,15-dioxygenated furanoeremophilanes, 1,6-dioxygenated furanoermophilanes and 6,15-dioxygenated eremophilanolides, respectively. The latter may exist due to decomposition of the labile furano-components during the drying process of the plant. Furthermore, it has been reported that the classification based on the chemical analysis agreed with the geographical distribution of the species [1].

No.	Sample	Place	Altitude (m)	Major compound
1	07 04	Yanyuan-Muli	3228	unknown, m/z = 248
2	07 46	Wuxuhai	3621	unknown, m/z = 248
3	07 30	Pingchuan	3162	**43**

Table 7. Samples of *L. vellerea*. Samples 1 and 2 were collected in the Sichuan province, whereas sample 3 was collected in the Gansu province of China. Samples were concentrated by the standard method and solved with AcOEt prior to separation.

Common compounds found in *L. vellerea*, collected in the Sichuan province of China were eremophilene (**67**), **89** and subspicatolide (**5**). Furthermore bakkenolide A (**66**) was found in sample 2 and 8-oxoeremophil-6(7)-en-12-oic acid (**79**) and its decarboxylated product **78** (Figure 65, m/z = 220 $[M]^+$, 205 = $[M\text{-}CH_3]^+$, 178 $[M\text{-ketene}(C_2H_2O)]^+$, 43 = base $[C_2H_3O]^+$) in sample 1.

The main compounds for both samples were assumed to be 6-hydroxy-eremophil-8(9),7(11)-dien-12,8-olide (**63**, Figure 66, m/z = 248 $[M]^+$, 140, 124,

109 = base) at retention time 12.35 minutes with 38.35% (sample 1) and 24.37% (sample 2) of relative distribution, respectively. This assumption was made by comparing the EI mass spectrum of compound **61** (Figure 165, m/z = 250) of the reference data, shown in chapter 6.3. **63** is presumably the dehydrogenation product of **61**.

In addition, sample 1 showed a peak at retention time 13.33 minutes, which could be 6,8-dihydroxy-eremophil-7(11)-en-12,8-olide (**62**, Figure 67, m/z = 266 $[M]^+$, 138, 123 = base, 109). By comparing the EI mass spectra (Figures 66 and 67) **63** is probably the dehydration product of **62**.

Other common compounds found in sample 1 and 2 are at retention times 11.18, 11.31, 11.54 and 11.65 minutes (Figures 60, 61, 62, and 63) and unknown.

At last sample 3, collected in the Gansu province of China showed a different chemical profile compared to the other samples. It is more consistent with the types proposed in [1]. The main compound is furanoeremophilan-15,6-olide (**43**) at retention time 11.41 minutes with 58.96% of relative distribution. Furthermore, 2-methyl-2-butenoic acid (**121** or **122**), β-pinene (**109**) and eremophilene (**67**) were found in the sample. It is most likely that the main compound **43** was generated from **49** by elimination of a hydroxy or an acyloxy group at C_6 and attacking the carboxyl group at C_{15} [1]. That could also explain the high amount of 2-methyl-2-butenoic acid (**121** or **122**) in the sample. Further peaks observed are unknown and occurred at retention times 11.90, 12.39, 12.46 and 13.40 minutes (Table 37). The peak at 16.35 minutes is likely to be 3β-angeloyloxy-furanoeremophilan-15,6-olide (**46**, Figure 58, m/z = 344 $[M]^+$, 244 [M-AngOH]+, 199 $[244\text{-}CO_2H]^+$, 185 $[199\text{-}CH_3]^+$, 172 = base $[C_{12}H_{12}O]^+$, 83 $[C_5H_7O]^+$, 55 $[C_4H_7]^+$). The corresponding mass spectral data are shown in chapter 6.2.4.

Intraspecific diversity was confirmed to be present in root chemicals of L. vellerea. Compared to the samples from northwestern to central Yunnan province of China [1] the samples from Sichuan province showed different chemical profiles, although some of the compounds were similar. The reason for this variation lies probably in the geographical separation of the samples. On the other hand the sample from Gansu province of China contained similar compounds to those from the Yunnan province as it showed 6,15-dioxygenated furanoeremophilanes (**43** and **46**) as part of the sample.

3.1.4. L. cyathiceps

L. cyathiceps belonging to the section Ligularia, series Ligularia, inhabits stream banks, valleys, and grassy slopes in the northwestern Yunnan province of China [4]. Seven samples of *L. cyathiceps* were collected in the Zhongdian (Shangrila) County of northwestern Yunnan in 2008 and examined by GC-MS (Table 8). The corresponding results are shown in chapter 6.2.5.

No.	Sample	Place	Altitude (m)	Major component
1	08 07	Hongshan (Geza)	3960	**35**
2	08 27	Tianchi	3719	**35**
3	08 29	Tianchi	3799	**35**
4	08 36	Tianchi	3880	**35**
5	08 39	Quianhushan	3655	**35**
6	08 40	Quianhushan	3548	**35**
7	08 41	Quianhushan	3548	**35**

Table 8. Samples of *L. cyathiceps*. Dried roots were extracted with AcOEt and oily extracts obtained by the standard method [4].

The chemical composition of all samples analyzed, provides 1,10β-epoxy-6β-isobutanoyloxy-furanoeremophilan-9-one (**35**) as the major component (Table 8), followed by cacalol (**15**) and 1,10β-epoxy-6β-angeloyloxy-furanoeremophilan-9-one (**34**) at retention times 11.29, 14.72 and 16.40 minutes, respectively. In addition, peaks at retention times 8.02, 8.88, 9.01, 9.16, 11.50, 14.18 and 14.85 minutes could be observed in some samples of *L. cyathiceps*. They correspond to eremophilene (**67**), valerianol (**80**), β-eudesmol (**84**), valeranone (**82**), 1,10β-epoxy-6β-isobutanoyloxy-furanoeremophilane (**38**, Figure 73, m/z = 318 $[M]^+$, 230 = $[M\text{-}C_4H_8O_2]^+$, 159 $[C_{11}H_{11}O]^+$, 145 $[C_{10}H_9O]^+$, 71 $[C_4H_7O]^+$, 43 = base $[C_3H_7]^+$), 1,10β-epoxy-6β-propanoyloxy-furanoeremophilan-9-one (**36**, Figure 69, m/z = 318 $[M]^+$, 262 $[M\text{-}C_3H_4O]^+$, 246 $[C_{15}H_{18}O_3]^+$, 228 $[246\text{-}H_2O]^+$, 178 = base $[C_{10}H_{10}O_3]^+$, 57 $[C_3H_5O]^+$) and 6β-angeloyloxy-10αH-furanoeremophilan-9-one (**127**, Figure 71, m/z = 330 $[M]^+$, 248 $[M\text{-}C_5H_6O]^+$, 230 $[M\text{-AngOH}]^+$, 83 = base $[C_5H_7O]^+$, 55 $[C_4H_7]^+$), respectively. According to the reference data (see chapter 6.3.) the last three compounds were assumed to have the same

carbon skeleton compared to **37**, **35** and **30** (Figures 167, 146 and 150), respectively. 6β-angeloyloxy-furanoeremophilan-9-one (**127** and **30**) might have two different configurations at C_{10}. Furthermore, sample 2 showed additional peaks at retention times 15.52 and 15.99 minutes, which could be 6β-angeloyloxy-furanoeremophil-1(10)-en-9-one (**32**, Figure 75, m/z = 328 $[M]^+$, 228 $[M\text{-AngOH}]^+$, 83 = base $[C_5H_7O]^+$, 55 $[C_4H_7]^+$) and 1,10β-epoxy-6β-isovaleroyloxy-furanoeremophilan-9-one (**128**, Figure 76, m/z = 346 $[M]^+$, 262 $[M\text{-}C_5H_8O]^+$, 244 $[M\text{-}C_5H_{10}O_2]^+$, 178 $[C_{10}H_{10}O_3]^+$, 85 $[C_4H_9CO]^+$, 57 = base $[C_4H_9]^+$), respectively.

In summary, 6-acyloxy-furanoeremophilan-9-ones (**35** and **34**) and cacalol (**15**) were common in L. cyathiceps. Given that the chemical pattern of each sample analyzed show similarities, intraspecific variations were limited. Hence the results suggest the presence of only one type, which could be limited to the location, as only samples from Yunnan were examined.

3.1.5. L. pleurocaulis

L. pleurocaulis, belonging to the section Senecillis, grows on highlands of around 4000m in altitude [11]. Nineteen samples of *L. pleurocaulis* (Table 9) were collected in northwestern Yunnan and southwestern Sichuan provinces of China from 2003 to 2009 and have been examined by GC-MS (see chapter 6.2.6).

Extracts of fresh roots were applied on TLC (hexane-AcOEt 7:3) to detect furanoeremophilanes by *Ehrlich*'s reaction. Three dark blue *Ehrlich* positive spots (R_f = 0.85, 0.43 and 0.38) were observed for all samples. In addition, it has been reported, that samples collected in Sichuan showed a light blue spot (R_f = 0.63) after several hours of coloring procedure. On the contrary samples collected in Yunnan showed a dark purple spot at the same R_f-value (0.63) [11].

No.	Sample	Place	Altitude (m)	Components[a)]
1	03 53	Wumingshan (Sichuan)	3800	**50**, **40**
2	03 61	Haizishan (Sichuan)	4300	**50**, **40**
3	04 36	Dabaoshan (Sichuan)	3400	**50**
4	04 44	Gezan (Yunnan)	4000	**50**, **52**
5	09 501	Qianhushan (Yunnan)	3631	**50**, **52**
6	09 502	Qianhushan (Yunnan)	3644	**50**, **52**
7	09 503	Qianhushan (Yunnan)	3649	**50**, **52**
8	09 504	Qianhushan (Yunnan)	3651	**50**, **52**
9	09 505	Qianhushan (Yunnan)	3622	**50**, **52**
10	09 506	Qianhushan (Yunnan)	3674	**50**, **52**
11	09 507	Qianhushan (Yunnan)	3657	**50**, **52**
12	09 508	Qianhushan (Yunnan)	3657	**50**, **52**
13	09 509	Qianhushan (Yunnan)	3657	**50**, **52**
14	09 510	Qianhushan (Yunnan)	3645	**50**, **52**
15	09 511	Qianhushan (Yunnan)	3624	**50**, **52**
16	09 37	Litang (Sichuan)	4296	**50**, **52**, **40**
17	09 55	Laima (Sichuan)	3746	**40**
18	09 101	Lianghe (Yunnan)	3534	**51**, **52**
19	09 112	Xiaojin/Baoxing (Sichuan)	3866	**50**

Table 9. Samples of *L. pleurocaulis*. Samples 5 to 15 were EtOH extracts of fresh roots, while samples 16 to 19 were MeOH extracts of dried roots (1 month of extraction). Samples 1 (corresponds to sample 5 reported in [11]) and 2 (corresponds to sample 6 reported in [11]) were collected in 2003, extracted with EtOH without drying and concentrated by the standard method, whereas samples 3 and 4 (corresponds to sample 4 reported in [11]), collected in 2004 were dried, extracted with EtOH and oily extracts obtained by the standard method [11]. a) Major compounds (6β-angeloyloxyfuranoeremophil-1(10)-en-3β-ol (**50**), 6β-tigloyloxyfuranoeremophil-1(10)-en-3β-ol (**51**) or furanoligularenone (**40**)) and compounds at R_f = 0.63 (3β-angeloyloxyfuranoeremophil-1(10)-en-6β-ol (**52**) and/or furanoligularenone (**40**))

Samples collected in Yunnan showed characteristic peaks at retention times 12.39, 13.38, 13.62 and 13.86 minutes, respectively. They relate to 6β-(isobutanoyloxy)-furanoeremophil-1(10)-en-3β-ol (**129**, Figure 78, MW = 318.40734, calc. for $C_{19}H_{26}O_4$, m/z = 230 = base $[C_{15}H_{18}O_2]^+$, 212 $[C_{15}H_{16}O]^+$, 197 $[C_{15}H_{16}O\text{-}CH_3]^+$, 172 $[C_{12}H_{12}O]^+$ RDA, 123 $[C_7H_7O_2]^+$ RDA, 71 $[C_4H_7O]^+$, 43 $[C_3H_7]^+$), 6β-(angeloyloxy)-furanoeremophil-1(10)-en-3β-ol (**50**, Figures 79 and

90, m/z = 330 $[M]^+$, 230 $[C_{15}H_{18}O_2]^+$, 212 $[C_{15}H_{16}O]^+$, 197 $[C_{15}H_{16}O\text{-}CH_3]^+$, 172 $[C_{12}H_{12}O]^+$ RDA, 123 $[C_7H_7O_2]^+$ RDA, 83 = base $[C_5H_7O]^+$, 55 $[C_4H_7]^+$), 6β-(tigloyloxy)-furanoeremophil-1(10)-en-3β-ol (**51**, Figure 80, m/z = 330 $[M]^+$, 230 $[C_{15}H_{18}O_2]^+$, 212 $[C_{15}H_{16}O]^+$, 197 $[C_{15}H_{16}O\text{-}CH_3]^+$, 172 $[C_{12}H_{12}O]^+$ RDA, 123 $[C_7H_7O_2]^+$ RDA, 83 = base $[C_5H_7O]^+$, 55 $[C_4H_7]^+$) and 3β-(angeloyloxy)-furanoeremophil-1(10)-en-6β-ol (**52**, Figure 81, m/z = 330 $[M]^+$, 312 $[M\text{-}H_2O]^+$, 230 $[C_{15}H_{18}O_2]^+$, 212 $[C_{15}H_{16}O]^+$, 197 $[C_{15}H_{16}O\text{-}CH_3]^+$, 172 $[C_{12}H_{12}O]^+$ RDA, 122 = base $[C_7H_6O_2]^+$ RDA, 83 $[C_5H_7O]^+$, 55 $[C_4H_7]^+$), respectively (Figure 7). Major components were assigned to be **50** (R_f = 0.43) and **51** (R_f = 0.38). In addition, to these compounds, **52** was common in samples collected in Yunnan and corresponds to the dark purple spot developed on TLC (R_f = 0.63) [11]. The difference to the samples collected in Sichuan was the presence of furanoligularenone (**40**) at retention time 10.24 minutes (light blue spot on TLC at R_f = 0.63) and the absence of **52** except for samples 3, 16 and 19. Sample 16 contained furanoligularenone (**40**) and **52**, whereas samples 3 and 19 showed no furanoligularenone (**40**), which probably could not be detected due to low concentration.

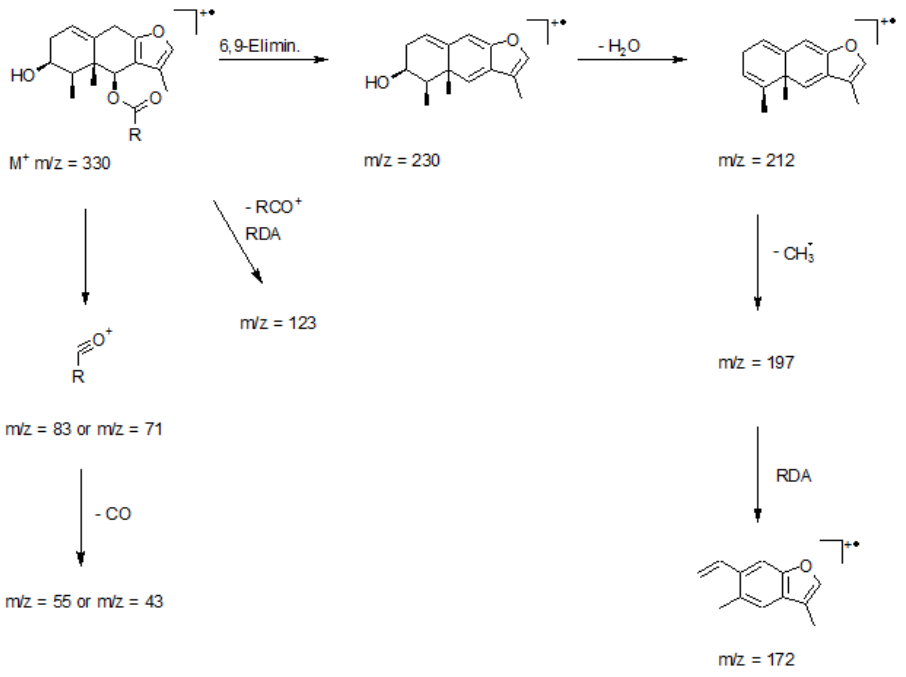

Figure 7. EI fragmentation pattern of 6β-isobutanoyloxy-furanoeremophil-1(10)-en-3β-ol (**129**), 6β-angeloyloxy-furanoeremophil-1(10)-en-3β-ol (**50**) and 6β-tigloyloxy-furanoeremophil-1(10)-en-3β-ol (**51**) [37]

Furthermore, selina-4,11-diene (**87**), β-caryophyllene (**98**), guaia-6,9-diene (**101**), α-caryophyllene (**97**), β-selinene (**83**), 10-epi-γ-eudesmol (**81**) and β-eudesmol could be observed for the samples collected in Yunnan. By comparison samples from Sichuan contained selina-4,11-diene (**87**), eremophilene (**67**) and 10-epi-γ-eudesmol (**81**) and even 3-desoxyneopetasol (**71**) was found in sample 3.

Besides all this monoterpenes were found in some samples, especially in extracts of fresh roots. Most of them contained a high amount of α-phellandrene (**112**), followed by β-pinene (**109**), α-pinene (**108**), p-cymene (**114**), β-myrcene (**107**) and 3-carene (**110**), respectively.

Intraspecific variation was present in *L. pleurocaulis*. The conclusions made in previous reports [11] were not consistent with the results found during this work. The statement that the different chemical composition between types correlates with the geographical separation could not be confirmed as some of the samples may not fit in this scheme. Two differences in chemical composition were proposed by Nagano and co-workers [11]. The first one was the presence of furanoligularenone (**40**) or **52** in Sichuan and Yunnan samples, respectively. This finding does not coincide with samples 3, 16 and 19, collected in Sichuan (Table 9). The second one was the difference in the ratio of the angelate (**50**) and tiglate (**51**). It was assumed that samples from Sichuan contained **50** and **51** in a 1:1.3 ratio, whereas samples from Yunnan gave compound **50** as the only major component [11]. This assumption was disproved with samples 17 and 19 for example as major compounds were furanoligularenone (**40**) in sample 17 and **51** in sample 18. Furthermore the presence of 6β-(angeloyloxy)- and 6β-(tigloyloxy)-furanoermeophil-1(10)-enes (**56** and **44**, R_f = 0.85), proposed in [11], could not be observed, which may not be detected due to low concentration.

3.1.6. L. dictyoneura

L. dictyoneura belonging to the section Senecillis grows on grassy slopes, banks, and forest understories ranging from 2000 to 3500m in altitude and is located in the northwestern Yunnan and southwestern Sichuan provinces of China [10].

Ten samples of *L. dictyoneura* were collected from 2003 to 2006 and analyzed by GC-MS. These samples have been examined previously by Nagano and co-workers [10]. The corresponding sample numbers are shown in table 10.

Ehrlich's test was carried out on TLC (hexane-AcOEt 7:3) for all samples to observe the diversity of the species. Seven different types could be distinguished (Table 10), whereas six of them showed *Ehrlich* positive reactions, indicating the presence of furanoeremophilane derivatives. Several *Ehrlich* positive spots were observed for type 1 (R_f = 0.74, 0.69, 0.63 and 0.38), type 2 (R_f = 0.63, 0.58 and 0.44), type 3 (R_f = 0.92 and 0.63), type 4 (orange colored spot at R_f = 0.79 and 0.58), type 5 (one strong spot at R_f = 0.62) and type 6 (one strong spot at R_f = 0.62), respectively. The components of *Ehrlich* negative samples were detected with $Ce(SO_4)_2$ [10].

No.	Sample	Place	Altitude (m)	Type	Sample No. [10] [a)]
1	03 35	Xiaoxueshan	3400	4	14
2	03 72	Rencun	2900	5	17
3	04 08	Sandawan	3200	1	1
4	04 09	Yulongxueshan	3000	2	2
5	04 19	Hutiaoxia	2200	2	3
6	04 35	Dabaoshan	3500	Ehrlich (-)	7
7	04 75	Mudiqing	3000	1	15
8	05 08	Shikashan	3500	3	9
9	06 56	Baimaxueshan	4345	6	20
10	06 68	Nixi	3365	Ehrlich (-)	

Table 10. Samples of *L. dictyoneura.* a) Corresponding sample numbers from reference article [10].

Further phytochemical analysis by GC-MS (see chapter 6.2.7) was consistent with the classification of seven different types. Samples 5 and 7 were assigned to be type 1. Sample 7 contained 3β-(acyloxy)-6β-(angeloyloxy)-furanoeremophilane (**47**) and 6β-(angeloyloxy)-furanoeremophilan-10β-ol (**24**, Figure 103, m/z = 332 $[M]^+$, 206 $[C_{12}H_{14}O_3]^+$ RDA (Figure 8), 124 = base $[C_7H_8O_2]^+$ RDA, 108 $[C_7H_8O]^+$, 83 $[C_5H_7O]^+$, 55 $[C_4H_7]^+$) at retention times 13.72 and 13.83 minutes, respectively. The major peak at 12.50 minutes is unknown (Figure 102, m/z = 290). In contrast, the major compound of sample 3 was 3β-(acyloxy)-6β-(angeloyloxy)-furanoeremophilane (**47**) at 13.72 minutes. Further peaks observed for this sample were at retention times 9.85, 11.54 and 14.68 minutes. They correspond to ligularol ethyl ether (**17**, Figure 105, m/z = 262 $[M]^+$, 152 = base $[C_9H_{12}O_2]^+$ RDA, 123 $[C_7H_7O_2]^+$), 6β-(angeloyloxy)-furanoeremophilane (**19**, Figure 106, m/z = 316 $[M]^+$, 216 $[M\text{-}AngOH]^+$, 159 $[C_{11}H_{11}O]^+$, 145 $[C_{10}H_9O]^+$, 83 = base $[C_5H_7O]^+$, 55 $[C_4H_7]^+$) and 3β-(acyloxy)-6β-(angeloyloxy)-furanoeremophilan-10β-ol (**48**, Figure 107, MW (g/mol) = 390.47, calc. for $C_{22}H_{30}O_6$, m/z = 290 $[M\text{-}AngOH]^+$, 206 $[C_{12}H_{14}O_3]^+$ RDA (Figure 8), 83 = base $[C_5H_7O]^+$, 55 $[C_4H_7]^+$, 43 $[C_2H_3O]^+$), respectively.

The major compound of *L. dictyoneura* type 2 was ligularol (**16**), followed by furanoeremophilan-15,6α-olide (**43**) at retention times 9.98 and 11.40 minutes, respectively (Samples 4 and 5). In addition, sample 4 contained ligularol ethyl and methyl ether (**17** and **18**), which seems to be an artifact during the extraction procedure. In contrast, sample 5 showed a small amount of ligularone (**39**), the oxidation product of ligularol (**16**).

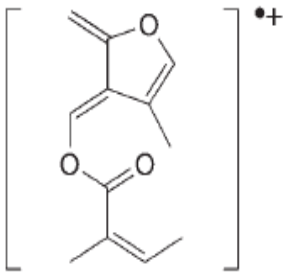

Figure 8. Retro-Diels-Alder fragment of 3β-(acetoxy)-6β-(angeloyloxy)-furanoeremophilan-10β-ol (**48**, m/z = 206) [10]

Sample 8 was assumed to be type 3. The major compound was fukinanolide (**66**), followed by furanoermemophilane (**44**) and ligularol methyl ether (**18**, Fig-

ure 111, m/z = 248 $[M]^+$, 138 = base $[C_8H_{10}O_2]^+$ RDA, 123 $[C_7H_7O_2]^+$) at retention times 9.96, 9.05 and 9.73 minutes, respectively (Table 62).

Although sample 1 showed a similar chemical composition in comparison with sample 8, it was assigned to be type 4. The major compound found in this sample was fukinanolide (**66**). In addition, ligularone (**39**), ligularol ethyl ether (**17**), dehydrofukinone (**70**) and furanoeremophilan-15,6α-olide (**43**) were detected (Table 63). These results agree with the findings reported by Nagano and coworkers [10]. In addition, the orange spot developed on TLC by *Ehrlich*'s reaction (R_f = 0.79) confirms the presence of ligularone (**39**) as the color indicates the presence of an oxo group at C_6 [3].

From sample 2[3] (type 5) dehydrofukinone (**70**), fukinanolide (**66**), ligularol (**16**), petasin (**74**) and 3β-(angeloyloxy)-ligularol (**42**, Figure 115, m/z = 332 $[M]^+$, 124 = base $[C_7H_8O_2]^+$ RDA, 109, 83 $[C_5H_7O]^+$, 55 $[C_4H_7]^+$) were detected at retention times 9.90, 9.95, 9.98, 12.97 and 13.83 minutes, respectively. The major peak at retention time 13.46 minutes is unknown (Figure 116, m/z = 316 $[M]^+$, 216 $[M\text{-}AngOH]^+$, 161 = base, 83 $[C_5H_7O]^+$, 55 $[C_4H_7]^+$), although it is known that this compound must have an angeloyloxy moiety.

The major compound of sample 9 (type 6) was 6β-acyloxy-1,10-epoxyfuranoeremophilane (**37**) at retention time 10.89 minutes. Further compounds found were selina-4,11-diene (**87**), eremophila-1(10),11-diene (**67**), γ-selinene (**85**), 6β-acyloxy-furanoeremophil-1(10)-ene (**55**, Figure 117, MW (g/mol) = 274.35478, calc. for $C_{17}H_{22}O_3$, m/z = 230 $[C_{15}H_{18}O_2]^+$, 214 $[C_{15}H_{18}O]^+$, 199 = base $[C_{14}H_{15}O]^+$, 172 $[C_{12}H_{12}O]^+$ RDA, 43 $[C_2H_3O]^+$), **57** (Figure 118, MW (g/mol) = 316.39146, calc. for $C_{19}H_{24}O_4$, m/z = 214 $[C_{15}H_{18}O]^+$, 199 = base $[C_{14}H_{15}O]^+$, 172 $[C_{12}H_{12}O]^+$ RDA, 69 $[C_4H_5O]^+$, 41 $[C_3H_5]^+$), **53** (Figure 119, MW (g/mol) = 332.39086, calc. for $C_{19}H_{24}O_5$, m/z = 230 $[M\text{-}C_4H_6O_3]^+$, 215 $[C_{15}H_{18}O_2\text{-}CH_3]^+$, 201, 188, 173, 159 $[C_{11}H_{11}O]^+$, 145 $[C_{10}H_9O]^+$, 69 = base $[C_4H_5O]^+$, 41 $[C_3H_5]^+$) at retention times 7.43, 8.01, 9.07, 10.66, 11.34 and 11.57 minutes, respectively. Compounds **53** and **57** were reported in [10] and compared to the EI mass spectral data described in the paper (Figures 119 and 118).

The TIC of samples 6 and 10 (*Ehrlich* negative type) showed characteristic peaks at retention times 7.34, 7.94, 8.04, 8.84, 9.60, 9.64, 9.90, 12.97, 13.36 and 13.42 minutes, respectively. They were assigned to be selina-4,11-diene

[3] GC-MS injection mode = splitless, because of low concentration of compounds

(**87**), isoledene (**100**), 10-epi-dihydroagarofuran (**104**), γ-eudesmol (**86**), 3-desoxyneopetasol (**71**), 3-desoxypetasol (**72**, Figure 121, m/z = 218 $[M]^+$, 203 $[M\text{-}CH_3]^+$, 150 $[C_{10}H_{14}O]^+$, 135 = base $[C_{10}H_{14}O\text{-}CH_3]^+$, 41 $[C_3H_5]^+$), dehydrofukinone (**70**), 3-tigloyloxy-eremophila-9,11-dien-8-one (**75**, Figure 122, m/z = 316 [M]+, 216 $[M\text{-TigOH}]^+$, 148 = base $[C_{10}H_{12}O]^+$, 83 $[C_5H_7O]^+$, 55 $[C_4H_7]^+$, 41 $[C_3H_5]^+$), neopetasin (**76**, Figure 123, m/z = 316 $[M]^+$, 216 $[M\text{-AngOH}]^+$, 148 = base $[C_{10}H_{12}O]^+$, 83 $[C_5H_7O]^+$, 55 $[C_4H_7]^+$, 41 $[C_3H_5]^+$) and petasin (**74**), respectively. The major compound of samples 6 and 10 was assumed to be **72**. The assumptions for compounds **72** and **75** were made by comparing the EI mass spectra of 3-desoxyneopetasol (**71**) and petasin (**74**, Figure 171) from the MassFinder library. It is obvious, that the identical EI mass spectra at different retention times are the result of compounds with the same carbon skeleton and different configurations.

Compared to previous reports [10], the major components identified could not be detected anymore in the majority of cases. This might be due to decomposition procedures occurred during the storage. To name just a few examples, samples 3, 7 (type 1) and 8 (type 3) did not contain ligularol (**16**). In addition, the major compound **48** stated for sample 7 (type 1) was not part of the extract according to GC-MS analysis. On the other hand, the results of samples 4 and 5 (type 2) were consistent with the findings in [10].

In summary *L. dictyoneura* is a highly diverse species containing non-furanoeremophilane derivatives and furanoeremophilane derivatives with different oxidation levels. It was also suggested that the transformation of eremophil-7(11)-en-8-one derivatives into furanoeremophilanes was taken place for ecological reasons as it is known that furanosesquiterpenes are used for defensive purposes. The conclusion that **2** was derived from **70** was made due to the fact that sample 8 (type 3) producing furanoeremophilane (**2**) was surrounded by samples producing derivatives of eremophil-7(11)-en-8-one and its isomer, 11-en-8-one (Samples 6 and 10).

3.1.7. L. tongolensis

L. tongolensis, belonging to the section Corymbosae, series Lapathifoliae, is widely distributed in the Hengduan Mountains, most of all in the Zhongdian County in Yunnan and inhabits various habitats like meadows, dry and sunny hillsides, and forest fringes, ranging from 2000 to 4000m in altitude [9].
Eight samples of *L. tongolensis*, collected in Yunnan and Sichuan provinces of China, were examined by GC-MS (Table 11).

No.	Sample	Place	Altitude (m)	Type	Major component
1	07 11	Liziping (Sichuan)	3280	1	unknown, m/z = 258
2	07 41	Wuxuhai (Sichuan)	3700	1	**124**
3	07 65	Pengbuxi (Sichuan)	3335	1	unknown, m/z = 258
4	07 76	Bajiaolou (Sichuan)	3440	1	unknown, m/z = 258
5	07 80	Yajiang (Sichuan)	3997	1	**124**
6	07 104	Jiawa (Sichuan)	3920	1	unknown, m/z = 258
7	09 46	Litang (Sichuan)	4260	2	**7**
8	09 103	Lianghe (Yunnan)	3534	2	**7**

Table 11. Samples of *L. tongolensis*. Samples 1 to 6 were dried, extracted with AcOEt and concentrated by the standard method, while samples 7 and 8 were extracted with EtOH without drying. Oily extract of sample 7 was obtained by the standard method.

It was observed that samples from 2007 showed different and complex chemical patterns in comparison to samples from 2009. For instance, sample 5 showed characteristic peaks at retention times 3.46, 4.60, 4.74, 5.92 and 8.02 minutes. They correspond to 2-methyl-2-butenoic acid (**121** or **122**), o-cymene (**115**), 4-methylhexanoic acid (**123**), cryptone (**120**) and eremophila-1(10),11-diene (**67**), respectively (Table 70). In addition to those peaks, sample 2 contained 3-methylpentanoic acid (**124**), β-pinene (**109**), β-phellandrene (**113**), α-curcumene (**105**) and β-caryophyllene epoxide (**99**) at retention times 3.97, 4.21, 4.64, 7.92 and 8.63 minutes, respectively (Table 71). Interestingly, both samples showed an unknown compound (Figure 129, m/z = 258) at retention time 13.07 minutes with a high percentage of relative distribution (Tables 70 and 71). On the other hand, compounds detected for sample 7 were α-

methylbutyric acid (**125**), angelic acid (**121**), β-methylvaleric acid (**124**), isobutylacetic acid (**126**), 1-phellandrene (**112**), o-cymene (**115**), β-phellandrene (**113**), 4-methylhexanoic acid (**123**), β-longipinene (**102**), β-bisabolene (**90**) and furanoeremophil-3-en-15,6α-olide (**7**, Figure 126, m/z = 244 = base $[M]^+$, 229 $[M\text{-}CH_3]^+$, 198 $[M\text{-}CO_2H]^+$, 187 $[M\text{-}C_4H_9]^+$, 159 $[C_{11}H_{11}O]^+$, 145 $[C_{10}H_9O]^+$) at 3.30, 3.81, 4.04, 4.11, 4.45, 4.62, 4.67, 4.83, 7.99, 8.08 and 11.64 minutes, respectively. In comparison to sample 7, sample 8 contained similar constituents. The results are shown in table 69.

The major compound of *L. tongolensis* type 2 was furanoeremophil-3-en-15,6α-olide (**7**), while those of type 1 was 2-methyl-2-butenoic acid (**121** or **122**) for sample 5 and 3-methyl-pentanoic acid (**124**) for sample 2, respectively.

It has been reported that the hydroxyl group at C_3 of furanoeremophilanes found in the plant are esterified with angelic acid for example [9]. It is obvious, that the presence of **121** in sample 5 may be due to the elimination of the acyloxy group at C_3 from **46**. In addition, it is likely that compound **7** was generated from **6** by elimination of a hydroxy or an acyloxy group at C_6 and attacking the carboxyl group at C_{15} [1] (Figure 9). Because of the instability of these compounds GC-MS may not be the appropriate method to examine the extracts.

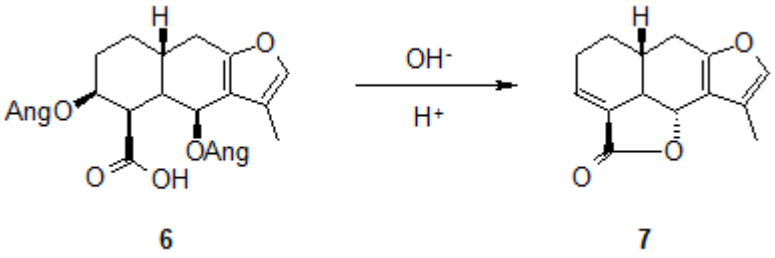

Figure 9. Plausible explanation for the formation of furanoeremophil-3-en-15,6α-olide (**7**) [38]

Interspecific variations were analyzed previously by comparing *L. tongolensis* with related species such as *L. cymbulifera*. While intraspecific diversity was present in *L. tongolensis*, *L. cymbulifera* was uniform with respect to their genetic and chemical composition. In addition, *L. tongolensis* inhabits a great variety of habitats, while *L. cymbulifera* usually grows in moist meadows. The absence of intraspecific diversity for *L. cymbulifera* could depend on the location. In contrast *L. tongolensis* seems to be in a process of differentiation through adapta-

tion to the environment [9]. Beside the differences between these two species it has been reported that 3,6,15-trioxygenated furanoeremophilanes were common to the section Corymbosae [9].

Compared to the results of *L. tongolensis*, similar compounds were found in *L. cymbulifera* by analyzing a sample, collected in 2009 in Litang (4334m), which is located in the Sichuan province of China. The GC-MS result suggest (Table 72) the presence of α-pinene (**108**), sabinene (**118**), β-pinene (**109**), p-cymene (**114**), β-thujene (**119**), eremophila-1(10),11-diene (**67**), eremophil-1(10)-en-11-ol (**80**, Figure 133, m/z = 222 $[M]^+$, 204 $[M-H_2O]^+$, 189 = base $[M-H_2O-CH_3]^+$), furanoeremophilan-10β-ol (**45**, Figure 134, m/z = 234 $[M]^+$, 216 $[C_{15}H_{20}O]^+$, 126, 109 = base $[C_7H_9O]^+$ RDA), ligularol (**16**), furanoeremophilan-15,6α-olide (**43**) and furanoeremophil-3-en-15,6α-olide (**7**, Figure 135, m/z = 244 = base $[M]^+$, 229 $[M-CH_3]^+$, 198 $[M-CO_2H]^+$, 187 $[M-C_4H_9]^+$, 121), respectively. Furthermore, the compound at 11.99 minutes was assumed to be 1-(methacryloyloxy)-ligularol (**29**, Figure 136, m/z = 318 $[M]^+$, 300 $[M-H_2O]^+$, 232 $[M-MeAcrOH]^+$, 124 $[C_7H_8O_2]^+$ RDA, 109 = base, 69 $[C_4H_5O]^+$, 41 $[C_3H_5]^+$) by comparing the reference EI mass spectrum of subspicatin B (**28**, Figure 149).

The major compounds of *L. cymbulifera* were furanoeremophil-3-en-15,6α-olide (**7**), followed by furanoeremophilan-10β-ol (**45**) at retention times 11.60 and 9.89 minutes, respectively. These results agree with the findings reported in [9].

3.1.8. L. przewalskii

L. przewalskii inhabits stream banks, grassy slopes, scrubs, forest margins and understories, ranging from 1100 to 4000m in altitude and is often cultivated in Europe for the use as an ornamental plant [21]. Two samples of *L. przewalskii* were collected in 2007 and two in 2009 in the Sichuan province of China and examined by GC-MS (Table 12). The results are shown in chapter 6.2.10.

No.	Sample	Place	Altitude (m)	Major component
1	07 79	Yajiang County	3663	**93**
2	07 62	Pengbuxi	3294	**92**
3	09 91	Zhuokeji	3037	**43**
4	09 106	Xiaojin/Baoxing	3185	**92**

Table 12. Samples of *L. przewalskii*. Roots were dried and extracted with AcOEt. Oily extracts of samples 1 and 2 were obtained by the standard method.

The major compound of sample 1 was euparin (**93**) at retention time 10.30 minutes, followed by eremophila-1(10),11-diene (**67**) and β-bisabolene (**90**) at 8.01 and 8.08 minutes, respectively (Table 73).

Sample 2 showed a more complex TIC profile, which contained 5,6-dimethoxy-2-(prop-1-en-2-yl)-benzofuran (**92**) as the major compound at retention time 9.87 minutes. Furthermore, β-caryophyllene (**98**), β-bisabolene (**90**), β-sesquiphellandrene (**106**), β-caryophyllene epoxide (**99**), euparin (**93**) and **91** were part of the extract (Table 74).

The major compound for sample 4 was the same as sample 2. Further common compounds were β-bisabolene (**90**) and euparin (**93**) (Table 76). In addition to these compounds β-pinene (**109**), p-cymene (**114**), α-longipinene (**103**), selina-4,11-diene (**87**) and γ-maaliene (**88**) were assigned to this extract.

For sample 3, furanoeremophilan-15,6α-olide (**43**) was detected at 11.40 minutes as the major compound, followed by 5,6-dimethoxy-2-(prop-1-en-2-yl)-benzofuran (**92**), 3-carene (**110**), α-phellandrene (**112**), α-pinene (**108**), valencene (**67**) and selina-4,11-diene (**87**), respectively.

By comparing the samples with each other, there exist similarities in chemical composition. Interestingly only sample 3 contained a furanoeremophilane derivative, while the others contained only constituents of the eremophilane and bisabolane type for instance.

Besides all this a small amount of monoterpene components were observed for the samples from 2009.

3.1.9. L. sagitta

L. sagitta belongs to the section Ligularia, series Ligularia and inhabits stream banks, grassy slopes, scrubs, forest margins and understories, ranging from 1300 to 4000m in altitude [12, 21]. Four samples of *L. sagitta* were collected in 2009 in the Sichuan province of China and analyzed by GC-MS (Table 13). The results are listed in chapter 6.2.11.

No.	Sample	Place	Altitude (m)	Major component
1	09 17	Reda	3392	**112**
2	09 52	Laima	3404	**112**
3	09 76	Tingka	3621	**112**
4	09 81	Niba	3283	**112**

Table 13. Samples of *L. sagitta.* Roots were dried and extracted with AcOEt.

In general, the major compound for all samples analyzed, was α-phellandrene (**112**) at retention time 4.42 minutes (Table 13). Furthermore, α-pinene (**108**), sabinene (**118**), β-pinene (**109**), 3-carene (**110**), o-cymene (**115**) and cis-ocimene (**111**) were found in samples of *L. sagitta* at retention times 3.81, 4.15, 4.20, 4.47, 4.58 and 4.66 minutes, respectively. In addition, samples of *L. sagitta* seems to have furanoeremophilane derivatives. It can be assumed that the EI mass spectra at retention times 11.58 and 12.25 minutes have the same carbon skeleton with different moieties. The compound at 11.58 minutes might have an methacryloyloxy-moiety (Figure 142, m/z = 316 $[M]^+$, 230 $[M\text{-}MeAcrOH]^+$, 69 = base $[C_4H_5O]^+$, 41 $[C_3H_5]^+$), while the other at 12.25 minutes have an angeloyloxy-moiety (Figure 143, m/z = 83 = base $[C_4H_7CO]^+$, 55 $[C_4H_7]^+$). Another reference that these compounds are of the furanoeremophilane type is that characteristic peaks at m/z 159 and 145 occurred [8].

According to the results of GC-MS analysis *L. sagitta* is uniform with regard to the chemical composition. This might be due to the fact, that the plants analyzed were collected at the same place and subsequently exposed to the same environment.

4. Summary and Conclusion

Several samples of the genus *Ligularia* have been examined with regard to their chemical composition using furanoeremophilane derivatives as chemical index. Therefore, extracts of *Ligularia sp.* were analyzed by GC-MS and LC-MS, respectively. In the majority of cases sesquiterpenoids of the eremophilane type were common. Prior to GC-MS analysis *Ehrlich*'s test on TLC was carried out (hexane-AcOEt 7:3) to detect the presence or absence of furanoeremophilane derivatives. Different colors occurred due to different substituents on the furanoeremophilane skeleton. It is empirically known that the substituent adjacent to the furan ring has an effect to the color of *Ehrlich*'s reaction. For instance the color of ligularol (**16**) is pink that of ligularone (**39**) orange and cacalol (**15**) is blue after 1 day of coloring procedure [3]. In contrast, sesquiterpenoids of the non-furanoeremophilane type (*Ehrlich* neg.) were detected with $Ce(SO_4)_2/H_2SO_4$ on TLC [4].

In comparison to MS direct measurements of *Ligularia* extracts, *Ehrlich*'s test can only reveal the presence or absence of furanoeremophilane derivatives. Thus the APCI mass spectrum of plant extracts were measured to give information about molecular and fragment ion peaks of different compounds prior to separation [7]. The resulting chemical profile of each extract could then be compared with the following LC-MS (APCI) data.

Due to the fact that this work is focusing on the volatile part of the extract GC-MS measurements of crude extracts were carried out. Approximately nine species of the genus *Ligularia* have been examined and their chemotypes determined. Intraspecific diversity was present for the species *virgaurea*, *subspicata*, *vellerea*, *pleurocaulis*, *dictyoneura* and *tongolensis* with different degrees of diversity. In contrast, *L. cyathiceps*, *przewalskii* and *sagitta* were assigned to be uniform. The absence of intraspecific variations should not be taken for granted since the chemical composition of plants sometimes depends on the location, plant development stage and environment. Therefore, more samples from different locations have to be examined with respect to their chemical and genetic composition to make a clear statement, whether the difference is based on the environment or genetics [11]. The same applies to those species, in which the

diversity in chemical composition was related to the geographical distribution of the samples [1].

While the two types of *L. pleurocaulis* had several compounds in common, *L. virgaurea* did not. Samples of *L. virgaurea* type 1 contained 6-oxygenated furanoeremophil-1(10)-en-2-ones (**8** and **9**) and their oxidized compounds (**13** and **14**), while type 2 contained ligularol (**16**) and its derivative (**17**) as major compounds [6]. In contrast, benzofuranosesquiterpenes (**94** and **15**) were detected for *L. virgaurea* type 3.

Furthermore, it can be said that *L. virgaurea* and *pleurocaulis* contained chemically distinct populations, while *L subspicata*, *dictyoneura*, and *kanaitzensis* [2] were rather continuous [32]. In the latter case they might be still in an early stage of differentiation from a type producing eremophilan-8-ones to a type containing furanoeremophilanes [5]. In general, C_1 and/or C_6 oxidized furanoeremophilane and eremophilan-8-one derivatives were detected as the major compounds in *L. subspicata*. C_1 oxidized compounds have been already isolated as minor compounds from samples of *L. vellerea* [1] and *dictyoneura* [10], but not detected via GC-MS for the present study.

The furanoeremophilane constituents obtained from *L. vellerea* were dioxygenated at C_6 and C_{15} [1]. Lactonization from 6β-acyloxy-furanoeremophilan-15-oic acid to a 6α,15-olide occurred due to elimination of an acyloxy group at C_6 and attacking the carboxyl group at C_{15} (Figure 9) [1]. Furthermore, there have been reports about the isolation of 6,15-dioxygenated enol lactones and the consideration that these compounds were decomposition products of the labile furanoeremophilanes after the drying process of the roots [1].

The furanoeremophilane components obtained from *L. vellera* were also found in *L. tongolensis*, *cymbulifera* and *atroviolacea*, belonging to the section Corymbosae, series Lapathifoliae. However, the oxidation level at C_3 was different, while the collection locality (Zhongdian area in northwestern Yunnan province of China) was the same [1]. Due to the thermal unstability of these compounds separation by GC was not available and the suggested characteristic 3,6,15-trioxygenated furanoeremophilanes for the section Corymbosae not detected [1,39].

In addition, the 6,15-dioxygenated eremophilanes and furanoeremophilan-15,6α-olide (**43**) found in *L. vellerea*, were also observed in *L. przewalskii* [15].

However, the major compounds found in *L. przewalskii* were benzofuranosesquiterpene derivatives (**92** and **93**). The presence of these compounds is consistent with the results reported earlier by Jia [14] and Bohlmann [31] as they have reported the isolation of similar compounds from the same species. Benzofuranosesquiterpene derivatives were also common in *L. cyathiceps*, *L. tsangchanensis* [13] and *L. virgaurea* type 3. Cacalol (**15**) was predominant in all samples. It was assigned to be the major compound for *L. virgaurea* type 3 and *L. tsangchanensis* [13], whereas *L. cyathiceps* contained 1,10β-epoxy-6β-isobutanoyloxy-furanoeremophilan-9-one (**35**) as the major compound, followed by **15**.

Besides all this other sesquiterpenoid components like β-bisabolene (**90**) or caryophyllene (**97** and **98**) were detected by GC-MS.

Interestingely, monoterpene components were obtained for samples of *L. virgaurea*, *pleurocaulis* and *sagitta*. The monoterpene composition consists of α-pinene (**108**), β-pinene (**109**), β-myrcene (**107**), α-phellandrene (**112**), β-phellandrene (**113**), o-cymene (**115**), p-cymene (**114**), cis-ocimene (**111**), 3-carene (**110**), α-terpinolene (**116**), sabinene (**118**) and limonene (**117**) for extracts of fresh roots collected in 2009. Some samples of *L. virgaurea* type 1 showed β-pinene (**109**) or cis-ocimene (**111**) as the major compound (Table 5). Previous reports of Bohlmann and co-workers [31] showed that various *Ligularia* sp. contained **111** most of all in aerial parts of the plant as well as in roots. Furthermore, α-phellandrene (**112**) was detected as the major compound in *L. sagitta* (Table 13). It has to be noticed, that these compounds can easily evaporate or rearrange during the drying, extraction, analysis, concentration and isolation procedure, respectively. For example, β-pinene (**109**) can be easily converted into β-myrcene (**107**) under high temperatures. However, the absence of monoterpenes in some samples could be due to the fact that evaporation has taken place during handling procedures. But this might not be only a problem for monoterpenes as it is known that furano-components are labile enough to decompose to a lactone system. The instability of these compounds is due to the presence of an electron-rich trisubstituted double enolether system, which decomposes easily under the presence of acids [33]. An example is given for *L. virgaurea* type 1 containing furanoeremophilanes of the 1(10)-en-2-one system in which the hydrogen at C_9 is highly acidic [6]. Under these conditions the

furano-components of *L. virgaurea* may decompose as reactions with electron deficient compounds easily occur [33]. In addition, ester hydrolysis under acidic and basic conditions may be the reason for the presence of highly unstable compounds in *L. tongolensis*. The presence of organic carboxyclic acids unbounded to the furanoeremophilane skeleton and the acidic hydrogen at C_4 of compound **46** probably catalyzes the reactions.
Besides all this the *retro*-Diels Alder reaction induced by EI-MS was observed occasionally for furanoeremophilane derivatives. This case was previously reported by Nagano and co-workers for furanoeremophilanes with an oxygen function such as hydroxyl, acyloxyl, and alkoxyl moiety on ring B. This fragmentation pattern was not predominant in all cases as sometimes peaks at m/z 159 or m/z 159 and 145, containing the furan moiety occurred [8].

In summary, sesquiterpenoids of the furanoeremophilane type were found to be predominant in the genus *Ligularia*. Most of them were esterified with organic acids such as angelic acid. The chemical composition is dependent on the plant material (fresh or dried roots), environment, soil condition, genotype, climate and method of extraction. In addition, furano-components are known to be unstable under acidic conditions, high temperature and oxygen. Further chemicals such as monoterpenes were found in extracts of fresh roots. Most of them are known for turpentine like smell, which might be the reason for the characteristic fragrance of the plant roots.
The compounds detected and listed in the tables are suggestions (chapter 6.2). Further phytochemical analysis would be necessary to prove the assumptions.
The present work is based on the analysis of crude extracts of the *Ligularia sp.* and delivers a first insight what the phytochemical profile of the given extract might be. That should ease further research on newly collected plants and help to find an overview about inter- and intraspecific diversity of this genus. Furthermore, it is recommended to standardize the extracts to be able to compare the samples with each other with respect to their amount.

5. References

1. Tori, M., Nakamizo, H., Mihara, K., Sato, M., Okamoto, Y., Nakashima, K., Tanaka, M., Saito, Y., Sono, M., Gong, X., Shen, Y., Hanai, R., Kuroda, C. Chemical and genetic diversity of *Ligularia vellerea* in Yunnan, China. Phytochemistry 69, 1158-1165 (2008).
2. Tori, M., Watanabe, A., Matsuo, S., Okamoto, Y., Tachikawa, K., Takaoka, S., Gong, X., Kuroda, C., Hanai, R. Diversity of *Ligularia kanaitzensis* in sesquiterpenoid composition and neutral DNA sequences. Tetrahedron 64, 4486-4495 (2008).
3. Kuroda, C., Nishio, E. Substituent Effect in Color of *Ehrlich*'s Test of Tetrahydrobenzofuran. Natural Product Communications, Vol. 2, No. 5, 581-585 (2007).
4. Nagano, H., Torihata, A., Matsushima, M., Hanai, R., Saito, Y., Baba, M., Tanio, Y., Okamoto, Y., Takashima, Y., Ichihara, M., Gong, X., Kuroda, C., Tori, M. Chemical and Genetic Study of *Ligularia cyathiceps* in Yunnan Province of China. Helvetica Chimica Acta, Vol. 92, 2071-2081 (2009).
5. Tori, M., Okamoto, Y., Tachikawa, K., Mihara, K., Watanabe, A., Sakaoku, M., Takaoka, S., Tanaka, M., Gong, X., Kuroda, C., Hattori, M., Hanai, R. Isolation of new eremophilane-type sesquiterpenoids, subspicatins A-D and subspicatolide from *Ligularia subspicata*, and chemical and genetic diversity of the species. Tetrahedron 64, 9136-9142 (2008).
6. Tori, M., Honda, K., Nakamizo, H., Okamoto, Y., Sakaoku, M., Takaoka, S., Gong, X., Shen, Y., Kuroda, C., Hanai, R. Chemical constituents of *Ligularia virgaurea* and its diversity in southwestern Sichuan of China. Tetrahedron 62, 4988-4995 (2006).
7. Okamoto, Y., Saito, Y., Kuroda, C., Hanai, R., Gong, X., Tori, M. Direct MS Measurement of the Extract of *Ligularia virgaurea* collected in Yunnan and Sichuan Provinces of China. Phytochemical Analysis, Vol. 21 (6), 513-523 (2010).
8. Nagano, H., Kuroda, C., Moriyama, Y., Tsuyuki, T., Takahashi, T. Mass Spectra of Furanoeremophilane Derivates. Bull. Chem. Soc. Jpn., 55, 1221-1227 (1982)

9. Hanai, R., Gong, X., Tori, M., Kondo, S., Otose, K., Okamoto, Y., Nishihama, T., Murota, A., Shen, Y., Wu, S., Kuroda, C. Chemical and Genetic Study of *Ligularia tongolensis*, *Ligularia cymbulifera*, and *Ligularia atroviolacea* in the Hengduan Mountains of China. Bull. Chem. Soc. Jpn. 78, 1302-1308 (2005).
10. Nagano, H., Iwazaki, Y., Matshushima, M., Sato, M., Gong, X., Shen, Y., Hirota, H., Kuroda, C., Hanai, R. High Diversity of *Ligularia dictyoneura* in Chemical Composition and DNA Sequence. Chemistry & Biodiversity, Vol. 4, 2874-2888 (2007).
11. Nagano, H., Iwazaki, Y., Gong, X., Shen, Y., Kuroda, C., Hanai, R. Chemical and Genetic Differentiation of *Ligularia pleurocaulis* in Northwestern Yunnan and Southwestern Sichuan Provinces of China. Bull. Chem. Soc. Jpn, Vol. 79, No. 2, 300-304 (2006).
12. Liu, S.-J., Liu, J.-Q., Zhang, M., Zhang, C.-F., Wang, Z.-T. Second metabolites of *Ligularia sagitta*. Biochemical Systematics and Ecology 35, 245-247 (2007)
13. Torihata, A., Hanai, R., Gong, X., Shen, Y., Kuroda, C. Chemical and Genetic Differentiation of *Ligularia tsangchanensis* in Yunnan and Sichuan Provinces of China. Chemistry & Biodiversity - Vol. 4, 500-506 (2007)
14. Jia, Z., Zhao, Y., Four new Furans from the roots of *Ligularia przewalskii*. JPN – Vol. 57, No.1, pp.146 –150 (1994)
15. Zhao, Y., Jia, Z., Peng, H. Eight new Eremophilane derivatives from the roots of *Ligularia przewalskii*. JPN - Vol. 58, No. 9, pp.1358 – 1364 (1995)
16. http://hengduan.huh.harvard.edu/fieldnotes (01.10.2011)
17. http://arboretum.harvard.edu/news-events/archived-news/biodiversity-of-the-hengduan-mountain-region-china/ (01.10.2011)
18. http://www.biodiversityhotspots.org/xp/hotspots/china/Pages/default.aspx (01.10.2011)
19. Zhang, Z., Fei, D., Jia, Z. Virgaurols A–D: Novel Asymmetric Eremophilane Dimers from the Roots of *Ligularia virgaurea*, Bull. Chem. Soc. Jpn. Vol. 81, No. 8, 1007-1011 (2008)
20. Fei, D., Wu, Q., Li, S., Gao, K. Two New Asymmetric Sesquiterpene Dimers from the Rhizomes of *Ligularia muliensis*. Chem. Pharm. Bull. 58(4) 467-469 (2010)

21. Wu, Z. Y., Raven, P. H., Hong, D. Y. Eds. *Flora of China. Vols. 20-21 (Asteraceae)*. Science Press, Beijing, and Missouri Botanical Garden Press, St. Louis. In Preparation. (24.11.2011)
22. http://chemwiki.ucdavis.edu/Analytical_Chemistry/Instrumental_Analysis/Gas_Chromatography (08.10.2011)
23. http://www.pharmxplorer.at/lernelemente/?leid=81 (09.10.11)
24. Gerhard Schomburg, Gaschromatographie. Grundlagen, Praxis, Kapillartechnik. Weinheim: VCH. 1987, ISBN 3-527-26461-2
25. Breitmaier. E. Terpenes: Flavors, Fragances, Pharmaca, Pheromones. WILEY-VCH Verlag GmbH & Co. KGaA, Weinheim, 2006
26. Jia, Z., Chen, H. Benzofuransesquiterpenes from *Ligularia virgaurea*. Phytochemistry, Vol. 30, No. 9, pp. 3132-3134 (1991).
27. http://pss.uvm.edu/pss123/perligul.html (20.11.2011)
28. http://www.botgarten.uni-tuebingen.de/tiki/tiki-index.php?page=Ligularia (20.11.2011)
29. Yang, J., Wang, R., Shi, Y. Phytochemicals and biological activities of *Ligularia* species. Nat. Prod. Bioprospect. 1, 1-24 (2011).
30. http://massfinder.com/wiki/MassFinder_4 (24.11.2011)
31. Bohlmann, F., Ehlers, D., Zdero, C., Grenz, M. Natürlich vorkommende Terpen-Derivate, 98: Über die Inhaltsstoffe der Gattung *Ligularia*. Chem. Ber. 110, 2640-2648 (1977)
32. Saito, Y., Hattori, M., Iwamoto, Y., Takashima, Y., Mihara, K., Sasaki, Y., Fujiwara, M., Sakaoku, M., Shimizu, A., Chao, X., Kuroda, C., Gong, X., Hanai, R., Tori, M. Overlapping chemical and genetic diversity in *Ligularia lamarum* and *Ligularia subspicata*. Isolation of ten new eremophilanes and a new seco-bakkane compound. Tetrahedron 67, 2220-2231 (2011)
33. Iida, K., Mitani, M. Kuroda, C. Fixation of Natural Furanoeremophilane by Diels-Alder Reaction. Bull. Chem. Soc. Jpn. Vol. 80, No. 5, 966-971 (2007)
34. Nagano, H., Moriyama, Y., Tanahashi, Y., Takahashi, T. Farfugin A and B, new sequiterpenes from Farfugium japonicum. Chemistry Letters, pp. 13-16 (1972)
35. Bohlmann, F., Zdero, C., Rao, N. Terpenderivate aus höheren Pflanzen, XIX: Neue Furansesquiterpene aus *Euryops*-Arten. Chem. Ber. 105, 3525-3531 (1972)

36. Bohlmann, F., Zdero, C. Neue Furanoeremophilane und andere Sesquiterpene aus Vertretern der Gattung *Euryops*. Phytochemistry 17, 1135-1153 (1978)
37. Bohlmann, F., Zdero, C., Grenz, M. Natürlich vorkommende Terpen-Derivate, XXXIX. Über die Inhaltsstoffe der Gattung *Euryops*. Chem. Ber. 107, 8, 2730-2759 (1974)
38. Bohlmann, F., Zdero, C., Grenz, M. Natürlich vorkommende Terpen-Derivate, XLII. Neue Sesquiterpene der Gattung *Othonna*. Chem. Ber. 107, 12, 3928-3945 (1974)
39. Kuroda, C., Murae, T., Tada, M., Nagano, H., Tsuyuki, T., Takahashi, T. 3β,6β-Bis(acyloxy)furanoeremophilan-14-als and -14-oic acids from *Syneilesis palmata* (THUNB.) MAXIM. Bull. Chem. Soc. Jpn., 55, 1228-1233 (1982)

6. Appendix

6.1. Chemical constituents of *Ligularia* sp.

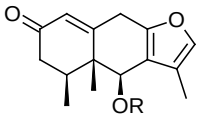

8 (virgaurenone A) R = Ang

9 (virgaurenone B) R = Ac

10 (virgaurenone C) R = H

11 R = C(=O)Me_2

12 R = MeAcr

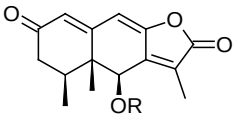

13 (virgaurenolide A) R = Ang

14 (virgaurenolide B) R = Ac

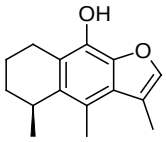

15 (cacalol)

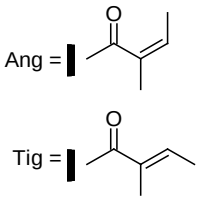

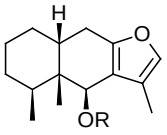

16 (ligularol) R = H

17 R = Et

18 R = Me

19 R = Ang

20 R = MeBu

21 R = C(=O)$CHMe_2$

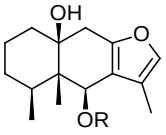

22 R = H

23 R = Ac

24 R = Ang

25 R = MeBu

26 R = C(=O)$CHMe_2$

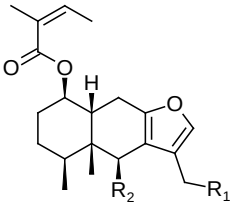

27 (subspicatin A) R_1 = OH, R_2 = H

28 (subspicatin B) R_1 = H, R_2 = OH

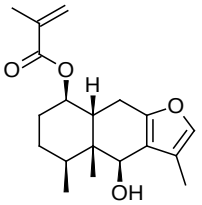

29

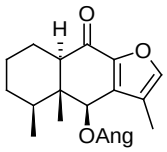

127

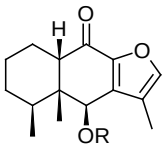

30 R = Ang

31 R = C(=O)$CHMe_2$

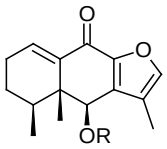

32 R = Ang

33 R = C(=O)$CHMe_2$

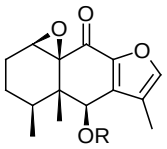

34 R = Ang

35 R = C(=O)$CHMe_2$

36 R = C(=O)Et

128 R = C(=O)$CH_2CH(CH_3)_2$

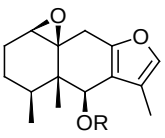

37 R = Ac

38 R = C(=O)$CHMe_2$

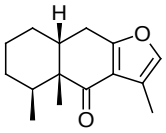

39

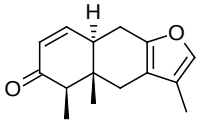

40

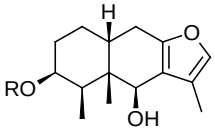

41 R = MeAcr

42 R = Ang

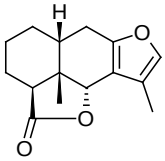

43

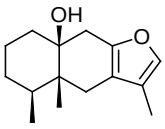

45

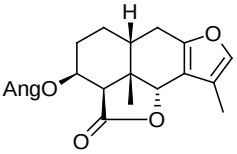

46

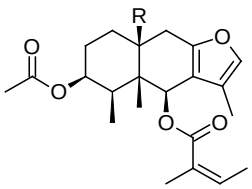

47 R = H

48 R = OH

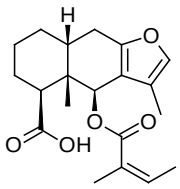

49

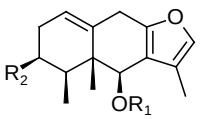

50 R_1 = Ang, R_2 = OH

51 R_1 = Tig, R_2 = OH

52 R_1 = H, R_2 = OAng

129 R_1 = C(=O)$CHMe_2$, R_2 = OH

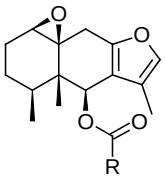

53 R = $HOCH_2C(=CH_2)$

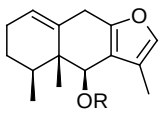

54 R = H
55 R = Ac
56 R = Ang
44 R = Tig

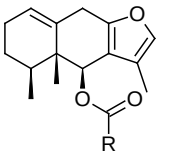

57 R = $HOCH_2C(=CH_2)$

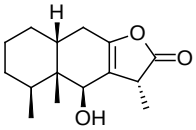

58 (eremofarfugin C)

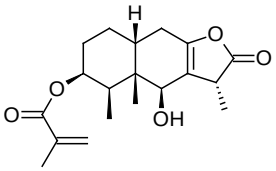

59 (eremofarfugin B)

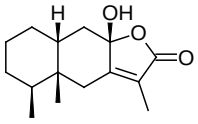

60

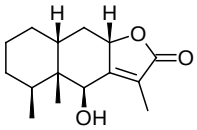

61

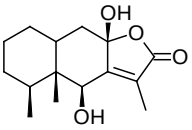

62

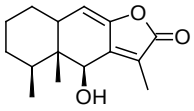

63

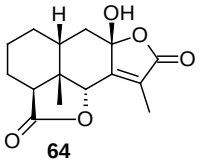

64

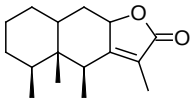

65

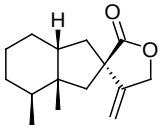

66 (fukinanolide)

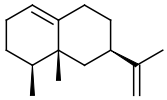

67

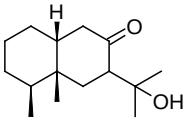

68

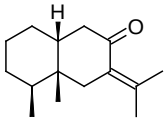

69 (fukinone)

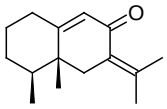

70 (dehydrofukinone)

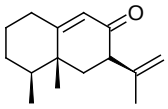

71 (alloeremophilone)

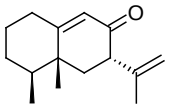

72

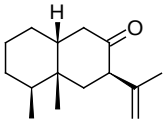

73

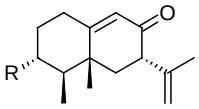

74 (petasin) R = OAng
75 R = OTig

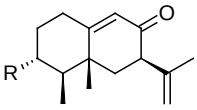

76 (neopetasin) R = OAng

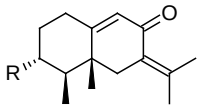

77 (isopetasin) R = OAng

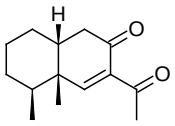

78

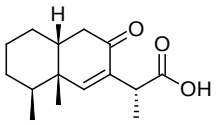

79

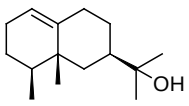

80

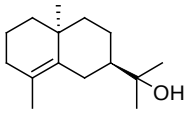

81

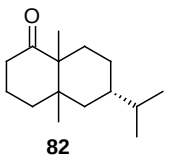

82

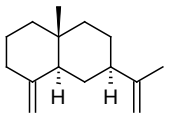

83

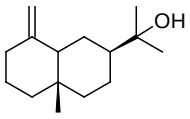

84

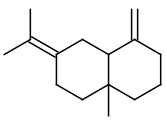

85

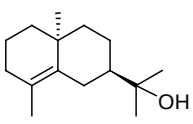

86

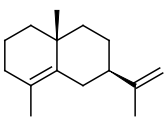

87

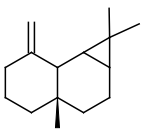

88

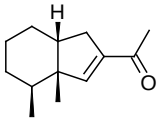

89

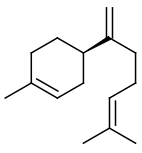

90

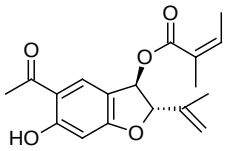

91

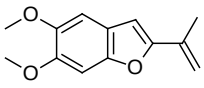

92

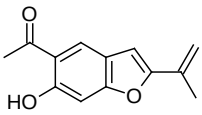

93 (euparin)

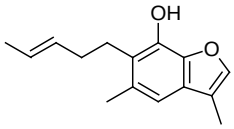

94

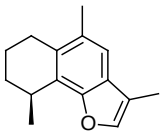

95 (farfugin A)

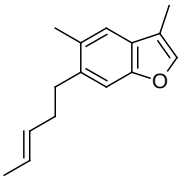

96 (farfugin B)

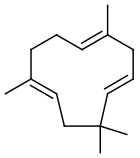

97

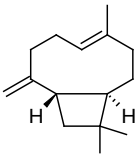

98

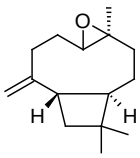

99

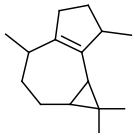

100

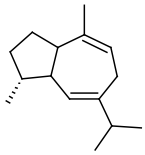

101

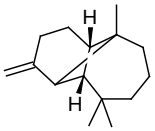

102

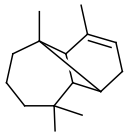

103

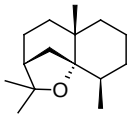

104

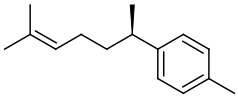

105

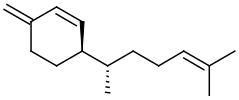

106

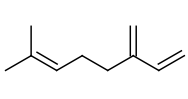

107

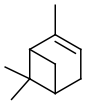

108

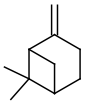

109

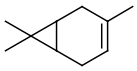

110

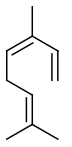

111

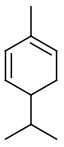

112

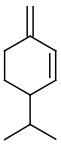

113

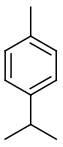

114

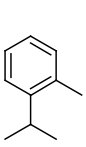

115

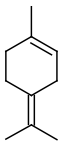

116

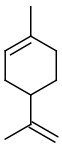

117

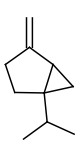

118

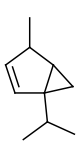

119

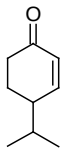

120

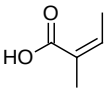

121

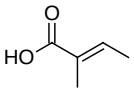

122

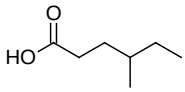

123

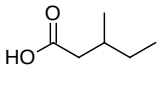

124

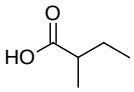

125

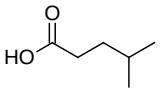

126

6.2. GC-MS results

6.2.1. L. virgaurea

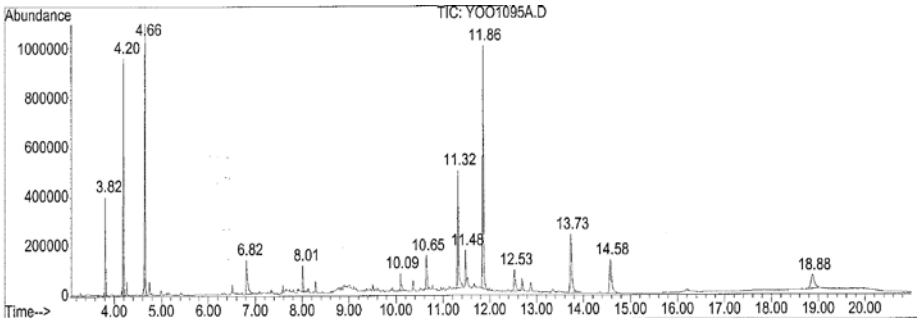

Figure 10. TIC of *L. virgaurea* type 1 (Sample 12)

RT (min)	Area %	Compound	Source
3.816	5.956	α-Pinene	Wiley
4.198	14.691	β-Pinene	Wiley
4.658	15.734	cis-Ocimene	Wiley
6.816	4.227	2-Methoxy-4-vinylphenol	Wiley
8.014	1.660	Eremophila-1(10),11-diene	Wiley
10.093	1.685	unknown, m/z = 207	
10.647	2.849	Palmitic acid ethyl ester	Wiley
11.317	10.104	unknown, m/z = 228	
11.484	2.114	9,12-Octadecadienoic acid, ethyl ester	Wiley
11.858	**19.387**	Virgaurenone B	Literature [6]
12.531	2.834	unknown, m/z = 244	
13.733	8.523	Virgaurenone A	Literature [6]
14.578	6.047	Virgaurenolide B	MassFinder
18.880	4.189	Virgaurenolide A	Literature [6]

Table 14. GC-MS result of *L. virgaurea* type 1 (Sample 12)

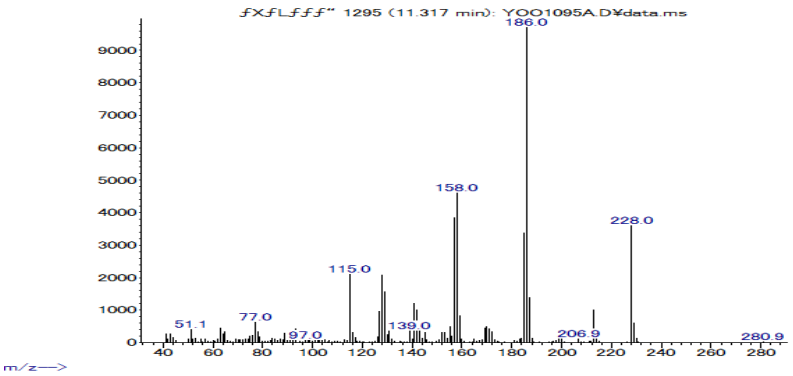

Figure 11. EI mass spectrum of *L. virgaurea* type 1 at RT 11.317 min. (Sample 12)

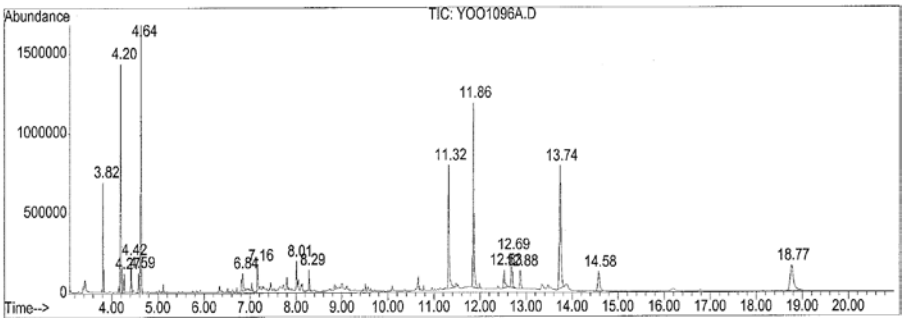

Figure 12. TIC of *L. virgaurea* type 1 (Sample 13)

RT (min)	Area %	Compound	Source
3.818	6.265	α-Pinene	Wiley
4.201	12.174	β-Pinene	Wiley
4.273	0.899	β-Myrcene	Wiley
4.420	1.572	α-Phellandrene	Wiley
4.588	1.043	p-Cymene	Wiley
4.638	**15.670**	cis-Ocimene	MassFinder
6.840	1.597	unknown, m/z = 150	
7.164	1.370	unknown, m/z = 207	
8.013	1.377	Eremophila-1(10),11-diene	Wiley
8.286	1.219	unknown, m/z = 204	
11.318	9.886	*unknown*, m/z = 228	
11.858	14.664	Virgaurenone B	Literature [6]
12.526	2.031	unknown, m/z = 244	
12.691	2.958	6β-OiBu-furanoeremophil-1(10)-en-2-one	
12.875	1.720	unknown, m/z = 288	
13.739	15.437	Virgaurenone A	Literature [6]
14.578	3.132	Viraurenolide B	MassFinder
18.767	6.988	Virgaurenolide A	Literature [6]

Table 15. GC-MS result of *L. virgaurea* type 1 (Sample 13)

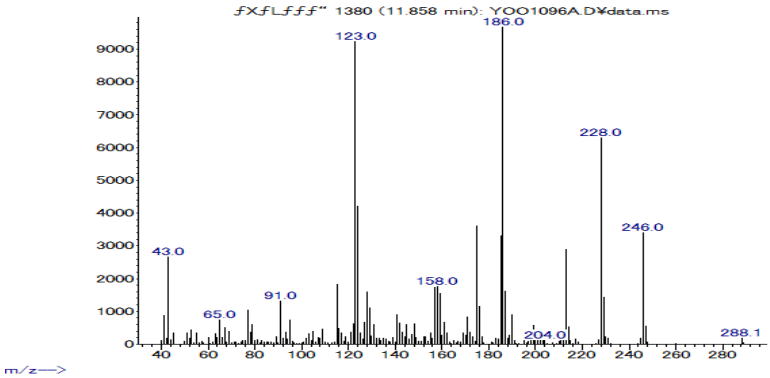

Figure 13. EI mass spectrum of *L. virgaurea* type 1 at RT 11.858 min. (Sample 13)

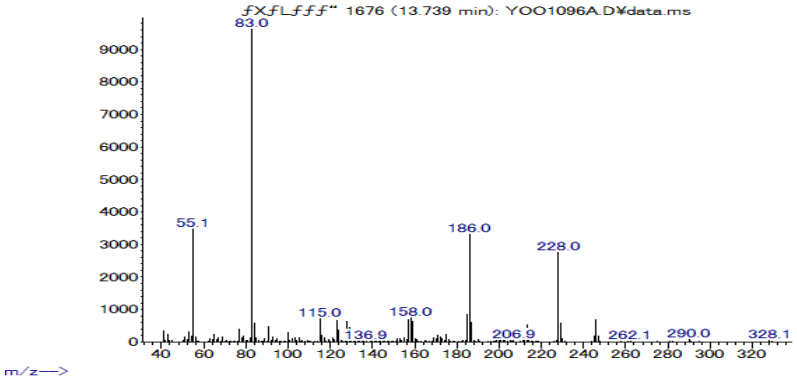

Figure 14. EI mass spectrum of *L. virgaurea* type 1 at RT 13.739 min. (Sample 13)

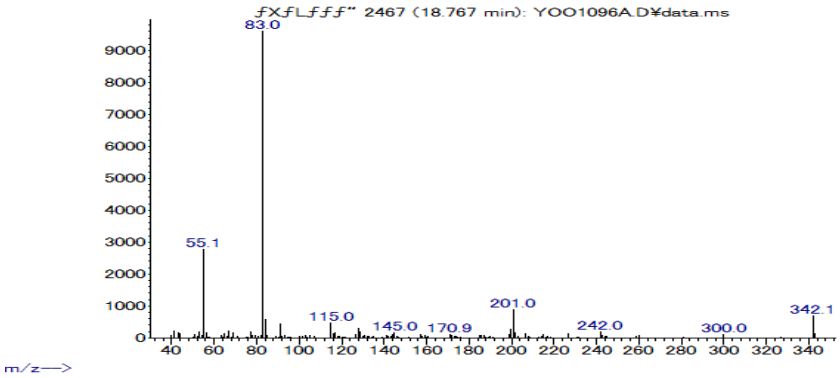

Figure 15. EI mass spectrum of *L. virgaurea* type 1 at RT 18.767 min. (Sample 13)

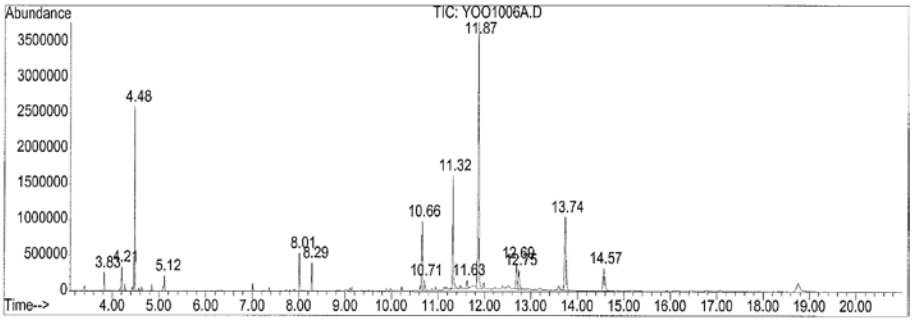

Figure 16. TIC of *L. virgaurea* type 1 (Sample 4)

RT (min)	Area %	Compound	Source
3.829	1.457	α-Pinene	Wiley
4.209	1.785	β-Pinene	Wiley
4.479	14.872	3-Carene	Wiley
5.118	1.461	α-Terpinolene	Wiley
8.015	2.892	Eremophila-1(10),11-diene	Wiley
8.287	2.115	unknown, m/z = 222	
10.663	5.866	unknown, m/z = 274	
10.714	1.031	1-Hexadecanol, acetate	Wiley
11.320	11.627	unknown, m/z = 228	
11.629	0.984	unknown, m/z = 306	
11.868	**32.104**	Virgaurenone B	Literature [6]
12.690	3.543	6β-OiBu-FE-1(10)-en-2-one	
12.747	2.966	6β-OMeAcr-FE-1(10)-en-2-one	
13.742	12.339	Virgaurenone A	Literature [6]
14.574	4.958	Viraurenolide B	MassFinder

Table 16. GC-MS result of *L. virgaurea* type 1 (Sample 4)

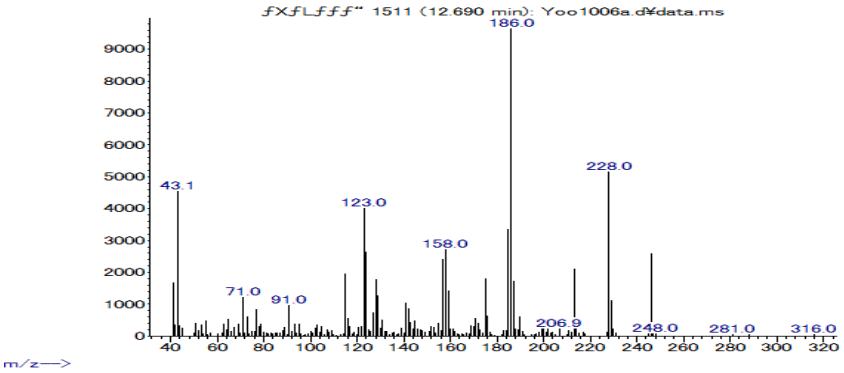

Figure 17. EI mass spectrum of *L. virgaurea* type 1 at RT 12.690 min. (Sample 4)

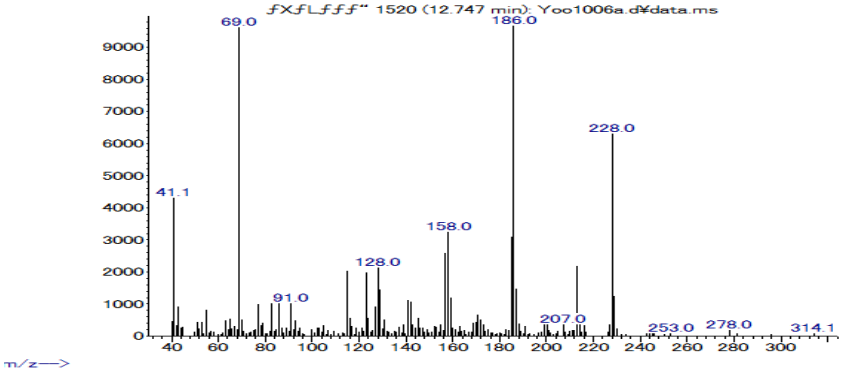

Figure 18. EI mass spectrum of *L. virgaurea* type 1 at RT 12.747 min. (Sample 4)

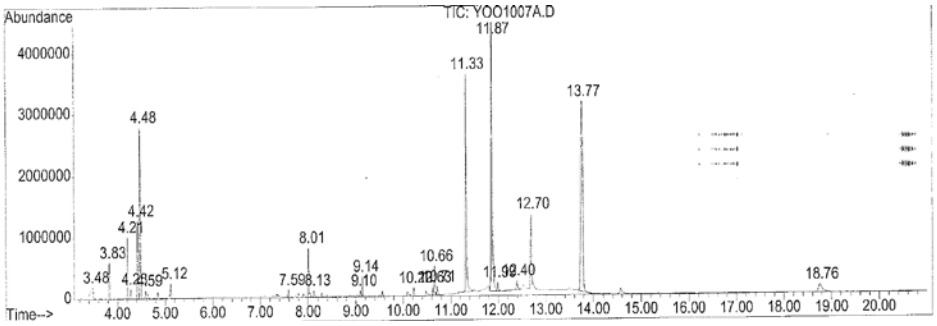

Figure 19. TIC of *L. virgaurea* type 1 (Sample 2)

RT (min)	Area %	Compound	Source
3.480	2.297	2-Methyl-2-butenoic acid	Wiley
3.828	1.605	α-Pinene	Wiley
4.208	3.111	β-Pinene	Wiley
4.278	0.465	β-Myrcene	Wiley
4.425	3.583	α-Phellandrene	Wiley
4.478	7.842	3-Carene	Wiley
4.591	0.328	o-Cymene	Wiley
5.118	0.700	α-Terpinolene	Wiley
7.592	0.367	β-Caryophyllene	Wiley
8.014	2.752	Eremophila-1(10),11-diene	Wiley
8.127	0.438	unknown, m/z = 220	
9.101	0.350	unknown, m/z = 220	
9.140	1.009	unknown, m/z = 216	
10.225	0.430	1-Pentadecanol, acetate	Wiley
10.626	0.428	unknown, m/z = 260	
10.661	1.581	unknown, m/z = 260	
10.715	0.620	1-Hexadecanol, acetate	Wiley
11.327	14.611	unknown, m/z = 228	
11.871	22.661	Virgaurenone B	Literature [6]
11.993	0.646	unknown, m/z = 281	
12.394	0.940	unknown, m/z = 246	
12.696	5.589	6β-OiBu-FE-1(10)-en-2-one	
13.771	**25.487**	Virgaurenone A	Literature [6]
18.763	2.160	Virgaurenolide A	Literature [6]

Table 17. GC-MS result of *L. virgaurea* type 1 (Sample 2)

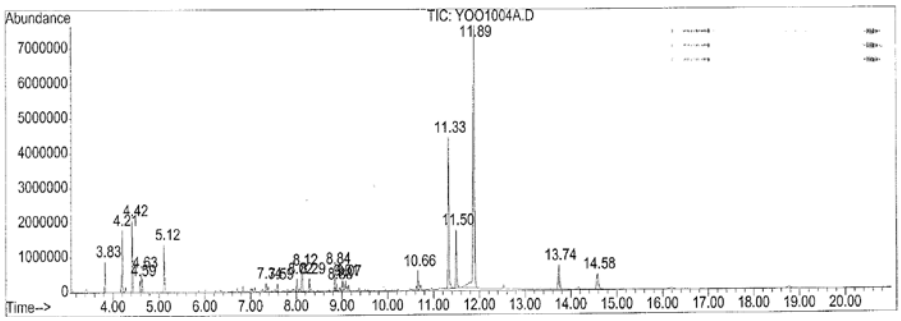

Figure 20. TIC of *L. virgaurea* type 1 (Sample 5)

RT (min)	Area %	Compound	Source
3.829	2.129	α-Pinene	Wiley
4.207	5.184	β-Pinene	Wiley
4.425	4.629	α-Phellandrene	Wiley
4.591	0.805	o-Cymene	Wiley
4.629	1.614	Limonene	Wiley
5.118	3.157	α-Terpinolene	Wiley
7.342	0.553	Selina-4,11-diene	MassFinder
7.592	0.591	β-Caryophyllene	Wiley
8.016	1.167	Eremophila-1(10), 11-diene	Wiley
8.120	2.981	unknown, m/z = 222	
8.287	0.866	unknown, m/z = 222	
8.844	1.641	unknown, m/z = 222	
8.882	0.611	unknown, m/z = 222	
9.012	1.073	unknown, m/z = 222	
9.075	0.615	unknown, m/z = 222	
10.661	1.489	unknown, m/z = 274	
11.331	15.958	unknown, m/z = 228	
11.502	5.746	Virgaurenone C	Literature [6]
11.889	**42.404**	Virgaurenone B	Literature [6]
13.740	3.639	Virgaurenone A	Literature [6]
14.580	3.148	Virgaurenolide B	MassFinder

Table 18. GC-MS result of *L. virgaurea* type 1 (Sample 5)

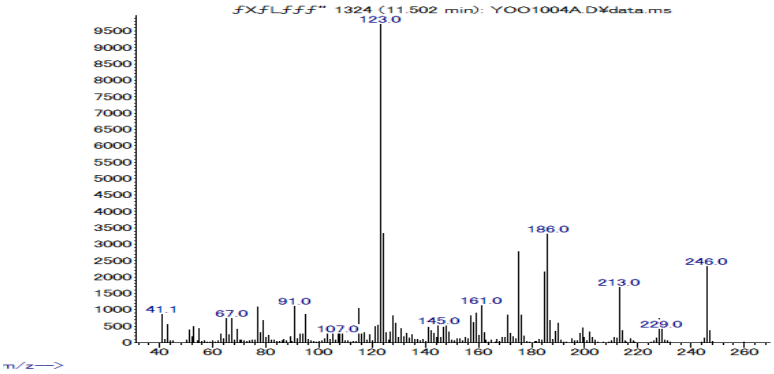

Figure 21. EI mass spectrum of *L. virgaurea* type 1 at RT 11.502 min. (Sample 5)

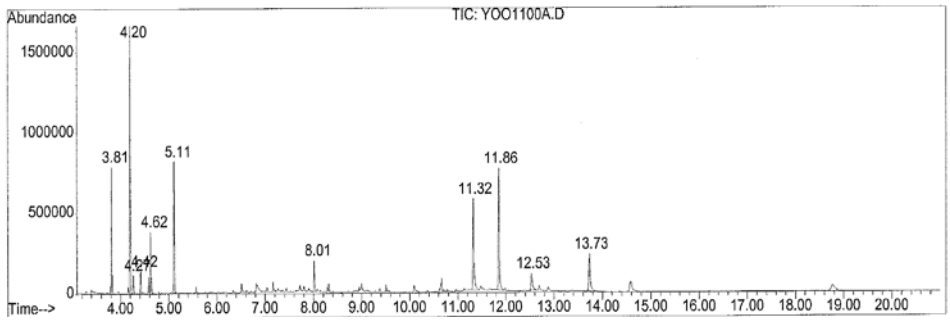

Figure 22. TIC of *L. virgaurea* type 1 (Sample 17)

RT (min)	Area %	Compound	Source
3.815	11.363	α-Pinene	Wiley
4.197	**23.744**	β-Pinene	Wiley
4.270	1.627	β-Myrcene	Wiley
4.417	2.013	α-Phellandrene	Wiley
4.621	6.671	α-Limonene	Wiley
5.113	11.053	α- Terpinolene	Wiley
8.013	3.165	Eremophila-1(10),11-diene	Wiley
11.320	13.215	unknown, m/z = 228	
11.856	15.463	Virgaurenone B	Literature [6]
12.530	3.807	unknown, m/z = 244	
13.733	7.879	Virgaurenone A	Literature [6]

Table 19. GC-MS result of *L. virgaurea* type 1 (Sample 17)

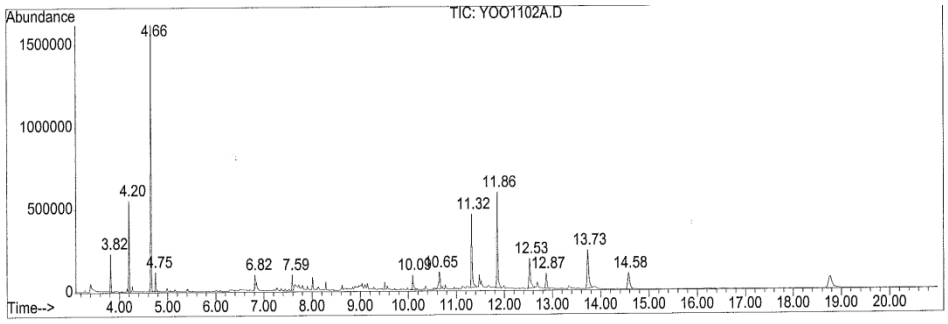

Figure 23. TIC of *L. virgaurea* type 1 (Sample 19)

RT (min)	Area %	Compound	Source
3.818	3.615	α-Pinene	Wiley
4.200	8.884	β-Pinene	Wiley
4.659	**28.093**	cis-Ocimene	Wiley
4.751	1.844	β-cis-Ocimene	Wiley
6.818	1.305	2-Methoxy-4-vinylphenol	Wiley
7.591	1.480	β-Caryophyllene	Wiley
10.093	2.352	unknown, m/z = 212	
10.647	4.041	Palmitic acid ethyl ester	Wiley
11.320	11.264	unknown, m/z = 228	
11.856	13.277	Virgaurenone B	Literature [6]
12.527	6.669	unknown, m/z = 244	
12.871	2.871	unknown, m/z = 288	
13.733	9.330	Virgaurenone A	Literature [6]
14.576	4.975	Virgaurenolide B	MassFinder

Table 20. GC-MS result of *L.virgaurea* type 1 (Sample 19)

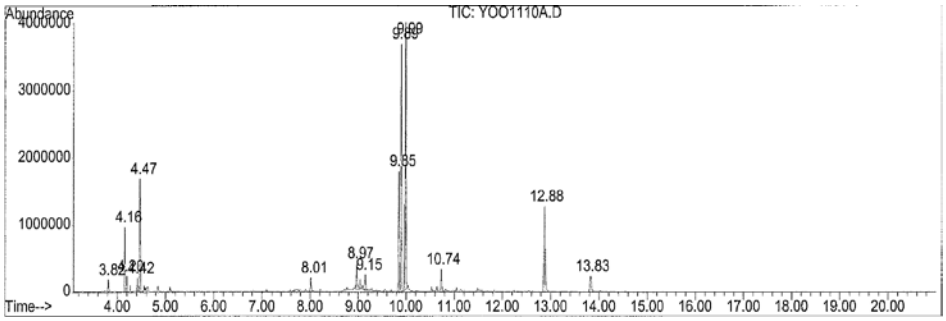

Figure 24. TIC of *L. virgaurea* type 2 (Sample 27)

RT (min)	Area %	Compound	Source
3.818	1.096	α-Pinene	Wiley
4.157	5.205	Sabinene	Wiley
4.200	1.362	β-Pinene	Wiley
4.418	0.993	α-Phellandrene	Wiley
4.471	9.818	3-Carene	Wiley
8.013	1.297	Eremophila-1(10),11-diene	Wiley
8.972	2.858	unknown, m/z = 236	
9.150	1.631	unknown, m/z = 216	
9.849	10.986	Ligularol ethyl ether	Literature [6]
9.894	22.153	*unknown*, m/z = 262	
9.988	**24.924**	Ligularol	MassFinder
10.737	2.129	FE-6β,10β-diol	Literature [6], [8]
12.875	12.635	6-OH-3-OMeAcr-FE	
13.828	2.913	6-OH-3-OAng-FE	

Table 21. GC-MS result of *L. virgaurea* type 2 (Sample 27)

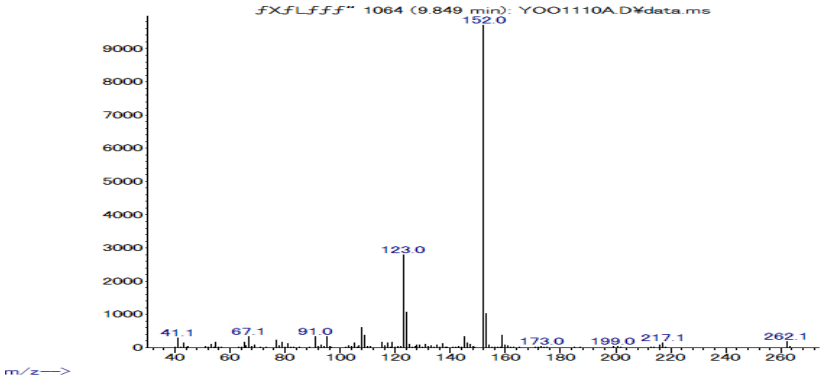

Figure 25. EI mass spectrum of *L. virgaurea* type 2 at RT 9.849 min. (Sample 27)

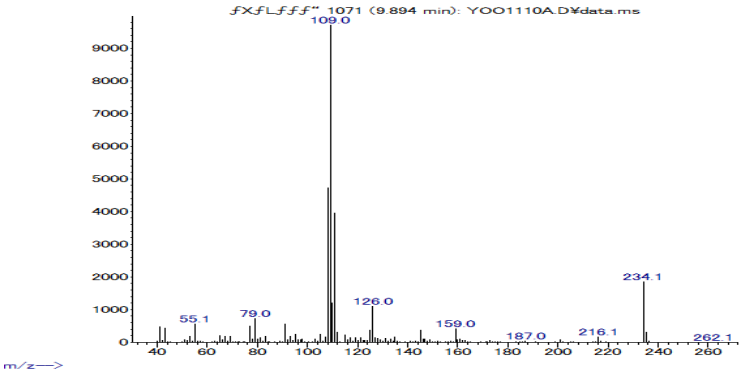

Figure 26. EI mass spectrum of *L. virgaurea* type 2 at RT 9.894 min. (Sample 27)

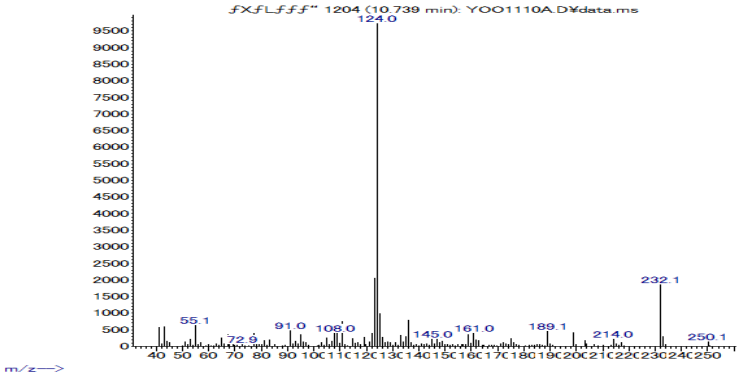

Figure 27. EI mass spectrum of *L. virgaurea* type 2 at RT 10.739 min. (Sample 27)

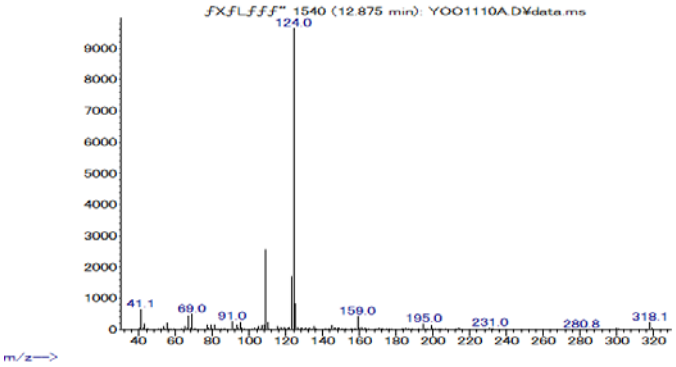

Figure 28. EI mass spectrum of *L. virgaurea* type 2 at RT 12.875 min. (Sample 27)

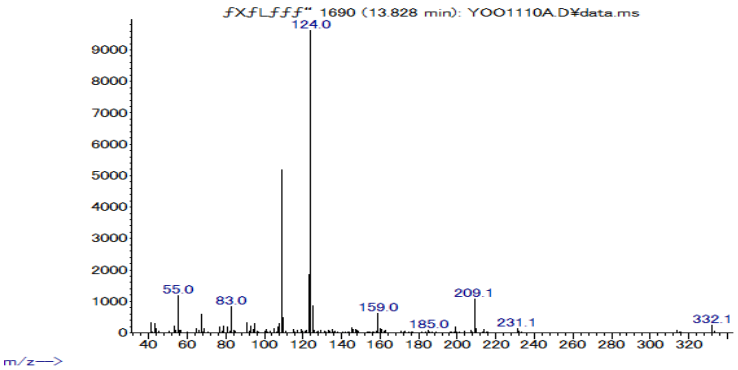

Figure 29. EI mass spectrum of *L. virgaurea* type 2 at RT 13.828 min. (Sample 27)

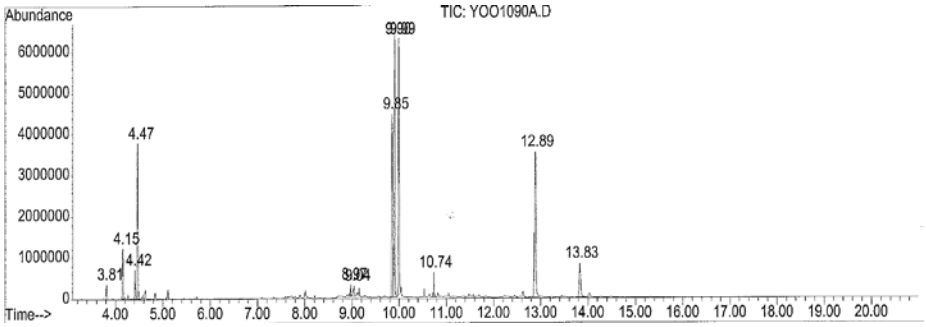

Figure 30. TIC of *L. virgaurea* type 2 (Sample 7)

RT (min)	Area %	Compound	Source
3.814	1.088	α-Pinene	Wiley
4.153	3.280	Sabinene	Wiley
4.416	1.888	α-Phellandrene	Wiley
4.469	10.721	3-Carene	Wiley
8.973	0.786	unknown, m/z = 204	
9.040	1.202	unknown, m/z = 216	
9.852	14.370	Ligularol ethyl ether	Literature [6]
9.903	**21.987**	unknown, m/z = 262	
9.993	20.066	Ligularol	MassFinder
10.735	1.914	FE- 6β,10β- diol	Literature [6], [8]
12.888	18.128	6-OH-3-OMeAcr-FE	
13.831	4.571	6-OH-3-OAng-FE	

Table 22. GC-MS result of *L. virgaurea* type 2 (Sample 7)

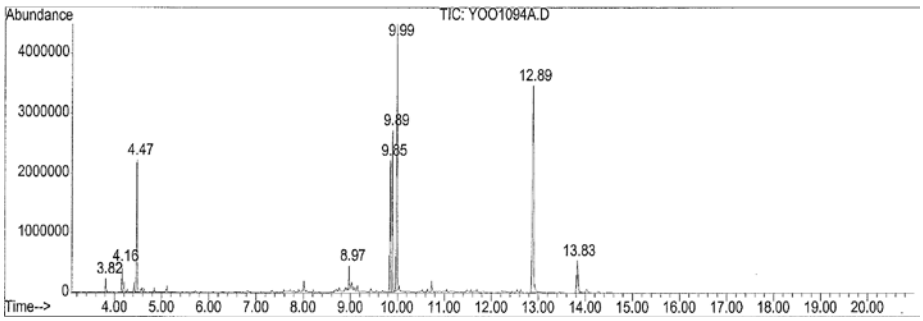

Figure 31. TIC of *L. virgaurea* type 2 (Sample 11)

RT (min)	Area %	Compound	Source
3.818	1.183	α-Pinene	Wiley
4.158	1.892	Sabinene	Wiley
4.473	10.798	3-Carene	Wiley
8.974	1.651	unknown, m/z = 203	
9.849	11.009	Ligularol ethyl ether	Literature [6]
9.894	13.311	unknown, m/z = 262	
9.988	23.390	Ligularol	MassFinder
12.887	**31.335**	6-OH-3-OMeAcr-FE	
13.829	5.430	6-OH-3-OAng-FE	

Table 23. GC-MS result of *L. virgaurea* type 2 (Sample 11)

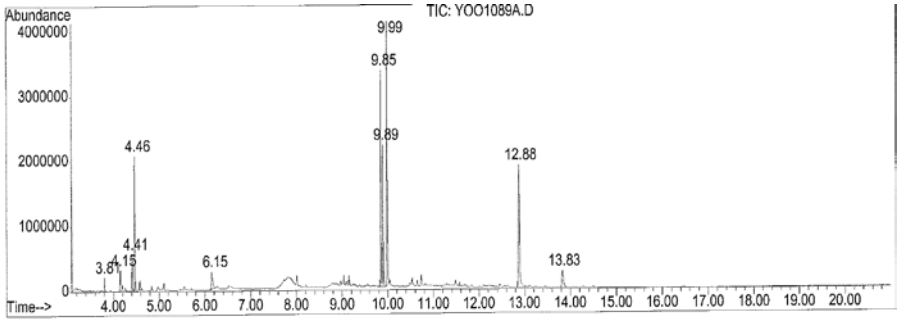

Figure 32. TIC of *L. virgaurea* type 2 (Sample 6)

RT (min)	Area %	Compound	Source
3.809	1.104	α-Pinene	Wiley
4.148	1.813	Sabinene	Wiley
4.410	2.937	α-Phellandrene	Wiley
4.464	11.442	3-Carene	Wiley
6.149	3.056	5-Hydroxymethylfurfural	Wiley
9.849	19.880	Ligularol ethyl ether	Literature [6]
9.893	12.590	*unknown*, m/z = 234	
9.987	**24.312**	Ligularol	MassFinder
12.879	19.524	6-OH-3-OMeAcr-FE	
13.828	3.342	6-OH-3-OAng-FE	

Table 24. GC-MS result of *L. virgaurea* type 2 (Sample 6)

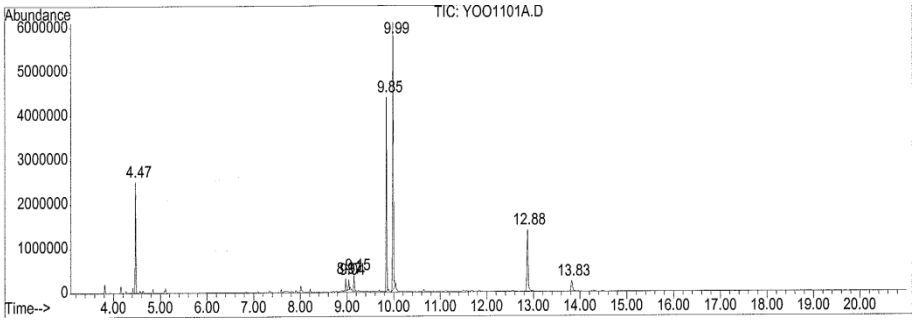

Figure 33. TIC of *L. virgaurea* type 2 (Sample 18)

RT (min)	Area %	Compound	Source
4.471	13.354	3-Carene	Wiley
8.974	1.483	unknown, m/z = 204	
9.043	1.545	unknown, m/z = 218	
9.152	2.352	unknown, m/z = 216	
9.849	25.275	Ligularol ethyl ether	Literature [6]
9.990	**39.572**	Ligularol	MassFinder
12.875	13.500	6-OH-3-OMeAcr-FE	
13.827	2.919	6-OH-3-OAng-FE	

Table 25. GC-MS result of *L. virgaurea* type 2 (Sample 18)

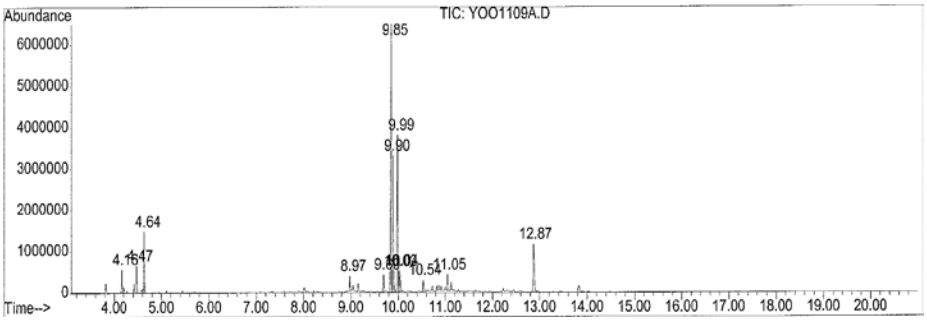

Figure 34. TIC of *L. virgaurea* type 2 (Sample 26)

RT (min)	Area %	Compound	Source
4.158	2.417	Sabinene	Wiley
4.473	2.855	3-Carene	Wiley
4.638	6.725	β-Phellandrene	Wiley
8.973	1.599	unknown, m/z = 204	
9.692	2.029	8-oxo-12-noreremophil-6-en-11-one	Literature [6]
9.852	**33.880**	Ligularol ethyl ether	Literature [6]
9.897	15.206	unknown, m/z = 262	
9.986	17.290	Ligularol	MassFinder
10.016	2.257	unknown, m/z = 262	
10.042	2.676	unknown, m/z = 262	
10.538	1.819	unknown, m/z = 306	
11.052	1.902	unknown, m/z = 306	
12.875	9.345	6-OH-3-OMeAcr-FE	

Table 26. GC-MS result of L. virgaurea type 2 (Sample 26)

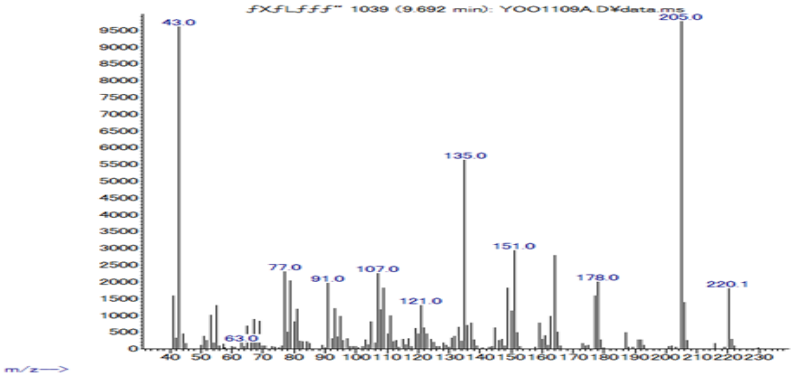

Figure 35. EI mass spectrum of *L. virgaurea* type 2 at RT 9.692 min. (Sample 26)

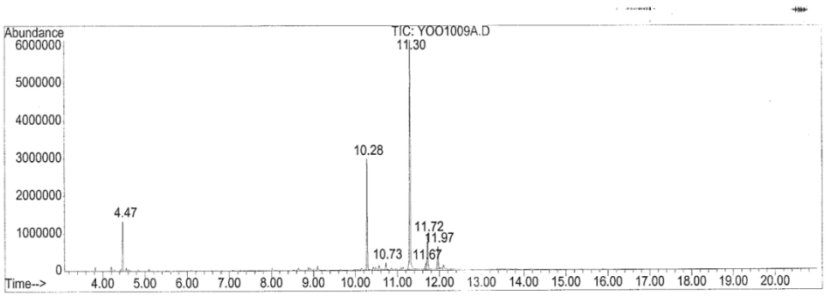

Figure 36. TIC of *L. virgaurea* type 3 (Sample 1)

RT(min)	Area %	Compound	Source
4.473	8.955	3-Carene	MassFinder
10.281	19.346	1-Hydroxy-2-(3'-pentenyl)-3,7-dimethylbenzofuran	Literature [26]
10.726	1.639	unknown, m/z = 230	
11.301	**53.234**	Cacalol	MassFinder
11.673	1.430	unknown, m/z = 246	
11.716	9.573	unknown, m/z = 248	
11.965	5.823	unknown, m/z = 247	

Table 27. GC-MS result of *L. virgaurea* type 3 (Sample 1)

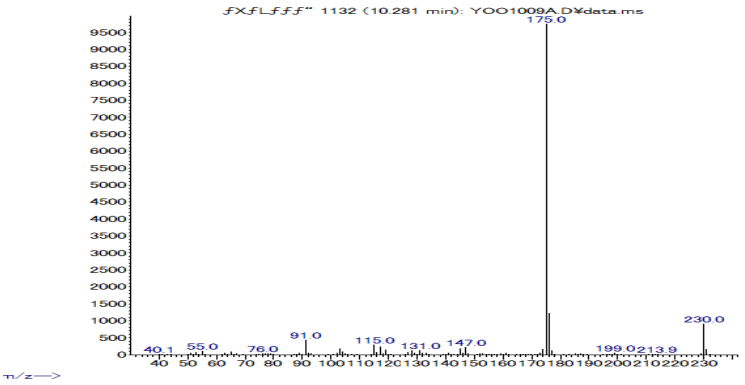

Figure 37. EI mass spectrum of *L. virgaurea* type 3 at RT 10.281min. (Sample 1)

6.2.2. L. subspicata

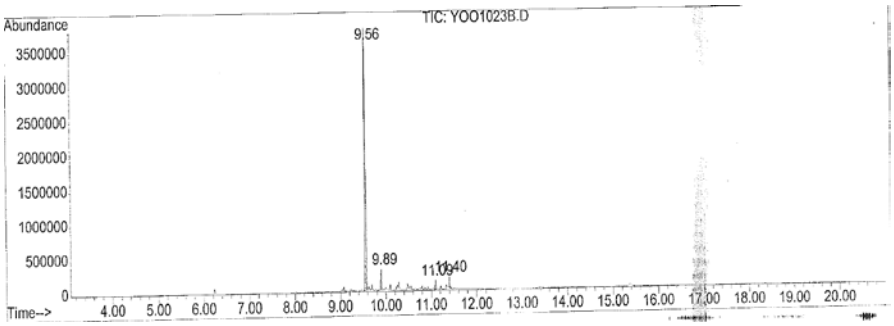

Figure 38. TIC of *L. subspicata* (Sample 4)

RT (min)	Area %	Compound	Source
9.562	**86.614**	Fukinone	MassFinder
9.894	6.559	Dehydrofukinone	MassFinder
11.094	2.927	unknown, m/z = 235	
11.399	3.900	8-Hydroxyeremophil-7(11)-ene-12,8-olide	MassFinder

Table 28. GC-MS result of *L. subspicata* (Sample 4)

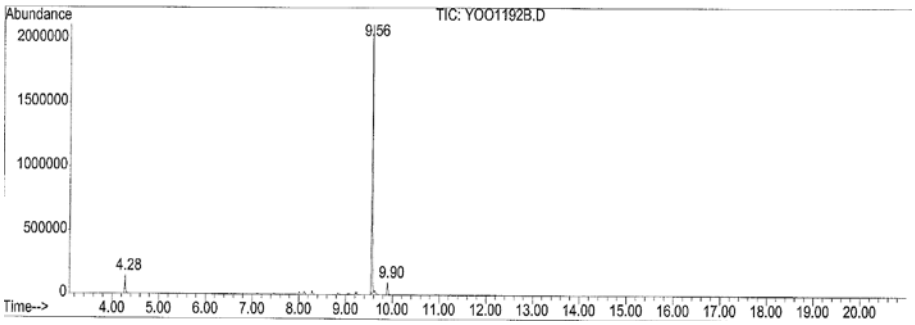

Figure 39. TIC of *L. subspicata* (Sample 5)

RT(min)	Area%	Compound	Source
4.279	6.458	β-Myrcene	Wiley
9.559	**87.636**	Fukinone	MassFinder
9.899	5.906	Dehydrofukinone	MassFinder

Table 29. GC-MS result of *L. subspicata* (Sample 5)

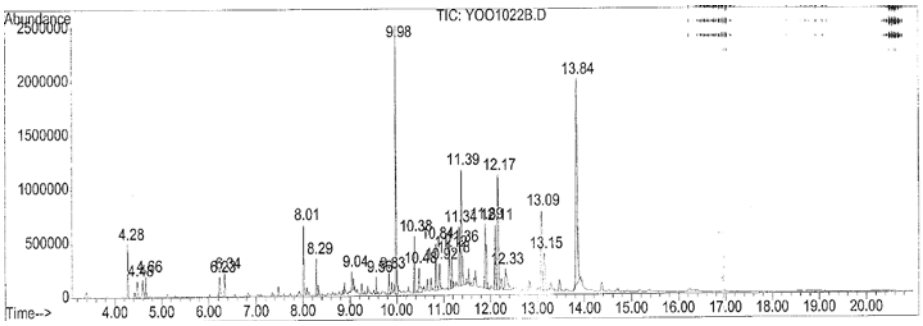

Figure 40. TIC of *L. subspicata* (Sample 1)

RT(min)	Area%	Compound	Source
4.279	2.030	β-Myrcene	Wiley
4.479	0.739	3-Carene	Wiley
4.664	1.187	cis-Ocimene	Wiley
6.229	1.385	unknown, m/z = 164	
6.338	0.949	Linalyl acetate	Wiley
8.015	3.135	Eremophila-1(10),11-diene	Wiley
8.287	1.597	unknown, m/z = 222	
9.042	0.800	unknown, m/z = 216	
9.559	0.743	unknown, m/z = 220	
9.834	1.109	unknown, m/z = 228	
9.985	12.035	Ligularol	MassFinder
10.378	2.570	unknown, m/z = 276	
10.479	2.041	Palmitic acid	Wiley
10.841	2.734	6-OAc-FE-10-ol	Literature [32]
10.923	1.460	6-OiBu-FE	Literature [32]
11.124	2.430	Eremofarfugin C	MassFinder
11.178	1.861	unknown, m/z = 304	
11.338	3.451	unknown, m/z = 280	
11.362	1.864	6-OMeBu-FE	Literature [32]
11.391	6.981	6-OiBu-FE-10-ol	MassFinder
11.893	5.883	6-OMeBu-FE-10-ol	MassFinder
12.107	3.704	6-OAng-FE-10-ol	MassFinder
12.168	7.451	6-OiBu-FE-9-one	MassFinder
12.328	2.987	unknown, m/z = 316	
13.093	6.058	6-OAng-FE-9-one	MassFinder
13.150	3.601	Subspicatin B	MassFinder
13.842	**19.214**	Subspicatin A	MassFinder

Table 30. GC-MS result of *L. subspicata* (Sample 1)

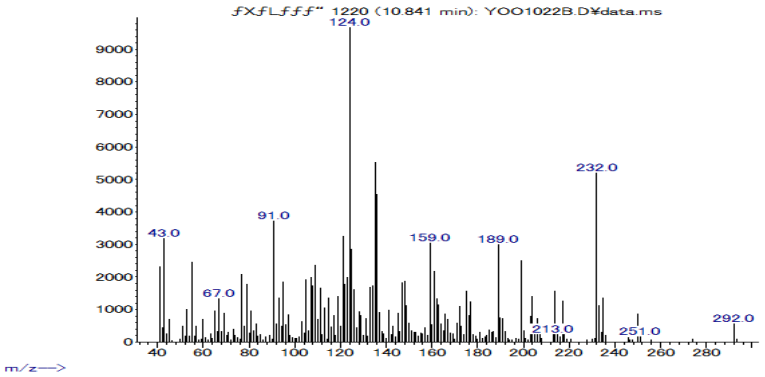

Figure 41. EI mass spectrum of *L. subspicata* at RT 10.841 min. (Sample 1)

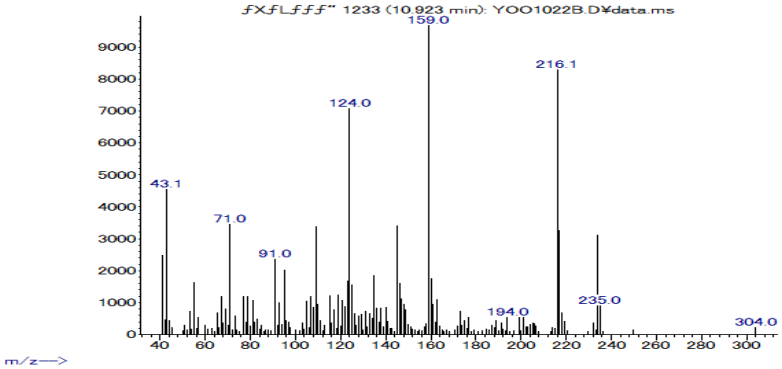

Figure 42. EI mass spectrum of *L. subspicata* at RT 10.923 min. (Sample 1)

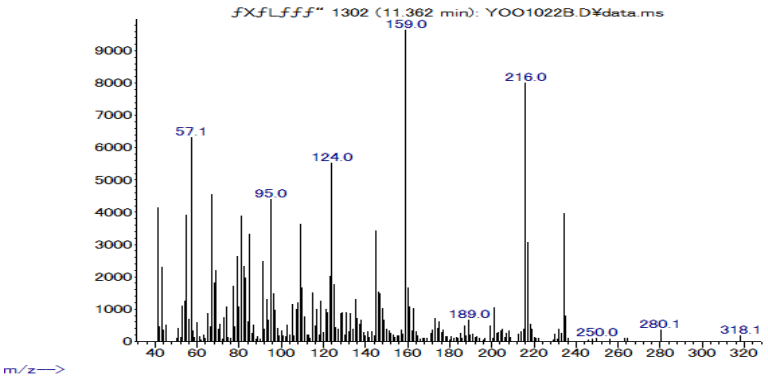

Figure 43. EI mass spectrum of *L. subspicata* at RT 11.362 min. (Sample 1)

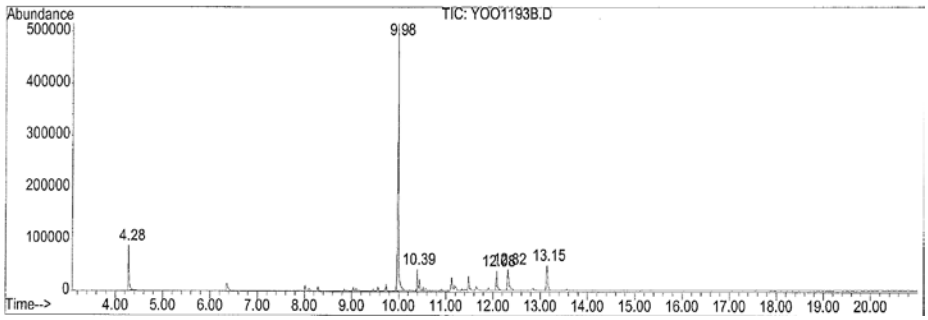

Figure 44. TIC of *L. subspicata* (Sample 6), measured after several days of extraction

RT (min)	Area %	Compound	Source
4.280	9.851	β-Myrcene	Wiley
9.982	**61.668**	Ligularol	MassFinder
10.392	3.662	unknown, m/z = 264	
12.080	6.053	unknown, m/z = 281	
12.318	9.077	unknown, m/z = 281	
13.145	9.690	Subspicatin B	MassFinder

Table 31. GC-MS result of *L. subspicata* (Sample 6), measured after several days of extraction

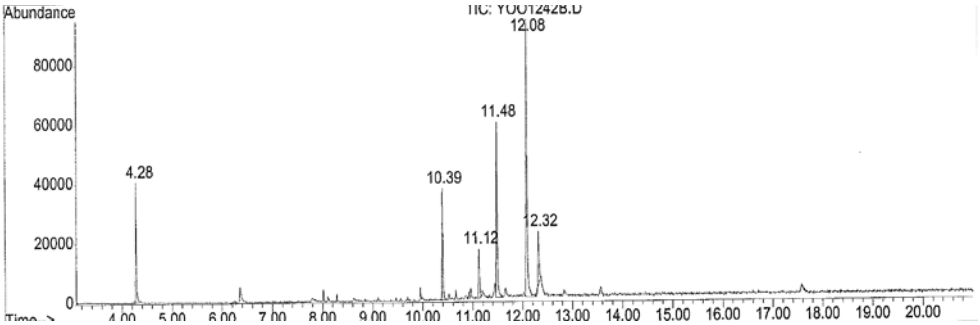

Figure 45. TIC of *L. subspicata* (Sample 6), extraction time = 1 month

RT (min)	Area %	Compound	Source
4.280	11.500	β-Myrcene	Wiley
10.393	11.609	unknown, m/z = 264	
11.124	6.072	6-OH-eremophil-7(8)-en-12,8-olide	MassFinder
11.483	22.248	*unknown*, m/z = 248	
12.080	**42.552**	*unknown*, m/z = 262	
12.319	6.019	6-OH-eremophil-7(11)-en-12,8-olide	MassFinder

Table 32. GC-MS result of *L. subspicata* (Sample 6), extraction time = 1 month

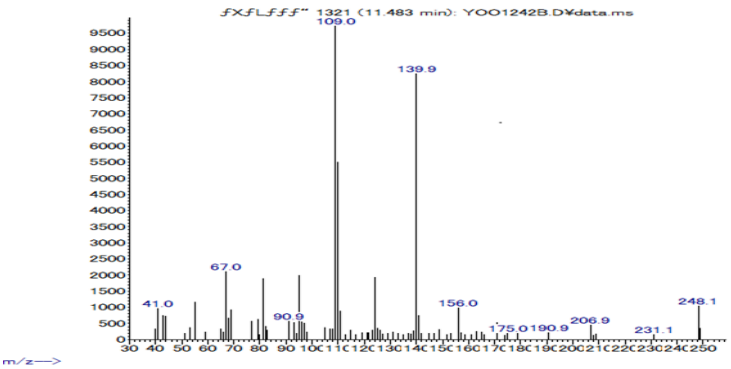

Figure 46. EI mass spectrum of *L. subspicata* at RT 11.483 min. (Sample 6)

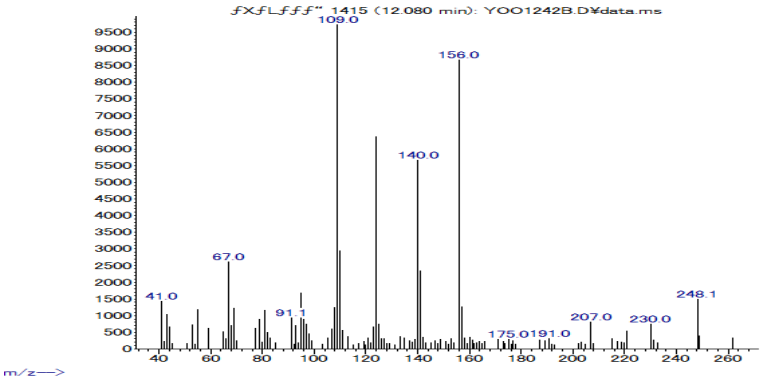

Figure 47. EI mass spectrum of *L. subspicata* at RT 12.080 min. (Sample 6)

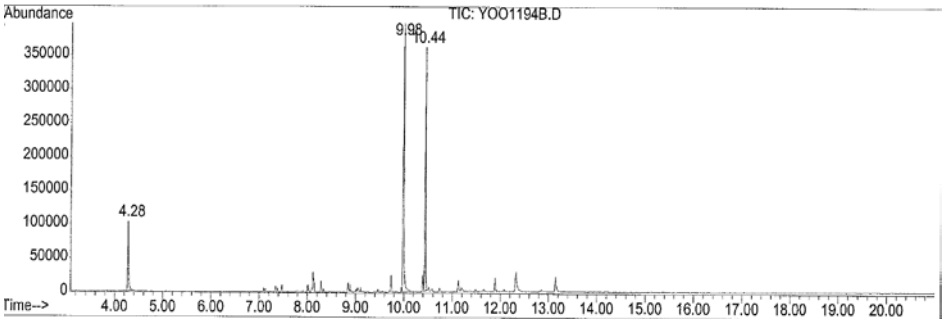

Figure 48. TIC of *L. subspicata* (Sample 7), measured after several days of extraction

RT (min)	Area %	Compound	Source
4.279	10.976	β-Myrcene	Wiley
9.983	**47.537**	Ligularol	MassFinder
10.441	34.752	*unknown*, m/z = 232	
12.328	6.735	unknown, m/z = 281	

Table 33. GC-MS result of *L. subspicata* (Sample 7), measured after several days of extraction

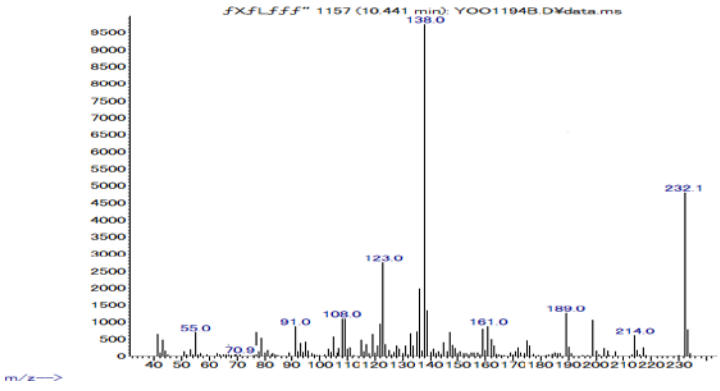

Figure 49. EI mass spectrum of *L. subspicata* at RT 10.441 min. (Sample 7)

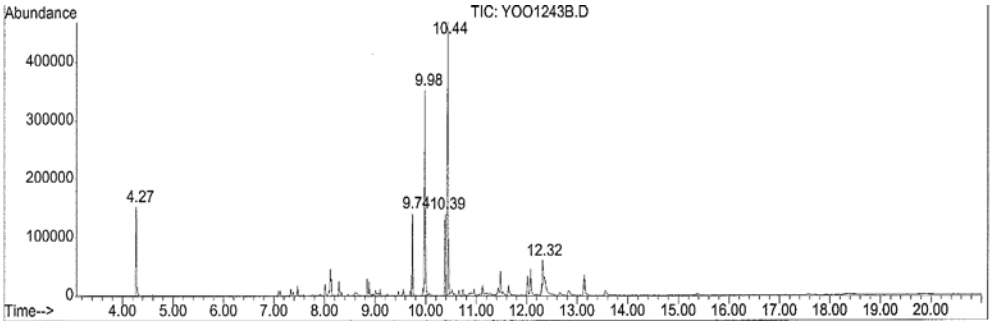

Figure 50. TIC of *L. subspicata* (Sample 7), extraction time = 1 month

RT (min)	Area %	Compound	Source
4.273	11.663	β-Myrcene	Wiley
9.734	10.040	Ligularol methyl ether	Literature [5]
9.981	28.939	Ligularol	MassFinder
10.389	11.092	unknown, m/z = 264	
10.440	**34.947**	*unknown*, m/z = 264	
12.316	3.319	6-OH-eremophil-7(11)-en-12,8-olide	MassFinder

Table 34. GC-MS result of *L. subspicata* (Sample 7), extraction time = 1 month

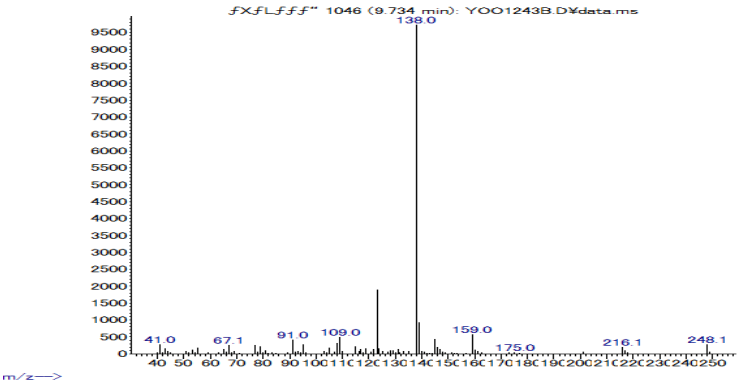

Figure 51. EI mass spectrum of *L. subspicata* at RT 9.734 min. (Sample 7)

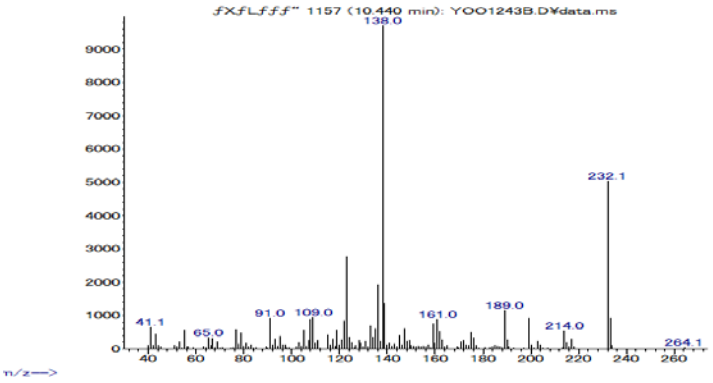

Figure 52. EI mass spectrum of *L. subspicata* at RT 10.440 min. (Sample 7)

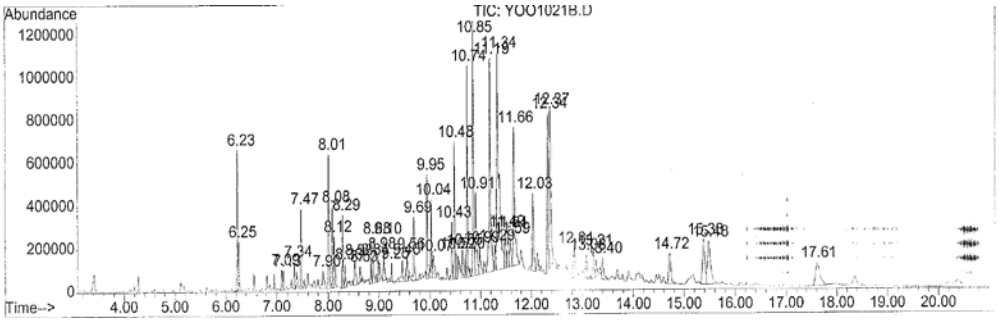

Figure 53. TIC of *L. subspicata* (Sample 3)

RT (min)	Area %	Compound	Source
8.014	2.435	Eremophila-1(10),11-diene	Wiley
9.949	1.796	Bakkenolide A	Wiley
10.740	3.874	Subspicatolide	MassFinder
10.855	6.001	8-oxoeremophil-6(7)-en-12-oic acid	MassFinder
11.337	**11.206**	*unknown*, m/z = 304	
11.191	7.103	unknown, m/z = 265	
12.335	4.754	6-hydroxy-8H-eremophil-7(11)-en-12,8-olide	MassFinder
12.373	5.887	6,8-hydroxy-eremophil-7(11)-en-12,8-olide	

Table 35. GC-MS result of *L. subspicata* (Sample 3), major peaks

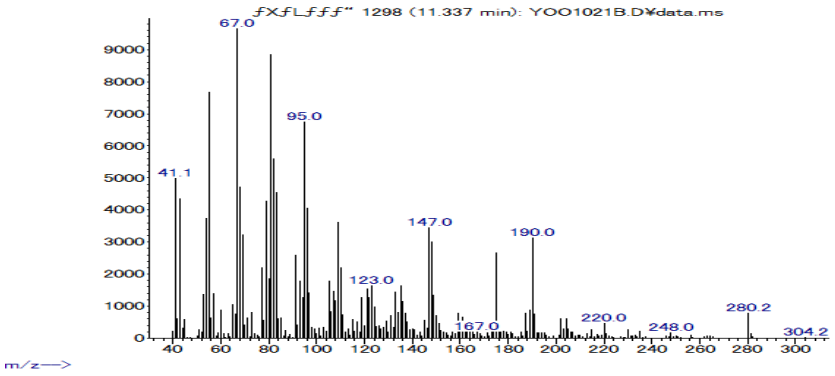

Figure 54. EI mass spectrum of *L. subspicata* at RT 11.337 min. (Sample 3)

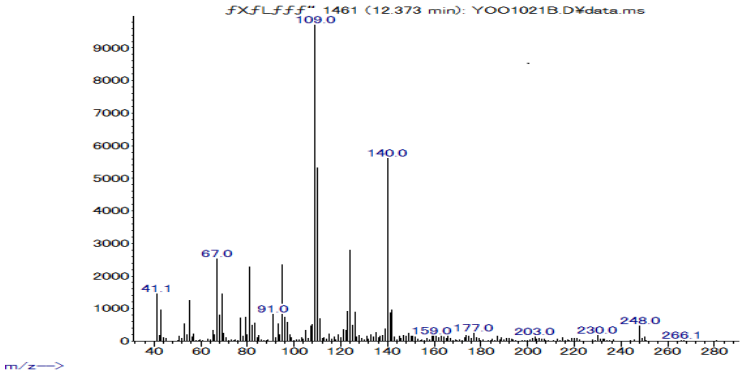

Figure 55. EI mass spectrum of *L. subspicata* at RT 12.373 min. (Sample 3)

6.2.3. L. lamarum

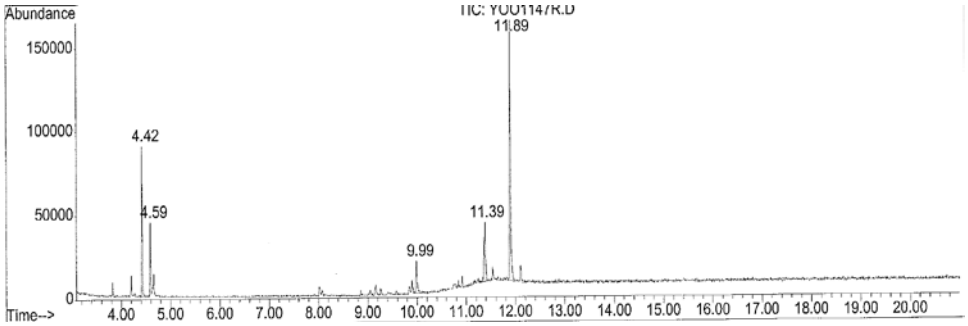

Figure 56. TIC of *L. lamarum* (No. 09 95)

RT (min)	Area %	Compound	Source
4.422	18.244	α-Phellandrene	Wiley
4.589	8.531	o-Cymene	Wiley
9.992	6.615	Ligularol	MassFinder
11.390	16.653	6-OiBu-FE-10-ol	MassFinder
11.893	**49.956**	6-OMeBu-FE-10-ol	MassFinder

Table 36. GC-MS result of *L. lamarum* (No. 09 95)

6.2.4. L. vellerea

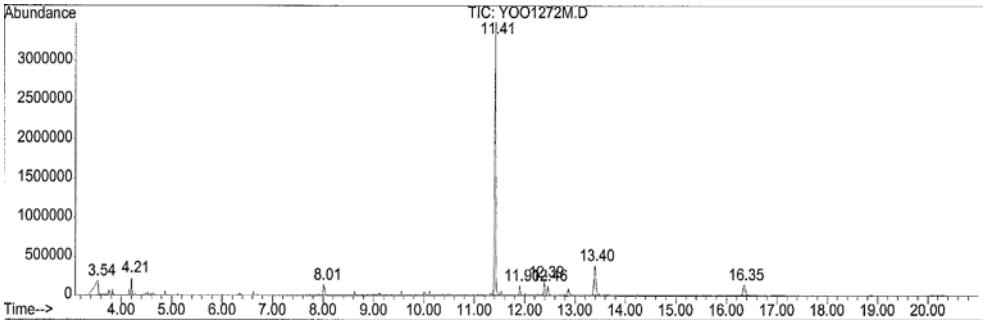

Figure 57. TIC of *L. vellerea* (Sample 3)

RT (min)	Area %	Compound	Source
3.537	11.440	2-methyl-2-butenoic acid	Wiley
4.207	2.366	β-Pinene	Wiley
8.013	2.624	Eremophila-1(10),11-diene	Wiley
11.413	**58.955**	FE-15,6-olide	MassFinder
11.903	1.979	unknown, m/z = 278	
12.393	3.399	unknown, m/z = 262	
12.462	2.426	unknown, m/z = 262	
13.399	11.476	unknown, m/z = 278	
16.353	5.335	3β-OAng-FE-15,6-olide	

Table 37. GC-MS result of *L. vellerea* (Sample 3)

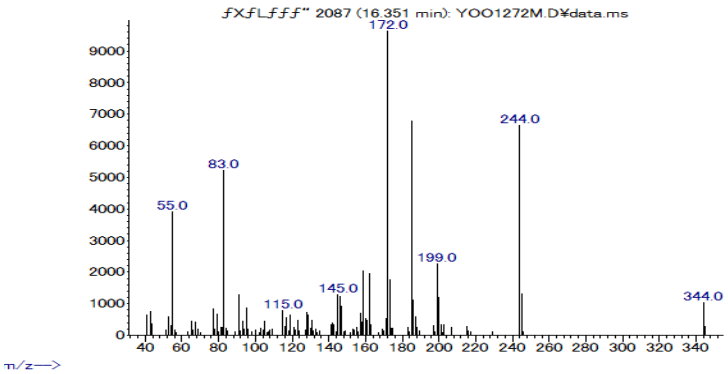

Figure 58. EI mass spectrum of *L. vellerea* at RT 16.351 min. (Sample 3)

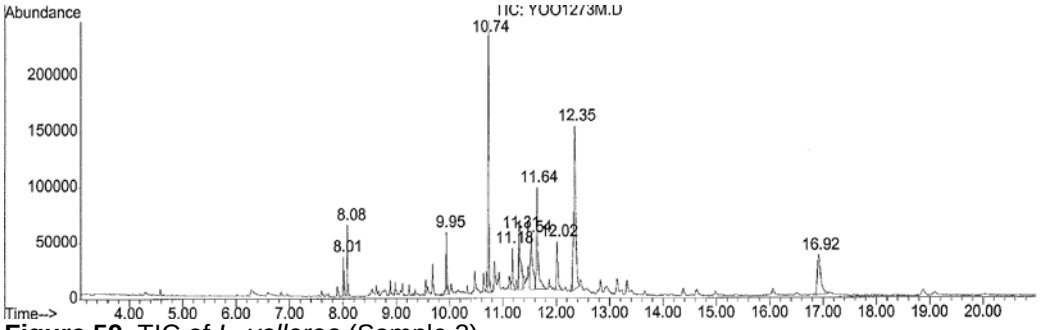

Figure 59. TIC of *L. vellerea* (Sample 2)

RT (min)	Area %	Compound	Source
8.011	2.245	Eremophila-1(10),11-diene	Wiley
8.083	4.089	Hexahydroindene-2-Ac-3a,4-diMe	MassFinder
9.947	4.468	Bakkenolide A	Wiley
10.737	16.585	Subspicatolide	MassFinder
11.187	3.417	*unknown*, m/z = 248	
11.308	8.089	*unknown*, m/z = 207	
11.536	8.893	*unknown*, m/z = 322	
11.645	12.567	*unknown*, m/z = 281	
12.019	5.378	unknown, m/z = 222	
12.350	**24.373**	6-hydroxy-eremophil-8(9),7(11)-diene-12,8-olide	
16.920	9.895	unknown, m/z = 246	

Table 38. GC-MS result of *L. vellerea* (Sample 2)

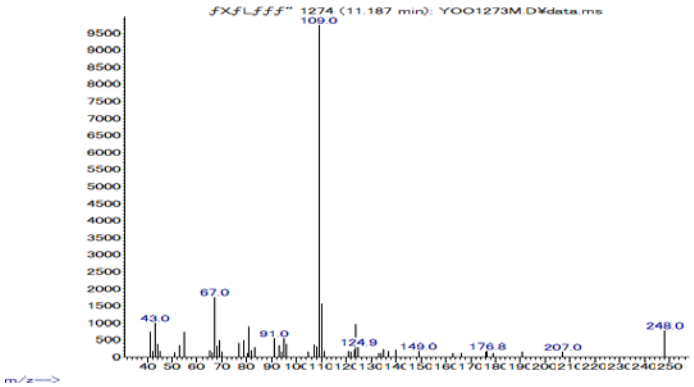

Figure 60. EI mass spectrum of *L. vellerea* at RT 11.187 min. (Sample 2)

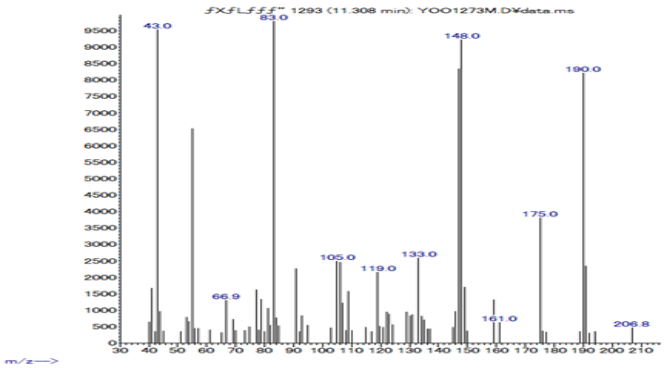

Figure 61. EI mass spectrum of *L. vellerea* at RT 11.308 min. (Sample 2)

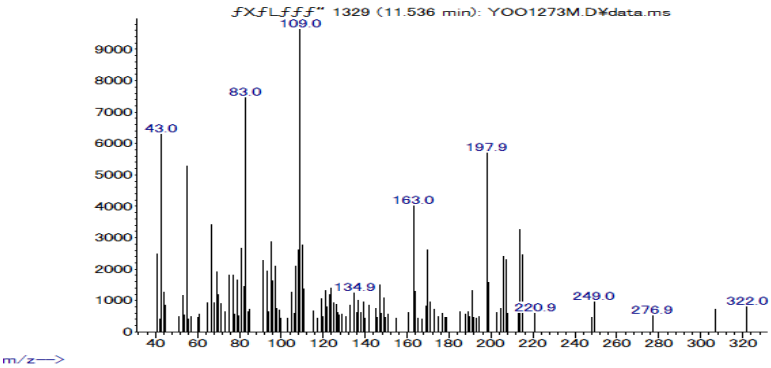

Figure 62. EI mass spectrum of *L. vellerea* at RT 11.536 min. (Sample 2)

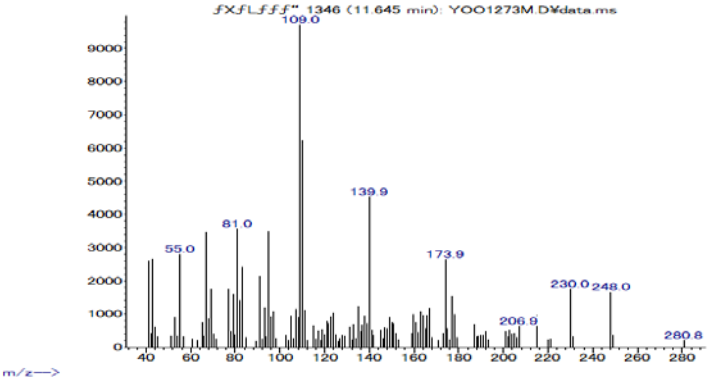

Figure 63. EI mass spectrum of *L. vellerea* at RT 11.645 min. (Sample 2)

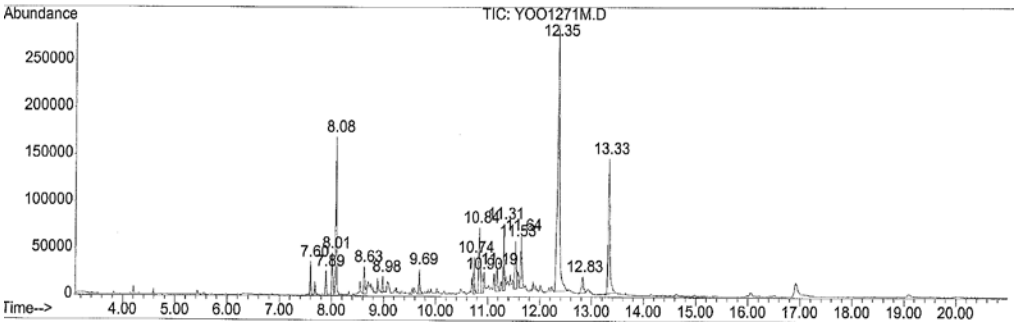

Figure 64. TIC of *L. vellerea* (Sample 1)

RT (min)	Area %	Compound	Source
7.598	1.803	unknown, m/z = 141	
7.894	1.671	unknown, m/z = 182	
8.014	3.146	Eremophila-1(10),11-diene	Wiley
8.083	8.627	Hexahydroindene-2-Ac-3a,4-diMe	MassFinder
8.632	1.978	unknown, m/z = 182	
9.686	1.652	8-oxo-12-noreremophil-6-en-11-one	
10.735	2.214	Subspicatolide	MassFinder
10.838	6.080	8-oxoeremophil-6(7)-en-12-oic acid	MassFinder
10.898	1.830	unknown, m/z = 235	
11.186	2.084	unknown, m/z = 248	
11.307	3.798	unknown, m/z = 207	
11.536	4.687	unknown, m/z = 322	
11.644	4.793	unknown, m/z = 248	
12.349	**38.354**	6-hydroxy-eremophil-8(9),7(11)-dien-12,8-olide	
12.832	2.134	unknown, m/z = 250	
13.328	15.148	6,8-dihydroxy-eremophil-7(11)-en-12,8-olide	

Table 39. GC-MS result of *L. vellerea* (Sample 1)

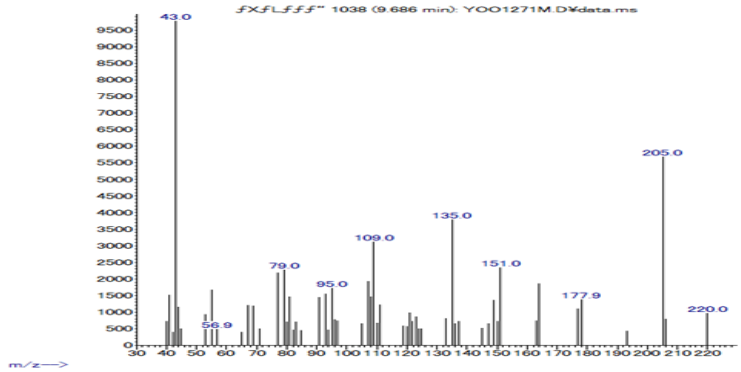

Figure 65. EI mass spectrum of *L. vellerea* at RT 9.686 min. (Sample 1)

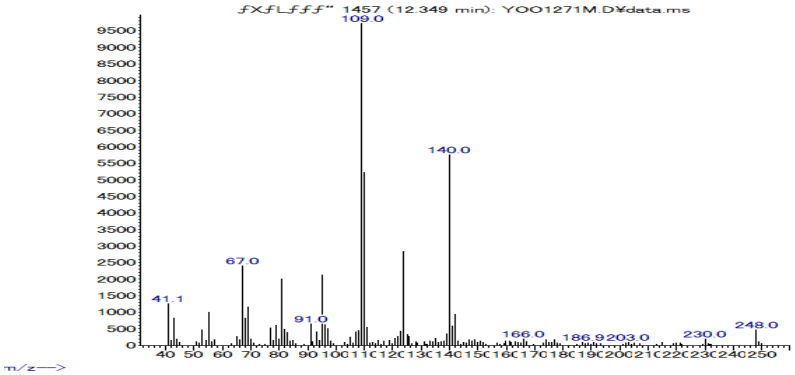

Figure 66. EI mass spectrum of *L. vellerea* at RT 12.349 min. (Sample 1)

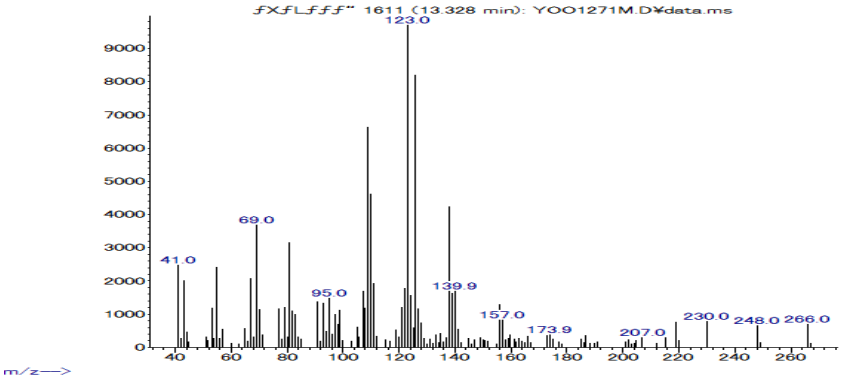

Figure 67. EI mass spectrum of *L. vellerea* at RT 13.328 min. (Sample 1)

6.2.5. L. cyathiceps

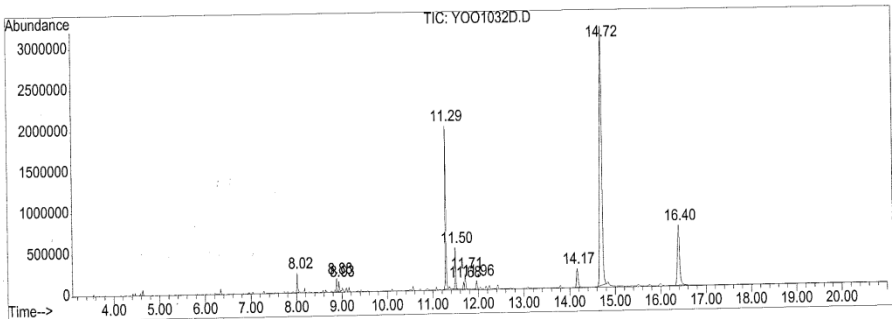

Figure 68. TIC of *L. cyathiceps* (Sample 4)

RT (min)	Area %	Compound	Source
8.015	1.483	Eremophila-1(10),11-diene	Wiley
8.883	1.028	Valerianol	MassFinder
8.933	0.781	unknown, m/z = 222	
11.294	12.920	Cacalol	MassFinder
11.502	3.249	1,10-epoxy-6-OiBu-FE	Literature [4]
11.677	0.642	unknown, m/z = 281	
11.713	1.582	unknown, m/z = 253	
11.962	0.931	unknown, m/z = 253	
14.171	3.194	1,10-epoxy-6-propanoyloxy-FE-9-one	Literature [4]
14.721	**59.919**	1,10-epoxy-6-OiBu-FE-9-one	MassFinder
16.402	14.270	1,10-epoxy-6-OAng-FE-9-one	MassFinder

Table 40. GC-MS result of *L. cyathiceps* (Sample 4)

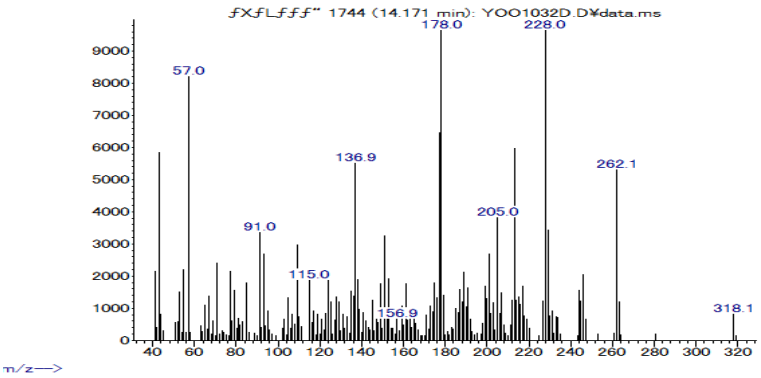

Figure 69. EI mass spectrum of *L. cyathiceps* at RT 14.171 min. (Sample 4)

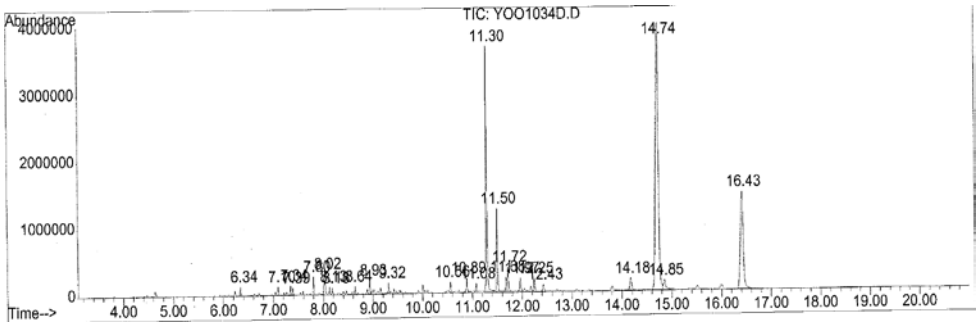

Figure 70. TIC of *L. cyathiceps* (Sample 6)

RT (min)	Area %	Compound	Source
8.016	1.732	Eremophila-1(10),11-diene	Wiley
11.299	13.621	Cacalol	MassFinder
11.502	4.578	1,10-epoxy-6-OiBu-FE	Literature [4]
14.176	1.419	1,10-epoxy-6-propanoyloxy-FE-9-one	Literature [4]
14.740	**48.654**	1,10-epoxy-6-OiBu-FE-9-one	MassFinder
14.851	1.491	6-OAng-FE-9-one	Literature [4]
16.426	16.831	1,10-epoxy-6-OAng-FE-9-one	MassFinder

Table 41. GC-MS result of *L. cyathiceps* (Sample 6), major peaks

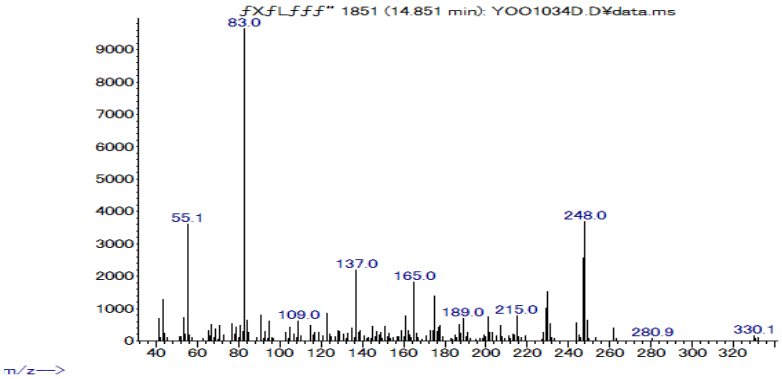

Figure 71. EI mass spectrum of *L. cyathiceps* at RT 14.851 min. (Sample 6)

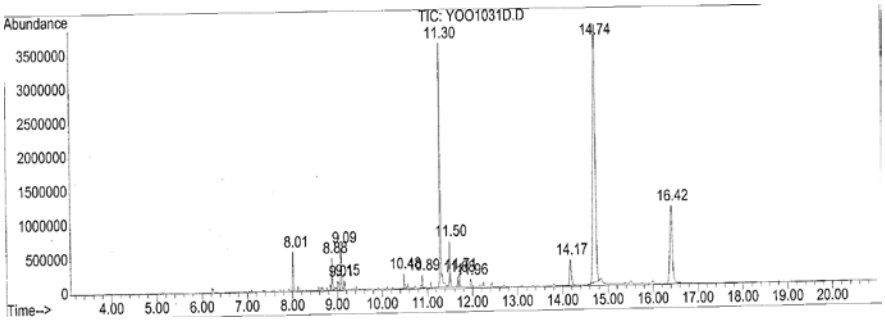

Figure 72. TIC of *L. cyathiceps* (Sample 3)

RT (min)	Area %	Compound	Source
8.015	2.339	Eremophila-1(10),11-diene	Wiley
8.883	1.796	Valerianol	MassFinder
9.012	0.890	β-Eudesmol	Wiley
9.088	2.631	unknown, m/z = 220	
9.155	0.586	Valeranone	Wiley
10.480	0.858	Palmitic acid	Wiley
10.890	0.813	unknown, m/z = 248	
11.297	16.316	Cacalol	MassFinder
11.497	3.015	1,10-epoxy-6-OiBu-FE	Literature [4]
11.676	0.673	unknown, m/z = 279	
11.713	0.976	unknown, m/z = 281	
11.963	0.596	unknown, m/z = 281	
14.173	3.425	1,10-epoxy-6-propanoyloxy-FE-9-one	Literature [4]
14.735	**49.974**	1,10-epoxy-6-OiBu-FE-9-one	MassFinder
16.416	15.111	1,10-epoxy-6-OAng-FE-9-one	MassFinder

Table 42. GC-MS result of *L. cyathiceps* (Sample 3)

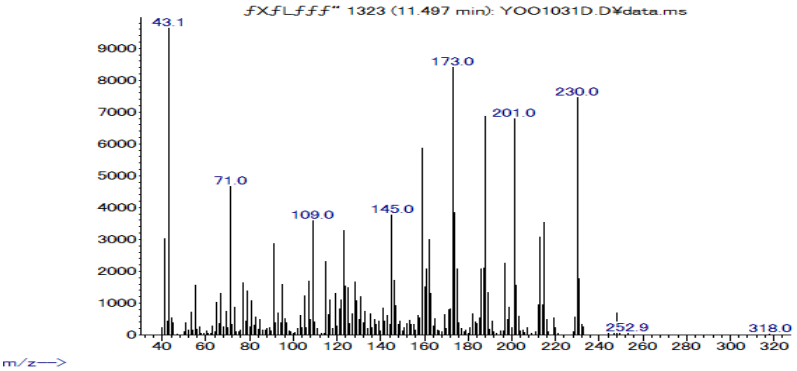

Figure 73. EI mass spectrum of *L. cyathiceps* at RT 11.497 min. (Sample 3)

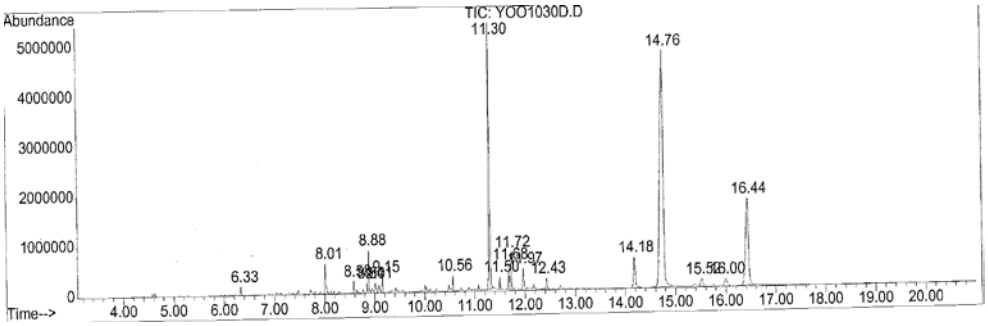

Figure 74. TIC of *L. cyathiceps* (Sample 2)

RT (min)	Area %	Compound	Source
6.334	0.413	Linalyl acetate	Wiley
8.014	1.748	Eremophila-1(10),11-diene	Wiley
8.580	0.575	unknown, m/z = 222	
8.843	0.454	unknown, m/z = 222	Wiley
8.882	2.070	unknown, m/z = 222	
9.012	0.813	β-Eudesmol	Wiley
9.154	0.835	Valeranone	Wiley
10.563	0.810	unknown, m/z = 252	
11.302	15.129	Cacalol	Wiley, MassFinder
11.501	0.703	1,10-epoxy-6-OiBu-FE	Literature [4]
11.678	1.398	unknown, m/z = 279	
11.719	2.234	unknown, m/z = 281	
11.967	1.541	unknown, m/z = 247	
12.429	0.960	unknown, m/z = 307	
14.180	3.402	1,10-epoxy-6-propanoyloxy-FE-9-one	Literature [4]
14.762	**49.319**	1,10-epoxy-6-OiBu-FE-9-one	MassFinder
15.519	0.997	6-OAng-FE-1(10)-en-9-one	Literature [4]
15.996	1.188	1,10-epoxy-6-isovaleroyloxy-FE-9-one	Literature [35]
16.438	15.411	1,10-epoxy-6-OAng-FE-9-one	MassFinder

Table 43. GC-MS result of L. cyathiceps (Sample 2)

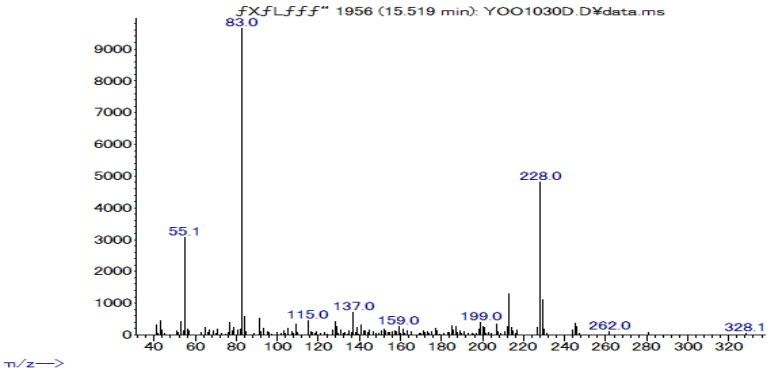

Figure 75. EI mass spectrum of *L. cyathiceps* at RT 15.519 min. (Sample 2)

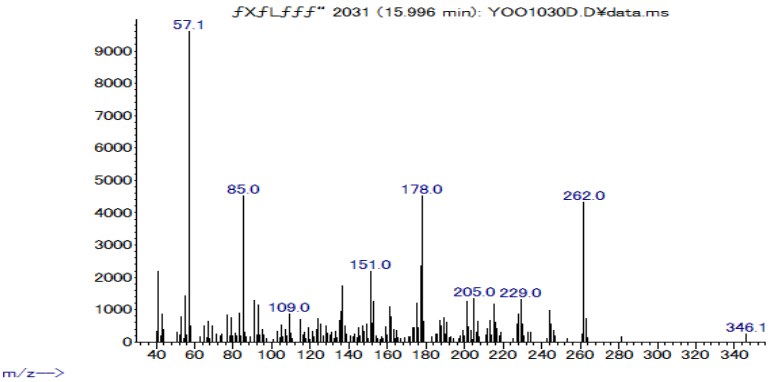

Figure 76. EI mass spectrum of *L. cyathiceps* at RT 15.996 min. (Sample 2)

6.2.6. L. pleurocaulis

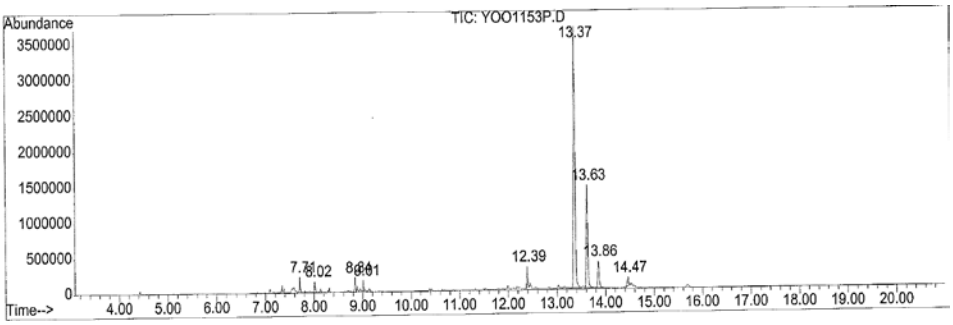

Figure 77. TIC of *L. pleurocaulis* Yunnan type (Sample 4)

RT(min)	Area %	Compound	Source
7.710	1.546	Guaia-6,9-diene	MassFinder
8.017	1.517	β-Selinene	Wiley
8.843	1.767	10-epi-γ-Eudesmol	MassFinder
9.013	1.386	β-Eudesmol	Wiley
12.391	3.221	6β-OiBu-FE-1(10)-en-3β-ol	
13.376	**60.332**	6β-OAng-FE-1(10)-en-3β-ol	Literature [11]
13.624	22.090	6β-OTig-FE-1(10)-en-3β-ol	Literature [11]
13.859	6.627	3β-OAng-FE-1(10)-en-6β-ol	Literature [11]
14.467	1.515	unknown, m/z = 346	

Table 44. GC-MS result of *L.pleurocaulis* Yunnan type (Sample 4)

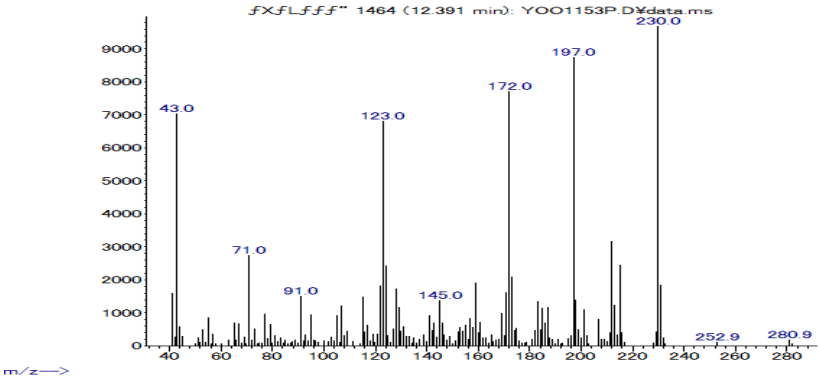

Figure 78. EI mass spectrum of *L. pleurocaulis* Yunnan type at RT 12.391 min. (Sample 4)

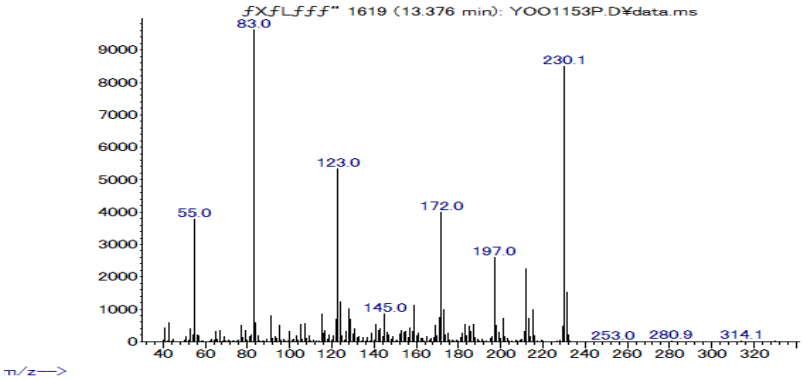

Figure 79. EI mass spectrum of *L. pleurocaulis* Yunnan type at RT 13.376 min. (Sample 4)

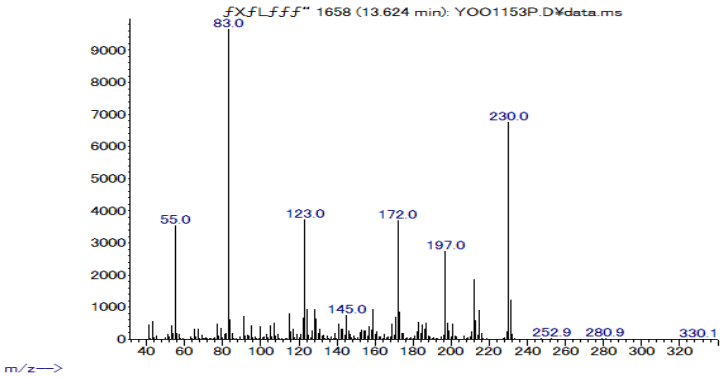

Figure 80. EI mass spectrum of *L. pleurocaulis* Yunnan type at RT 13.624 min. (Sample 4)

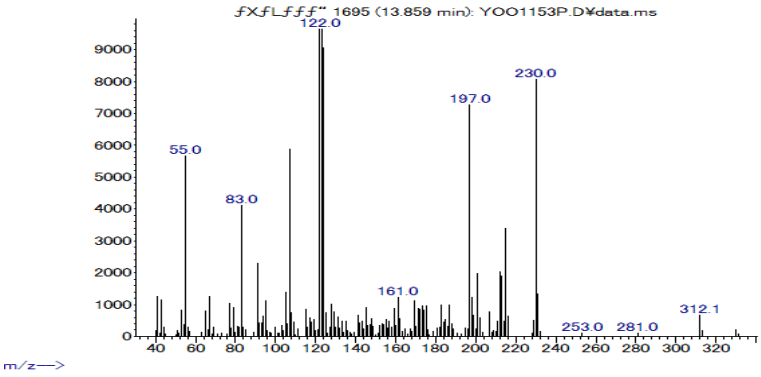

Figure 81. EI mass spectrum of *L. pleurocaulis* Yunnan type at RT 13.859 min. (Sample 4)

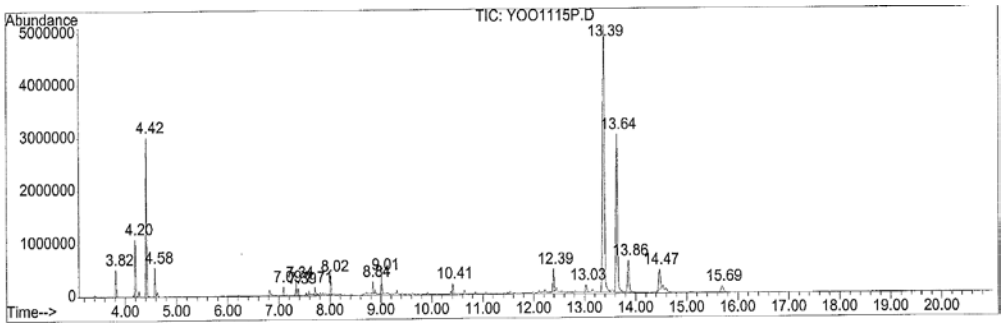

Figure 82. TIC of *L. pleurocaulis* Yunnan type (Sample 6)

RT(min)	Area %	Compound	Source
3.816	1.997	α-Pinene	Wiley
4.198	4.018	β-Pinene	Wiley
4.418	10.322	α-Phellandrene	Wiley
4.584	1.702	p-Cymene	Wiley
7.094	0.533	unknown, m/z = 204	
7.340	1.012	Selina-4,11-diene	MassFinder
7.385	0.470	unknown, m/z = 204	
7.711	0.602	Guaia-6,9-diene	MassFinder
8.019	1.351	β-Selinene	Wiley
8.843	0.774	10-epi-γ-Eudesmol	MassFinder
9.012	1.527	β-Eudesmol	Wiley
10.413	0.907	unknown, m/z = 230	
12.392	1.903	6β-OiBu-FE-1(10)-en-3β-ol	
13.034	0.898	unknown, m/z = 230	
13.390	**41.540**	6β-OAng-FE-1(10)-en-3β-ol	Literature [11]
13.637	21.939	6β-OTig-FE-1(10)-en-3β-ol	Literature [11]
13.860	4.472	3β-OAng-FE-1(10)-en-6β-ol	Literature [11]
14.470	2.712	unknown, m/z = 346	
15.693	1.321	unknown, m/z = 326	

Table 45. GC-MS result of *L. pleurocaulis* Yunnan type (Sample 6)

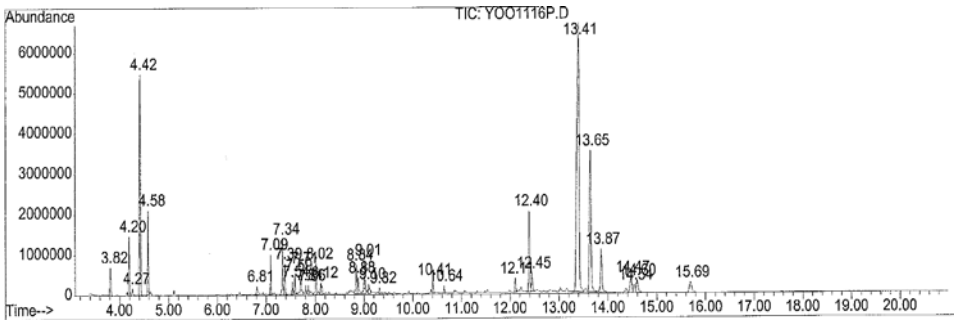

Figure 83. TIC of *L. pleurocaulis* Yunnan type (Sample 7)

RT(min)	Area %	Compound	Source
3.815	1.420	α-Pinene	Wiley
4.197	2.738	β-Pinene	Wiley
4.269	0.308	β-Myrcene	Wiley
4.417	11.311	α-Phellandrene	Wiley
4.583	3.357	p-Cymene	Wiley
6.812	0.623	2-Methoxy-4-vinylphenol	Wiley
7.095	1.554	unknown, m/z = 204	
7.340	2.557	Selina-4,11-diene	MassFinder
7.385	1.270	unknown, m/z = 204	
7.537	0.532	unknown, m/z = 204	
7.590	0.705	β-Caryophyllene	Wiley
7.711	1.489	Guaia-6,9-diene	MassFinder
7.811	0.442	α-Caryophyllene	Wiley
7.864	0.380	unknown, m/z = 204	
8.018	1.462	β-Selinene	Wiley
8.117	0.730	unknown, m/z = 222	
8.843	1.326	10-epi-γ-Eudesmol	MassFinder
8.882	0.885	unknown, m/z = 222	
9.012	2.003	β-Eudesmol	Wiley
9.097	0.653	unknown, m/z = 222	
9.316	0.256	unknown, m/z = 222	
10.412	0.734	unknown, m/z = 230	
10.643	0.310	unknown, m/z = 276	
12.109	0.728	6β-propanoyloxy-FE-1(10)-en-3β-ol	
12.397	4.688	6β-OiBu-FE-1(10)-en-3β-ol	
12.450	1.178	6β-OMeAcr-FE-1(10)-en-3β-ol	
13.410	**34.423**	6β-OAng-FE-1(10)-en-3β-ol	Literature [11]
13.650	13.154	6β-OTig-FE-1(10)-en-3β-ol	Literature [11]
13.866	3.830	3β-OAng-FE-1(10)-en-6β-ol	Literature [11]
14.473	1.476	unknown, m/z = 346	
14.536	0.758	3β-OTig-FE-1(10)-en-6β-ol	
14.598	1.340	6β-OMeSen-FE-1(10)-en-3β-ol	
15.691	1.383	3β-OMeSen-FE-1(10)-en-6β-ol	Literature [36]

Table 46. GC-MS result of *L. pleurocaulis* Yunnan type. (Sample 7)

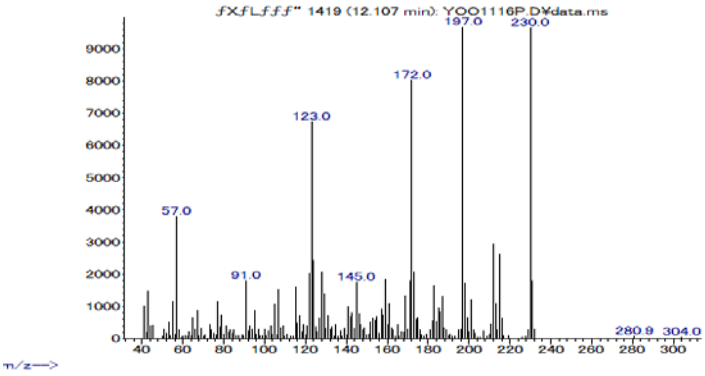

Figure 84. EI mass spectrum of *L. pleurocaulis* Yunnan type at RT 12.107 min. (Sample 7)

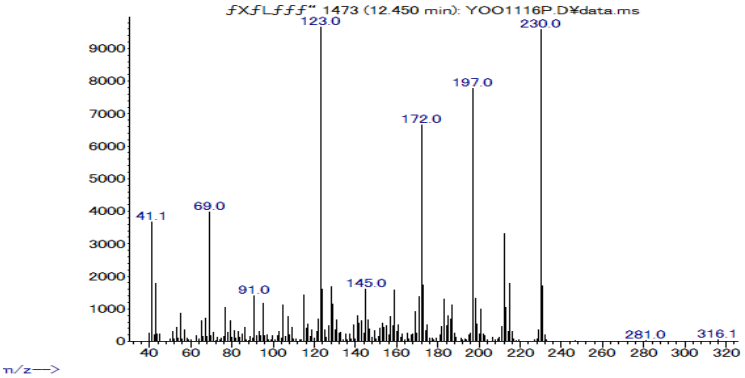

Figure 85. EI mass spectrum of *L. pleurocaulis* Yunnan type at RT 12.450 min. (Sample 7)

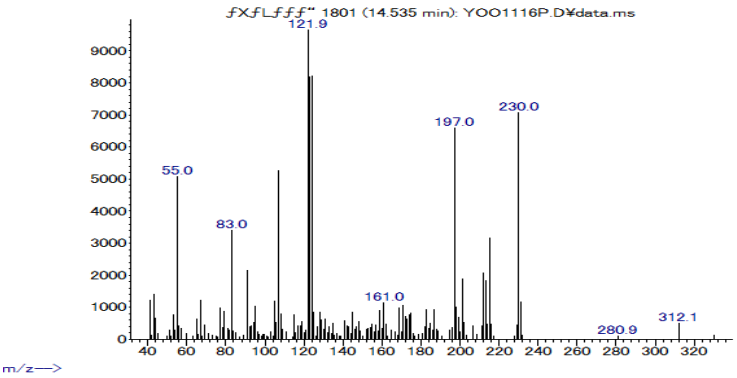

Figure 86. EI mass spectrum of L. pleurocaulis Yunnan type at RT 14.535 min. (Sample 7)

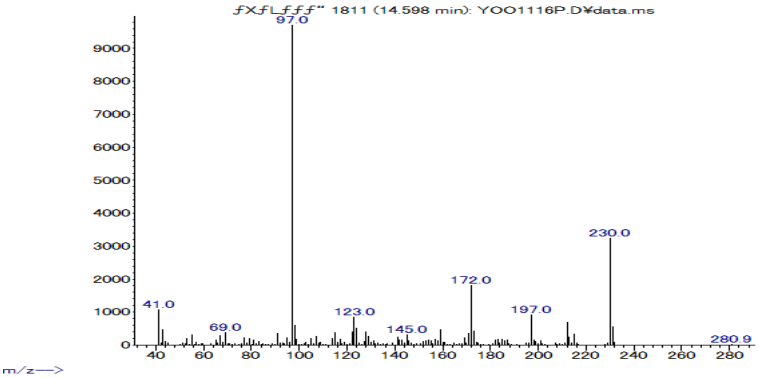

Figure 87. EI mass spectrum of *L. pleurocaulis* Yunnan type at RT 14.598 min. (Sample 7)

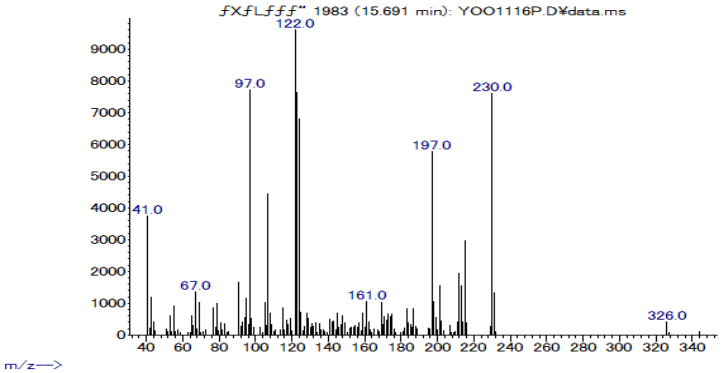

Figure 88. EI mass spectrum of *L. pleurocaulis* Yunnan type at RT 15.691 min. (Sample 7)

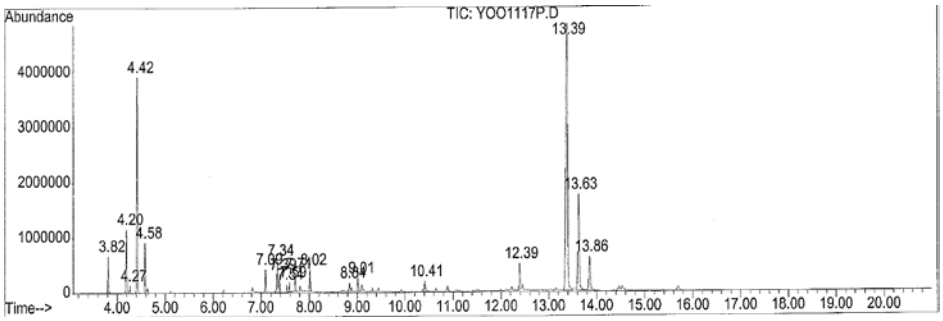

Figure 89. TIC of *L. pleurocaulis* Yunnan type (Sample 8)

RT(min)	Area %	Compound	Source
3.816	2.594	α-Pinene	Wiley
4.198	4.487	β-Pinene	Wiley
4.271	0.479	β-Myrcene	Wiley
4.418	14.530	α-Phellandrene	Wiley
4.584	2.912	p-Cymene	Wiley
7.095	1.464	unknown, m/z = 204	
7.340	2.692	Selina-4,11-diene	MassFinder
7.385	1.214	unknown, m/z = 204	
7.538	0.502	unknown, m/z = 204	
7.591	0.739	β-Caryophyllene	Wiley
7.711	1.264	Guaia-6,9-diene	MassFinder
8.019	1.697	β-Selinene	Wiley
8.843	0.708	unknown, m/z = 222	
9.014	1.022	β-Eudesmol	Wiley
10.413	0.911	unknown, m/z = 230	
12.392	2.459	6β-OiBu-FE-1(10)-en-3β-ol	
13.384	**42.046**	6β-OAng-FE-1(10)-en-3β-ol	Literature [11]
13.632	13.395	6β-OTig-FE-1(10)-en-3β-ol	Literature [11]
13.859	4.885	3β-O-Ang-FE-1(10)-en-6β-ol	Literature [11]

Table 47. GC-MS result of *L. pleurocaulis* Yunnan type (Sample 8)

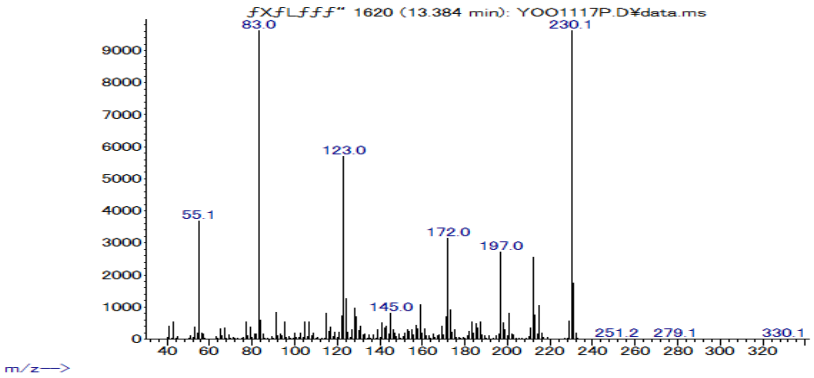

Figure 90. EI mass spectrum of *L. pleurocaulis* Yunnan type at RT 13.384 min. (Sample 8)

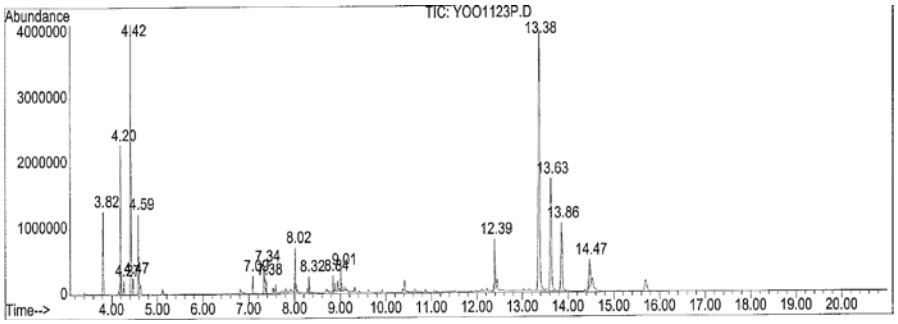

Figure 91. TIC of *L. pleurocaulis* Yunnan type (Sample 14)

RT(min)	Area %	Compound	Source
3.816	4.449	α-Pinene	Wiley
4.198	8.040	β-Pinene	Wiley
4.271	0.760	β-Myrcene	Wiley
4.418	14.958	α-Phellandrene	Wiley
4.470	0.870	3-Carene	Wiley
4.586	3.899	p-Cymene	Wiley
7.094	0.962	unknown, m/z = 204	
7.339	1.776	Selina-4,11-diene	MassFinder
7.385	0.798	unknown, m/z = 204	
8.018	2.786	β-Selinene	Wiley
8.319	0.985	unknown, m/z = 222	
8.843	0.837	10-epi-γ-Eudesmol	MassFinder
9.013	1.480	β-Eudesmol	Wiley
12.392	3.704	6β-OiBu-FE-1(10)-en-3β-ol	
13.376	**30.511**	6β-OAng-FE-1(10)-en-3β-ol	Literature [11]
13.628	12.440	6β-OTig-FE-1(10)-en-3β-ol	Literature [11]
13.861	7.756	3β-O-Ang-FE-1(10)-en-6β-ol	Literature [11]
14.468	2.987	unknown, m/z = 346	

Table 48. GC-MS result of *L. pleurocaulis* Yunnan type (Sample 14)

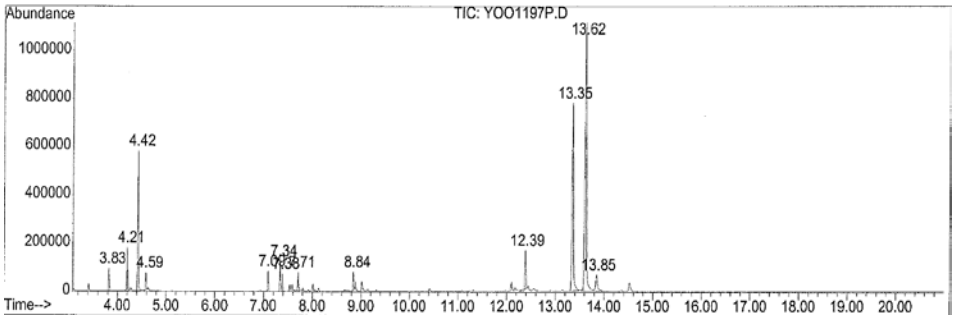

Figure 92. TIC of *L. pleurocaulis* (Sample 18), measured after several days of extraction

RT (min)	Area %	Compound	Source
3.827	1.730	α-Pinene	Wiley
4.207	3.428	β-Pinene	Wiley
4.424	10.788	α-Phellandrene	Wiley
4.592	1.346	p-Cymene	Wiley
7.094	1.465	unknown, m/z = 204	
7.340	2.543	Selina-4,11-diene	MassFinder
7.384	1.452	unknown, m/z = 204	
7.711	1.402	Guaia-6,9-diene	MassFinder
8.844	1.298	10-epi-γ-Eudesmol	MassFinder
12.387	3.501	6β-OiBu-FE-1(10)-en-3β-ol	
13.350	26.667	6β-OAng-FE-1(10)-en-3β-ol	Literature [11]
13.615	**40.745**	6β-OTig-FE-1(10)-en-3β-ol	Literature [11]
13.849	3.634	3β-OAng-FE-1(10)-en-6β-ol	Literature [11]

Table 49. GC-MS result of *L. pleurocaulis* Yunnan type (Sample 18), measured after several days of extraction

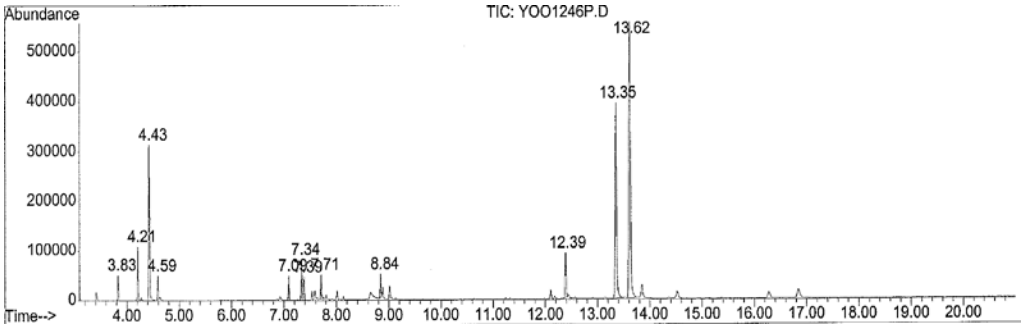

Figure 93. TIC of *L. pleurocaulis* Yunnan type (Sample 18), extraction time = 1 month

RT (min)	Area %	Compound	Source
3.829	1.965	α-Pinene	Wiley
4.208	3.904	β-Pinene	Wiley
4.425	11.504	α-Phellandrene	Wiley
4.593	1.892	p-Cymene	Wiley
7.095	1.701	unknown, m/z = 204	
7.340	3.050	Selina-4,11-diene	MassFinder
7.386	1.684	unknown, m/z = 204	
7.711	1.625	Guaia-6,9-diene	MassFinder
8.844	1.688	10-epi-γ-Eudesmol	MassFinder
12.390	4.278	6β-OiBu-FE-1(10)-en-3β-ol	
13.354	26.067	6β-OAng-FE-1(10)-en-3β-ol	Literature [11]
13.616	**40.642**	6β-OTig-FE-1(10)-en-3β-ol	Literature [11]

Table 50. GC-MS result of *L. pleurocaulis* Yunnan type (Sample 18), extraction time = 1 month

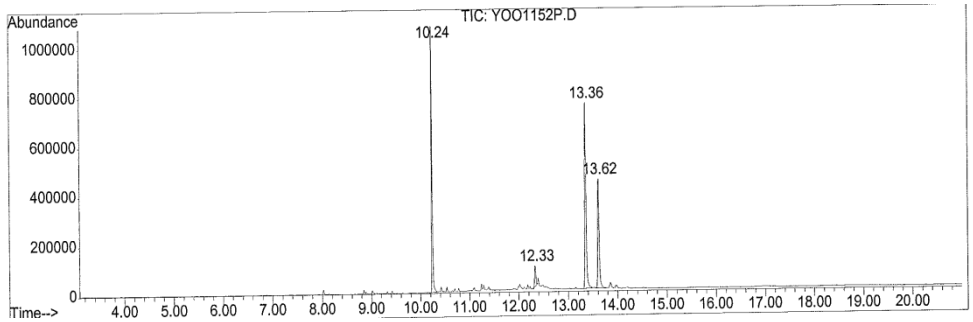

Figure 94. TIC of *L. pleurocaulis* Sichuan type (Sample 1)

RT(min)	Area %	Compound	Source
10.241	33.484	Furanoligularenone	MassFinder
12.331	3.510	unknown, m/z = 331	
13.356	**38.434**	6β-OAng-FE-1(10)-en-3β-ol	Literature [11]
13.617	24.573	6β-OTig-FE-1(10)-en-3β-ol	Literature [11]

Table 51. GC-MS result of *L. pleurocaulis* Sichuan type (Sample 1)

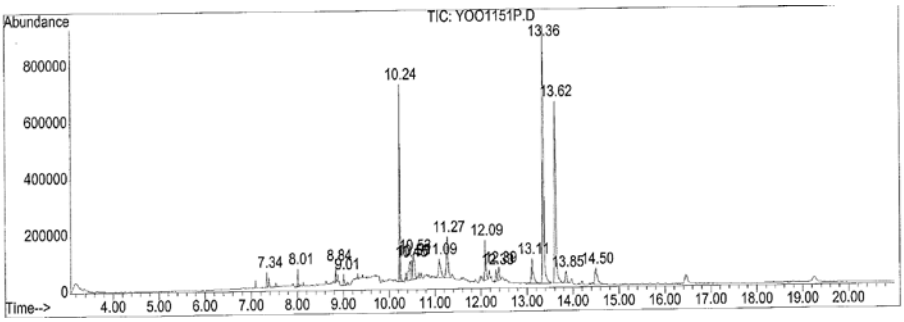

Figure 95. TIC of *L. pleurocaulis* Sichuan type (Sample 2)

RT (min)	Area %	Compound	Source
7.338	0.960	Selina-4,11-diene	MassFinder
8.012	1.178	Eremophila-1(10), 11-diene	Wiley
8.840	0.897	unknown	Wiley
9.010	0.914	β-Eudesmol	Wiley
10.238	10.808	Furanoligularenone	MassFinder
10.454	2.839	GC Septum bleed	
10.497	2.666	GC Septum bleed	
10.532	3.964	GC Septum bleed	
11.094	3.295	unknown	
11.273	6.179	GC Septum bleed	
12.092	4.080	GC Septum bleed	
12.327	1.086	unknown	
12.391	1.177	unknown	
13.116	4.079	GC Septum bleed	
13.357	**28.361**	6β-OAng-FE-1(10)-en-3β-ol	Literature [11]
13.618	22.252	6β-OTig-FE-1(10)-en-3β-ol	Literature [11]
13.853	1.641	3β-OAng-FE-1(10)-en-6β-ol	Literature [11]
14.502	3.625	GC Septum bleed	

Table 52. GC-MS result of *L. pleurocaulis* Sichuan type (Sample 2)

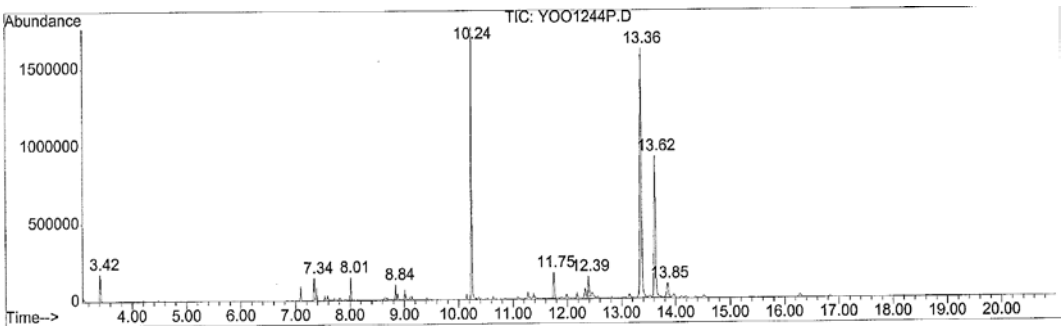

Figure 96. TIC of *L. pleurocaulis* Sichuan type (Sample 16)

RT (min)	Area %	Compound	Source
3.416	2.443	1-Nonene	Wiley
7.340	1.640	Selina-4,11-diene	MassFinder
8.014	2.024	Eremophila-1(10),11-diene	Wiley
10.239	23.362	Furanoligularenone	MassFinder
11.755	2.884	unknown, m/z = 276	
12.389	2.487	6β-OiBu-FE-1(10)-en-3β-ol	
13.362	**40.351**	6β-OAng-FE-1(10)-en-3β-ol	Literature [11]
13.619	22.098	6β-OTig-FE-1(10)-en-3β-ol	Literature [11]
13.850	2.710	3β-OAng-FE-1(10)-en-6β-ol	Literature [11]

Table 53. GC-MS result of *L.pleurocaulis* Sichuan type. (Sample 16)

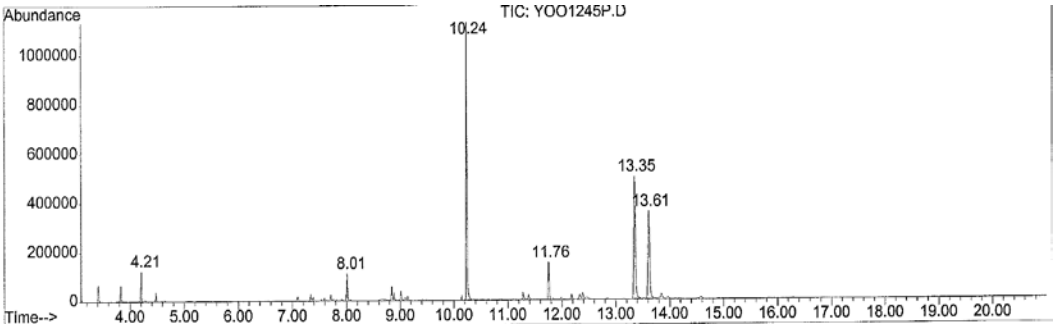

Figure 97. TIC of *L. pleurocaulis* Sichuan type (Sample 17)

RT (min)	Area %	Compound	Source
4.209	3.694	β-Pinene	Wiley
8.014	3.598	Eremophila-1(10),11-diene	Wiley
10.239	**38.392**	Furanoligularenone	MassFinder
11.757	5.667	unknown, m/z = 276	
13.354	27.333	6β-OAng-FE-1(10)-en-3β-ol	Literature [11]
13.615	21.316	6β-OTig-FE-1(10)-en-3β-ol	Literature [11]

Table 54. GC-MS result of *L.pleurocaulis* Sichuan type (Sample 17)

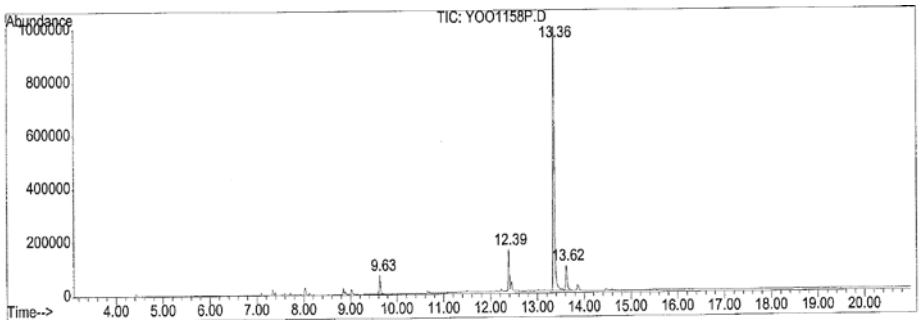

Figure 98. TIC of *L. pleurocaulis* (Sample 3)

RT(min)	Area %	Compound	Source
9.632	4.774	3-Desoxyneopetasol	MassFinder
12.392	7.700	6β-OiBu-FE-1(10)-en-3β-ol	
13.358	**78.684**	6β-OAng-FE-1(10)-en-3β-ol	Literature [11]
13.618	8.843	6β-OTig-FE-1(10)-en-3β-ol	Literature [11]

Table 55. GC-MS result of *L. pleurocaulis* (Sample 3)

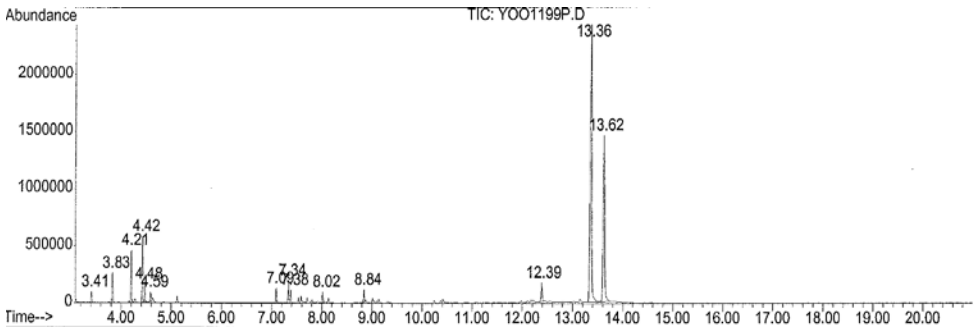

Figure 99. TIC of *L. pleurocaulis* (Sample 19), measured after several days of extraction

RT (min)	Area %	Compound	Source
3.413	1.013	1-Nonene	Wiley
3.826	2.559	α-Pinene	Wiley
4.205	4.625	β-Pinene	Wiley
4.423	5.516	α-Phellandrene	Wiley
4.476	1.643	3-Carene	Wiley
4.591	0.736	p-Cymene	Wiley
7.094	1.160	unknown, m/z = 204	
7.339	2.119	Selina-4,11-diene	MassFinder
7.384	1.170	unknown, m/z = 204	
8.016	1.083	Eremophila-1(10),11-diene	Wiley
8.843	0.972	10-epi-γ-Eudesmol	MassFinder
12.389	2.037	6β-OiBu-FE-1(10)-en-3β-ol	
13.363	**46.264**	6β-OAng-FE-1(10)-en-3β-ol	Literature [11]
13.622	29.104	6β-OTig-FE-1(10)-en-3β-ol	Literature [11]

Table 56. GC-MS result of *L. pleurocaulis* (Sample 19), measured after several days of extraction

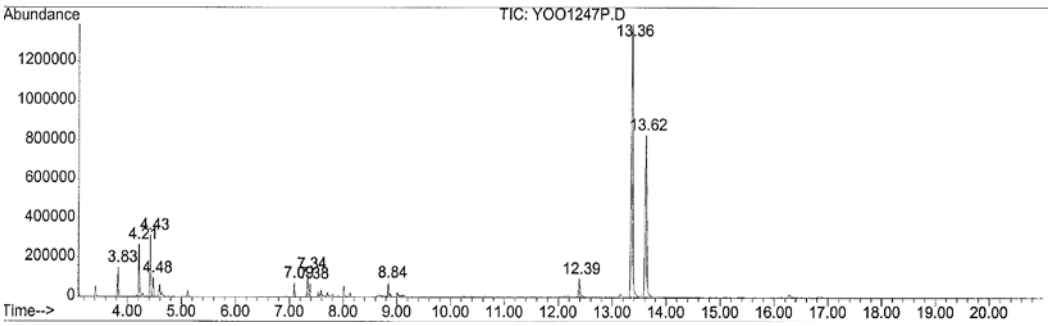

Figure 100. TIC of *L. pleurocaulis* (Sample 19), extraction time = 1 month

RT (min)	Area %	Compound	Source
3.829	2.701	α-Pinene	Wiley
4.208	4.827	β-Pinene	Wiley
4.425	5.587	α-Phellandrene	Wiley
4.478	1.719	3-Carene	Wiley
4.593	0.867	p-Cymene	Wiley
7.095	1.251	unknown, m/z = 204	
7.340	2.261	Selina-4,11-diene	MassFinder
7.384	1.226	unknown, m/z = 204	
8.843	1.113	10-epi-γ-Eudesmol	MassFinder
12.389	2.239	6β-OiBu-FE-1(10)-en-3β-ol	
13.361	**46.236**	6β-OAng-FE-1(10)-en-3β-ol	Literature [11]
13.619	29.973	6β-OTig-FE-1(10)-en-3β-ol	Literature [11]

Table 57. GC-MS result of *L. pleurocaulis* (Sample 19), extraction time = 1 month

6.2.7. L. dictyoneura

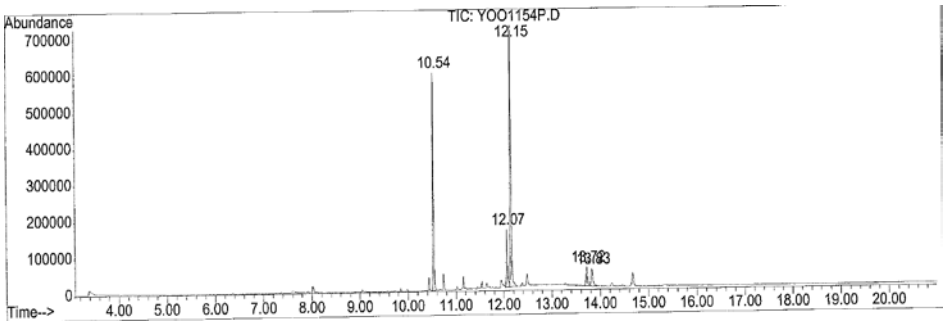

Figure 101. TIC of *L. dictyoneurea* type 1 (Sample 7)

RT(min)	Area %	Compound	Source
10.536	29.115	unknown, m/z = 278	
12.065	11.349	unknown, m/z = 290	
12.150	**48.571**	*unknown*, m/z = 290	
13.719	4.939	3β-OAc-6β-OAng-FE	MassFinder
13.827	6.026	6β-OAng-FE-10β-ol	Literature [10]

Table 58. GC-MS result of *L. dictyoneura* type 1 (Sample 7)

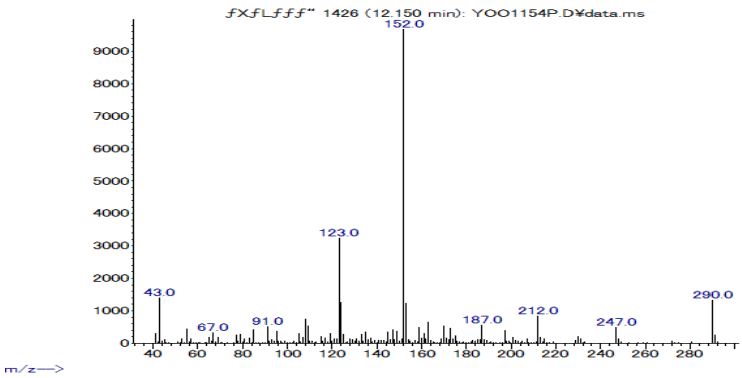

Figure 102. EI mass spectrum of *L. dictyoneura* type 1 at RT 12.150 min. (Sample 7)

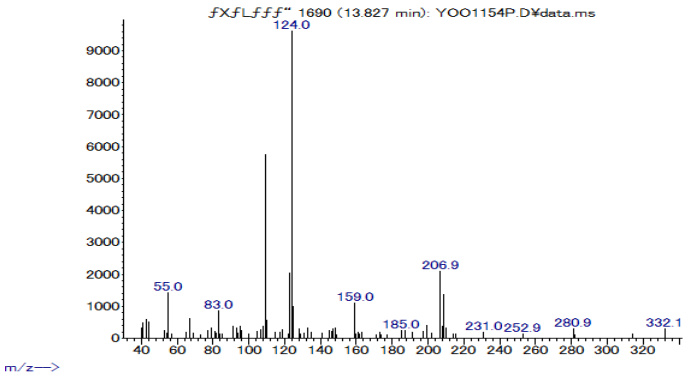

Figure 103. EI mass spectrum of *L. dictyoneura* type 1 at RT 13.827 min. (Sample 7)

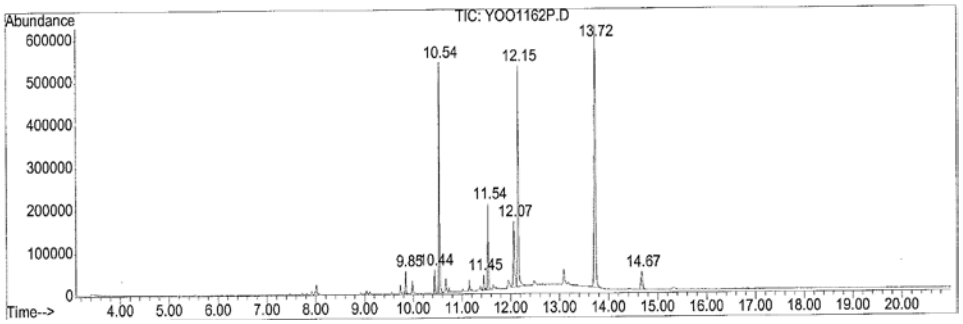

Figure 104. TIC of *L. dictyoneurea* type 1 (Sample 3)

RT(min)	Area%	Compound	Source
9.846	1.764	Ligularol ethyl ether	
10.439	1.739	unknown, m/z = 232	
10.536	16.505	unknown, m/z = 232	
11.448	1.295	unknown, m/z = 281	
11.543	7.217	6β-OAng-FE	
12.065	7.851	unknown, m/z = 290	
12.150	22.982	unknown, m/z = 290	
13.723	**37.705**	3β-OAc-6β-OAng-FE	MassFinder
14.677	2.941	3β-OAc-6β-OAng-FE-10β-ol	Literature [10]

Table 59. GC-MS result of *L. dictyoneura* type 1 (Sample 3)

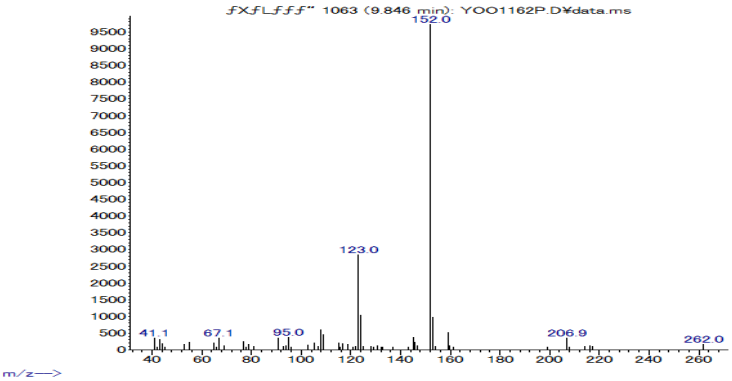

Figure 105. EI mass spectrum of L. dictyoneura type 1 at RT 9.846 min. (Sample 3)

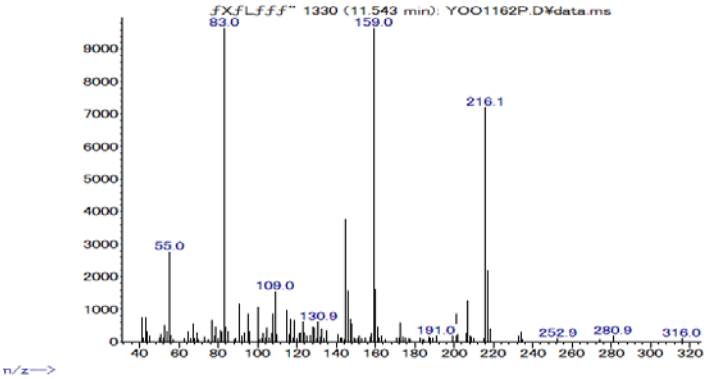

Figure 106. EI mass spectrum of *L. dictyoneura* type 1 at RT 11.543 min. (Sample 3)

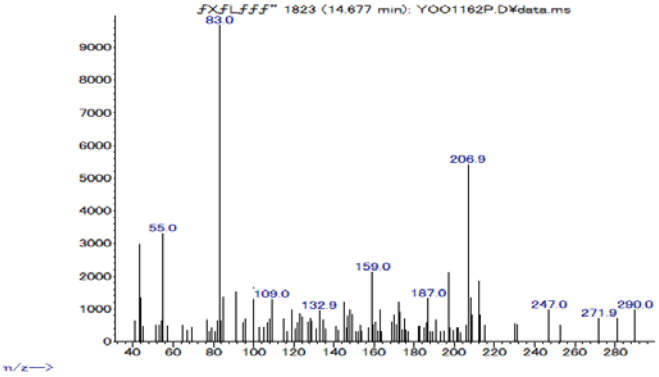

Figure 107. EI mass spectrum of *L. dictyoneura* type 1 at RT 14.677 min. (Sample 3)

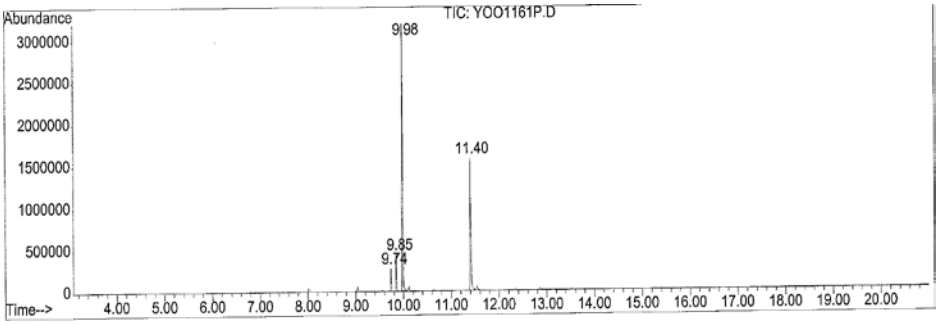

Figure 108. TIC of *L. dictyoneura* type 2 (Sample 4)

RT(min)	Area %	Compound	Source
9.738	4.374	Ligularol methyl ether	
9.846	7.078	Ligularol ethyl ether	
9.984	**54.721**	Ligularol	MassFinder
11.401	33.826	FE-15,6α-olide	MassFinder

Table 60. GC-MS result of *L. dictyoneura* type 2 (Sample 4)

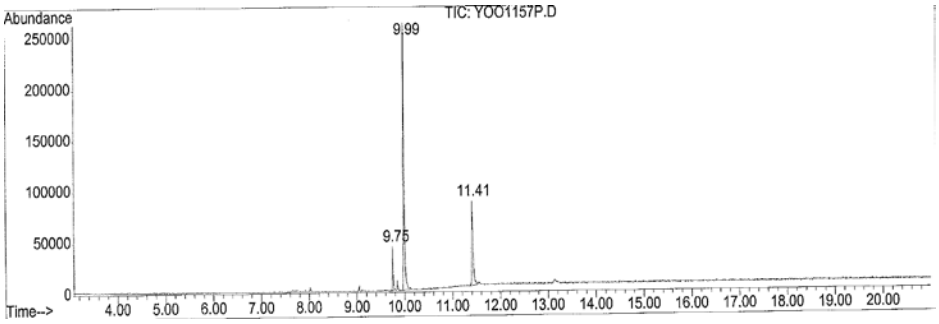

Figure 109. TIC of *L. dictyoneura* type 2 (Sample 5)

RT(min)	Area %	Compound	Source
9.750	9.217	Ligularone	MassFinder
9.988	**62.085**	Ligularol	MassFinder
11.410	28.698	FE-15,6α-olide	MassFinder

Table 61. GC-MS result of *L. dictyoneura* type 2 (Sample 5)

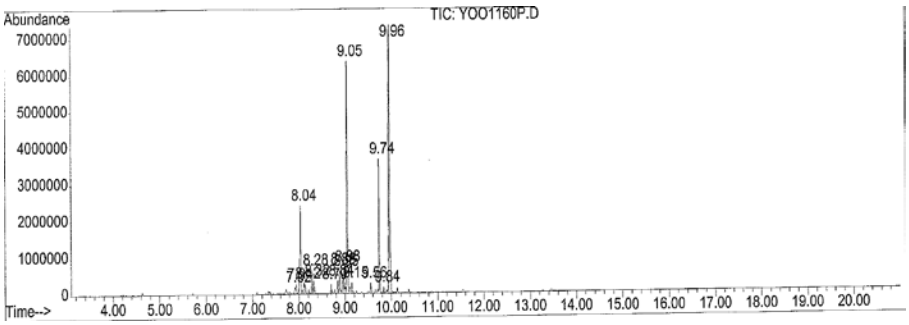

Figure 110. TIC of *L. dictyoneura* type 3 (Sample 8)

RT(min)	Area %	Compound	Source
8.035	10.245	unknown, m/z = 222	
9.049	23.097	Furanoeremophilane	MassFinder
9.738	11.837	Ligularol methyl ether	
9.962	**36.342**	Fukinanolide	MassFinder

Table 62. GC-MS result of *L. dictyoneura* type 3 (Sample 8), major peaks

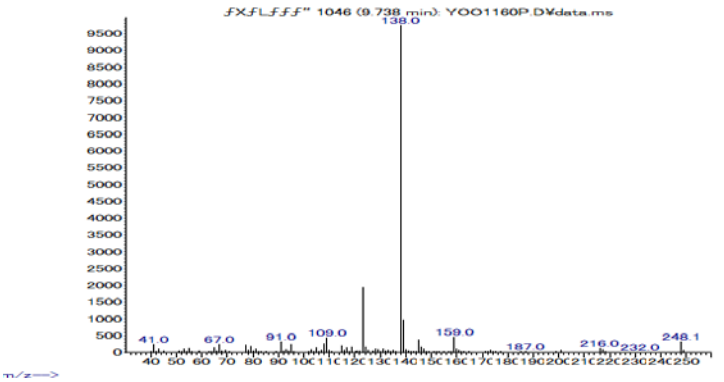

Figure 111. EI mass spectrum of *L. dictyoneura* type 3 at RT 9.738 min. (Sample 8)

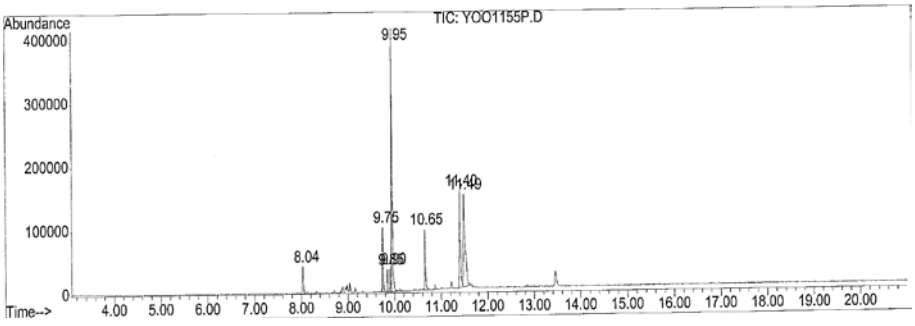

Figure 112. TIC of *L. dictyoneura* type 4 (Sample 1)

RT (min)	Area %	Compound	Source
8.038	4.013	unknown, m/z = 253	
9.747	7.821	Ligularone	MassFinder
9.845	2.205	Ligularol ethyl ether	
9.904	3.011	Dehydrofukinone	MassFinder
9.951	**32.858**	Fukinanolide	MassFinder
10.651	9.058	Ethyl palmitate	MassFinder
11.405	15.191	FE-15,6α-olide	MassFinder
11.492	25.843	9,12-Octadecadienoic acid, ethyl ester	Wiley

Table 63. GC-MS result of *L. dictyoneura* type 4 (Sample 1)

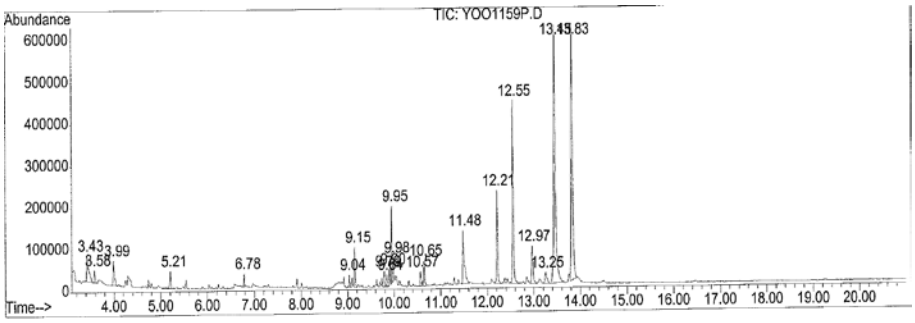

Figure 113. TIC of *L. dictyoneura* type 5 (Sample 2), Injection = splitless

RT (min)	Area %	Compound	Source
9.900	0.855	Dehydrofukinone	MassFinder
9.949	3.537	Fukinanolide	MassFinder
9.983	1.057	Ligularol	MassFinder
10.647	1.598	Ethyl palmitate	MassFinder
11.484	5.418	9,12-Octadecadienoic acid ethyl ester	Wiley
12.215	5.967	unknown, m/z = 314	
12.555	12.275	unknown, m/z = 314	
12.966	3.230	Petasin	MassFinder
13.253	1.387	unknown, m/z = 331	
13.455	**27.167**	unknown, m/z = 316	
13.826	24.442	3β-OAng-ligularol	Literature [10]

Table 64. GC-MS result of *L. dictyoneura* type 5 (Sample 2), major peaks

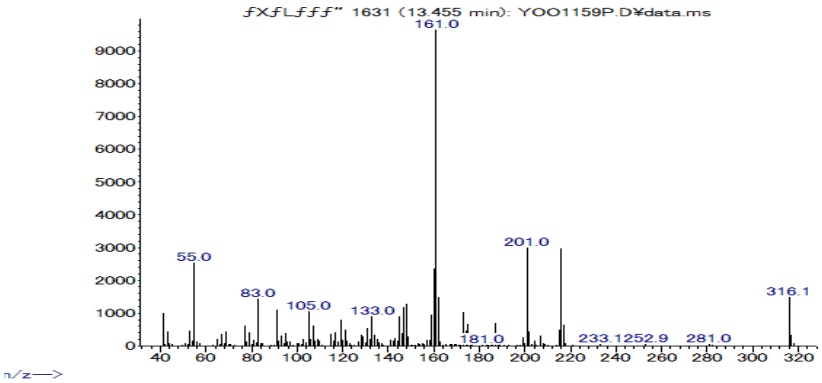

Figure 114. EI mass spectrum of *L. dictyoneura* type 5 at RT 13.455 min. (Sample 2)

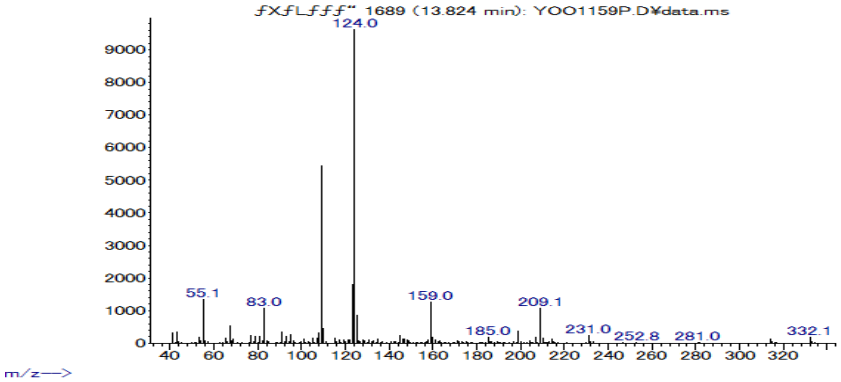

Figure 115. EI mass spectrum of *L. dictyoneura* type 5 at RT 13.824 min. (Sample 2)

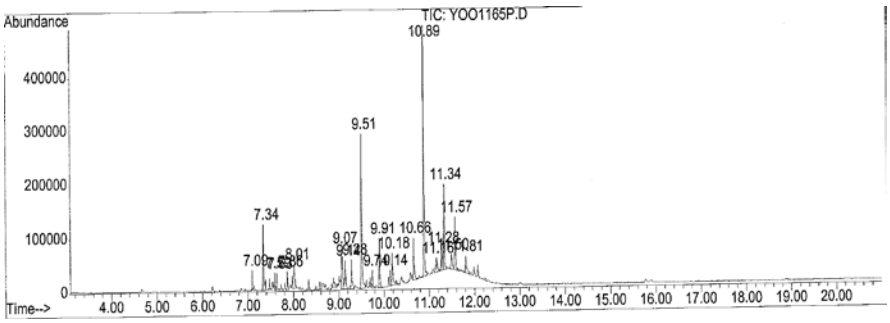

Figure 116. TIC of *L. dictyoneura* type 6 (Sample 9)

RT (min)	Area %	Compound	Source
7.340	5.931	Selina-4,11-diene	MassFinder
8.014	3.202	Eremophila-1(10),11-diene	Wiley
9.069	4.592	γ-Selinene	Wiley
9.509	14.684	unknown, m/z = 260	
9.907	4.114	unknown, m/z = 276	
10.142	1.252	unknown, m/z = 232	
10.184	3.455	unknown, m/z = 230	
10.658	4.545	6β-OAc-FE-1(10)-ene	
10.889	**19.140**	6β-OAc-1,10-epoxy-FE	MassFinder
11.160	2.462	unknown, m/z = 281	
11.281	3.133	unknown, m/z = 281	
11.338	9.313	6β-{2-[(hydroxymethyl)prop-2-enoyl]oxy}-FE-1(10)-ene	Literature [10]
11.496	1.733	unknown, m/z = 281	
11.573	5.334	6β-{2-[(hydroxymethyl)prop-2-enoyl]oxy}-1,10-epoxy-FE	Literature [10]
11.810	2.487	unknown, m/z = 281	

Table 65. GC-MS result of *L. dictyoneura* type 6 (Sample 9), major peaks

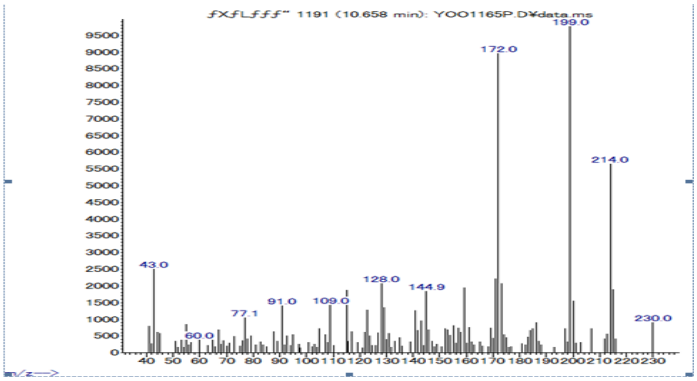

Figure 117. EI mass spectrum of *L. dictyoneura* type 6 at RT 10.658 min. (Sample 9)

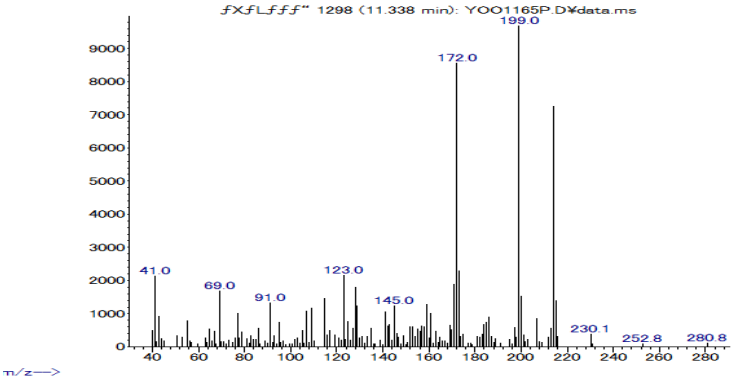

Figure 118. EI mass spectrum of *L. dictyoneura* type 6 at RT 11.338 min. (Sample 9)

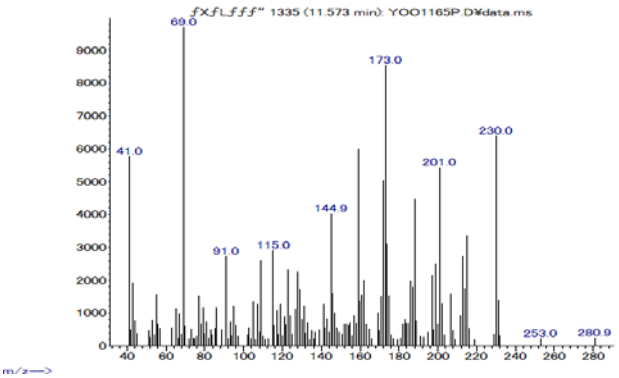

Figure 119. EI mass spectrum of *L. dictyoneura* type 6 at RT 11.573 min. (Sample 9)

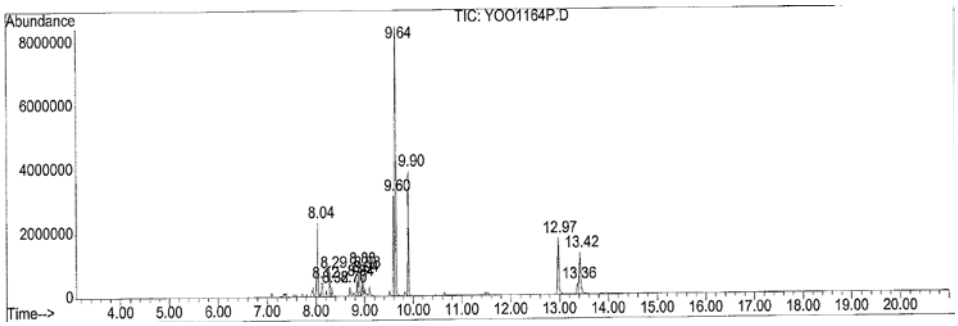

Figure 120. TIC of *L. dictyoneura* Ehrlich neg. (Sample 6)

RT (min)	Area %	Compound	Source
8.036	8.933	10-epi-Dihydroagarofuran	MassFinder
8.119	2.529	unknown, m/z = 222	
8.285	1.989	unknown, m/z = 222	
8.321	1.320	unknown, m/z = 222	
8.697	1.082	unknown, m/z = 207	
8.841	1.451	γ-Eudesmol	Wiley
8.880	2.831	unknown, m/z = 222	
8.945	1.650	unknown, m/z = 222	
8.976	1.795	unknown, m/z = 222	
9.601	9.397	3-Desoxyneopetasol	MassFinder
9.637	**36.854**	3-Desoxypetasol	Literature [10]
9.898	11.113	Dehydrofukinone	MassFinder
12.974	9.217	3-OTig-eremophila-9,11-dien-8-one	Literature [10]
13.361	1.703	Neopetasin	
13.419	8.136	Petasin	MassFinder

Table 66. GC-MS result of *L. dictyoneura* Ehrlich neg. (Sample 6)

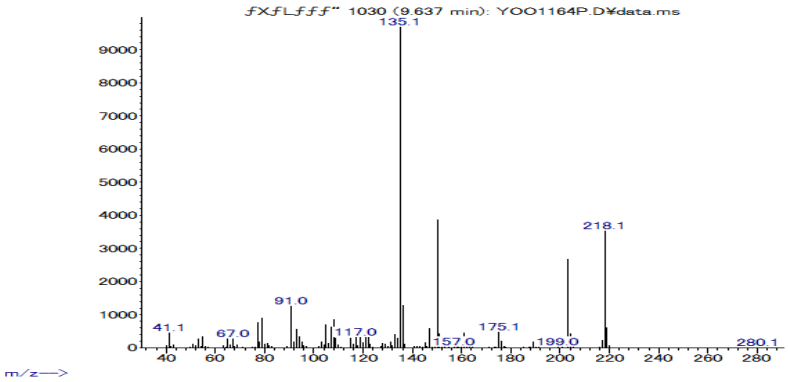

Figure 121. EI mass spectrum of L. dictyoneura Ehrlich neg. at RT 9.637 min. (Sample 6)

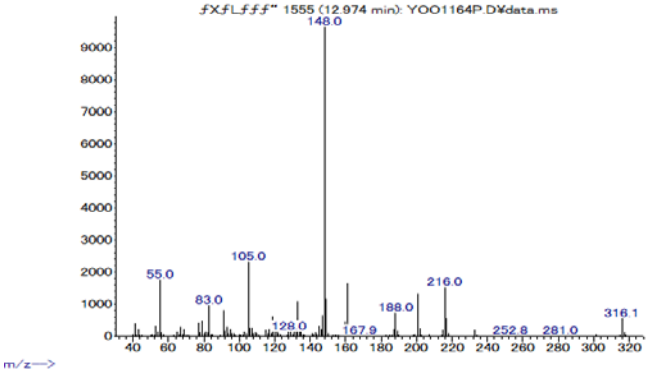

Figure 122. EI mass spectrum of L. dictyoneura Ehrlich neg. at RT 12.974 min. (Sample 6)

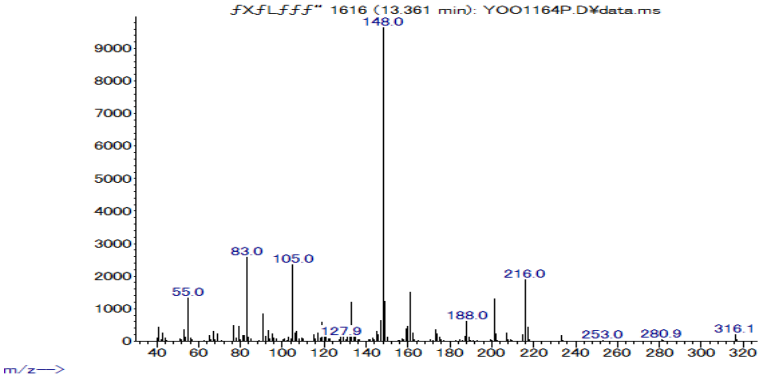

Figure 123. EI mass spectrum of L. dictyoneura Ehrlich neg. at RT 13.361 min. (Sample 6)

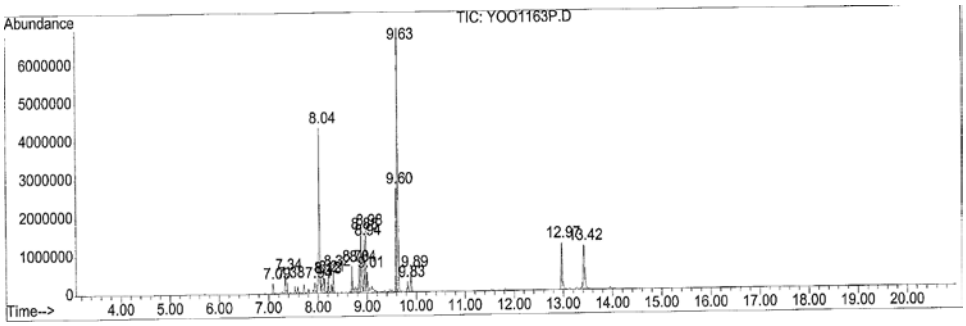

Figure 124. TIC of *L. dictyoneura* Ehrlich neg. (Sample 10)

RT (min)	Area %	Compound	Source
7.092	0.895	unknown, m/z = 204	
7.337	1.729	Selina-4,11-diene	MassFinder
7.382	0.907	unknown, m/z = 204	
7.941	1.222	Isoledene	Wiley
8.035	16.790	10-epi-Dihydroagarofuran	MassFinder
8.115	1.317	unknown, m/z = 222	
8.133	1.218	unknown, m/z = 222	
8.210	1.405	unknown, m/z = 220	
8.316	1.825	unknown, m/z = 222	
8.696	2.112	unknown, m/z = 220	
8.840	2.162	γ-Eudesmol	Wiley
8.880	4.482	unknown, m/z = 222	
8.945	3.986	unknown, m/z = 222	
8.978	4.779	unknown, m/z = 222	
9.007	1.682	unknown, m/z = 220	
9.598	8.092	3-Desoxyneopetasol	MassFinder
9.632	**28.489**	3-Desoxypetasol	Literature [10]
9.830	0.957	unknown, m/z = 222	
9.895	1.699	Dehydrofukinone	Wiley
12.972	6.372	3-OTig-eremophila-9,11-dien-8-one	Literature [10]
13.420	7.878	Petasin	MassFinder

Table 67. GC-MS result of *L. dictyoneura* Ehrlich neg. (Sample 10)

6.2.8. L. tongolensis

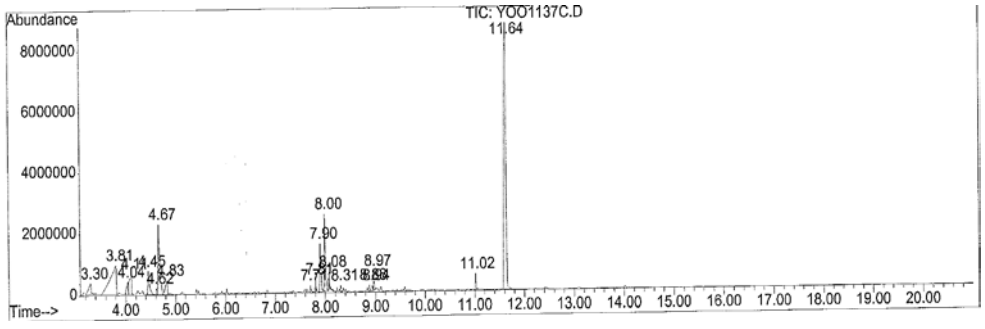

Figure 125. TIC of *L. tongolensis* type 2 (Sample 7)

RT (min)	Area %	Compound	Source
3.304	2.189	α-Methylbutyric acid	Wiley
3.807	14.630	Angelic acid	Wiley
4.040	1.658	β-Methylvaleric acid	Wiley
4.107	3.831	Isobutylacetic acid	Wiley
4.452	3.058	1-Phellandrene	Wiley
4.618	0.518	o-Cymene	Wiley
4.666	9.542	β-Phellandrene	Wiley
4.827	2.120	4-Methylhexanoic acid	Wiley
7.709	0.515	unknown, m/z = 204	
7.808	0.824	unknown, m/z = 204	
7.901	4.214	unknown, m/z = 204	
7.998	5.907	β-Longipinene	MassFinder
8.075	0.875	β-Bisabolene	Wiley
8.312	0.509	unknown, m/z = 204	
8.881	0.354	unknown, m/z = 222	
8.940	0.293	unknown, m/z = 234	
8.973	1.167	unknown, m/z = 222	
11.016	1.031	unknown, m/z = 244	
11.643	**46.765**	FE-3-en-15,6α-olide	Literature [9]

Table 68. GC-MS result of *L. tongolensis* type 2 (Sample 7)

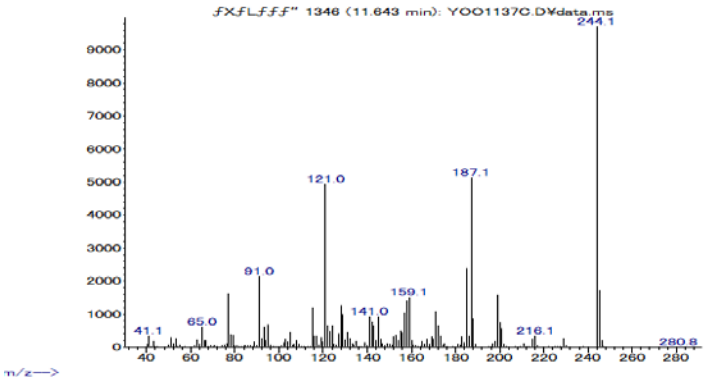

Figure 126. EI mass spectrum of *L. tongolensis* type 2 at RT 11.643 min. (Sample 7)

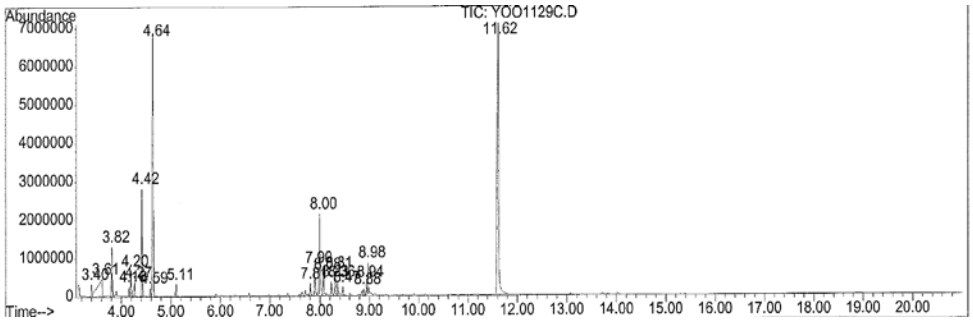

Figure 127. TIC of *L. tongolensis* type 2 (Sample 8)

RT (min)	Area %	Compound	Source
3.402	0.890	1-Nonene	Wiley
3.611	7.341	2-Methyl-2-butenoic acid	Wiley
3.817	3.284	α-Pinene	Wiley
4.156	0.621	Sabinene	Wiley
4.199	1.714	β-Pinene	Wiley
4.270	0.941	β-Myrcene	Wiley
4.418	6.444	1-Phellandrene	Wiley
4.586	0.565	o-Cymene	Wiley
4.641	22.308	β-Phellandrene	MassFinder
5.113	0.709	α-Terpinolene	Wiley
7.809	1.002	unknown, m/z = 204	
7.901	2.100	γ-Curcumene	Wiley
7.998	6.139	β-Longipinene	MassFinder
8.076	1.704	β-Bisabolene	Wiley
8.233	0.920	unknown, m/z = 204	
8.313	1.844	unknown, m/z = 204	
8.359	0.805	unknown, m/z = 204	
8.467	0.608	Germacra-1(10),4,7(11)-triene	Wiley
8.884	0.469	unknown, m/z = 222	
8.941	0.749	unknown, m/z = 234	
8.975	1.812	unknown, m/z = 236	
11.623	**37.030**	FE-3-en-15,6α-olide	Literature [9]

Table 69. GC-MS result of *L. tongolensis* type 2 (Sample 8)

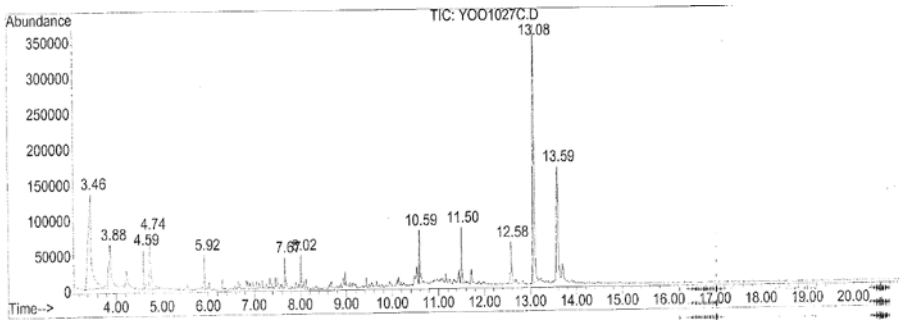

Figure 128. TIC of *L. tongolensis* type 1 (Sample 5)

RT (min)	Area %	Compound	Source
3.460	**25.430**	2-Methyl-2-butenoic acid	Wiley
3.879	7.533	unknown, m/z = 100	
4.593	2.129	o-Cymene	Wiley
4.736	6.550	4-Methylhexanoic acid	Wiley
5.916	1.995	Cryptone	MassFinder
7.669	1.718	unknown, m/z = 168	
8.016	1.887	Eremophila-1(10),11-diene	MassFinder
10.593	3.901	unknown, m/z = 250	
11.501	4.053	unknown, m/z = 232	
12.577	4.652	unknown, m/z = 276	
13.072	26.288	*unknown*, m/z = 258	
13.587	13.865	*unknown*, m/z = 276	

Table 70. GC-MS result of *L. tongolensis* type 1 (Sample 5)

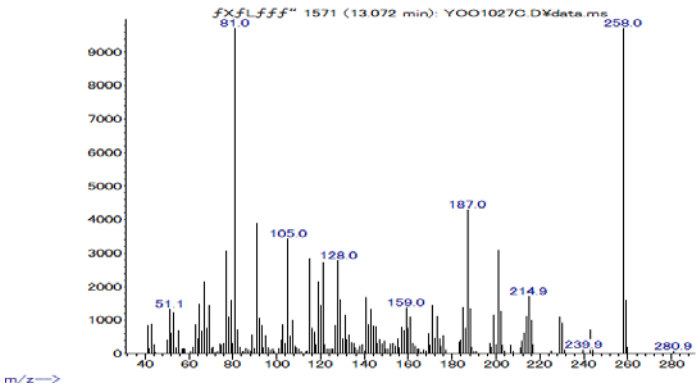

Figure 129. EI mass spectrum of *L. tongolensis* type 1 at RT 13.072 min. (Sample 5)

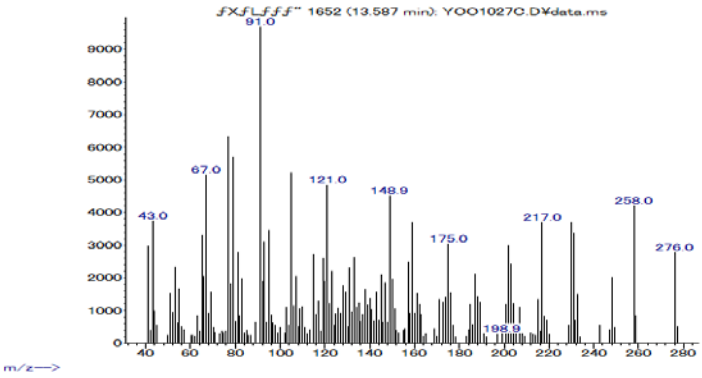

Figure 130. EI mass spectrum of *L. tongolensis* type 1 at RT 13.587 min. (Sample 5)

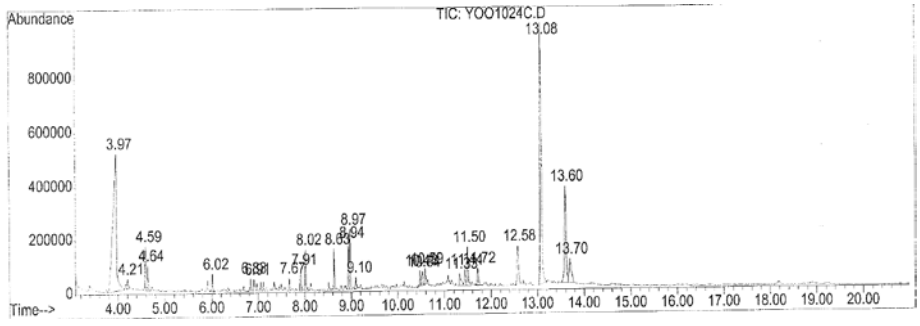

Figure 131. TIC of *L. tongolensis* type 1 (Sample 2)

RT (min)	Area %	Compound	Source
3.968	**31.701**	3-Methylpentanoic acid	Wiley
4.206	0.419	β-Pinene	Wiley
4.589	1.764	o-Cymene	Wiley
4.640	1.100	β-Phellandrene	Wiley
5.914	0.522	Cryptone	MassFinder
7.915	1.582	α-Curcumene	Wiley
8.016	2.433	Eremophila-1(10),11-diene	Wiley
8.630	1.819	β-Caryophyllene epoxide	Wiley
10.476	0.926	Palmitic acid	Wiley
11.329	1.277	cis,cis-Linoleic acid	Wiley
11.444	1.203	unknown, m/z = 232	
11.499	2.552	unknown, m/z = 232	
11.717	1.371	unknown, m/z = 232	
12.579	3.647	unknown, m/z = 276	
13.084	23.104	unknown, m/z = 258	
13.602	10.300	unknown, m/z = 276	
13.699	3.445	unknown, m/z = 260	

Table 71. GC-MS result of *L. tongolensis* type 1 (Sample 2), characteristic peaks

6.2.9. L. cymbulifera

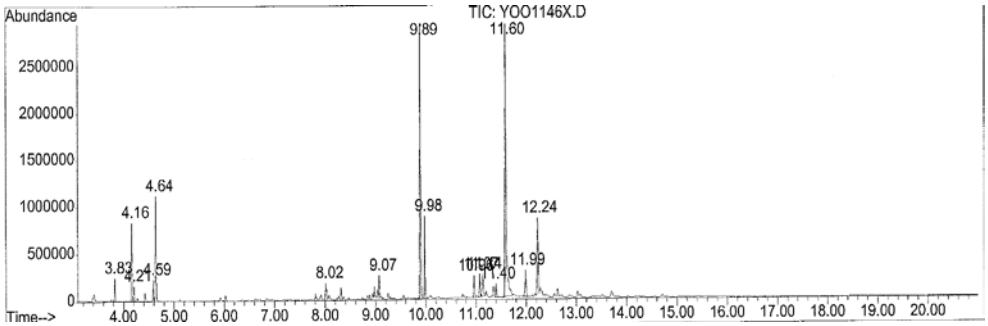

Figure 132. TIC of *L. cymbulifera* (No. 09 43)

RT (min)	Area %	Compound	Source
3.828	1.516	α-Pinene	Wiley
4.165	5.326	Sabinene	Wiley
4.208	1.160	β-Pinene	Wiley
4.591	1.435	p-Cymene	Wiley
4.642	7.641	β-Thujene	Wiley
8.015	1.973	Eremophila-1(10),11-diene	Wiley
9.076	1.556	Eremophil-1(10)-en-11-ol	Literature [9]
9.889	20.902	FE-10β-ol	Literature [9]
9.983	6.396	Ligularol	MassFinder
10.965	1.906	unknown, m/z = 250	
11.075	1.744	unknown, m/z = 250	
11.135	2.905	unknown, m/z = 250	
11.400	1.275	FE-15,6α-olide	MassFinder
11.599	**33.215**	FE-3-en-15,6α-olide	Literature [9]
11.993	3.015	1-OMeAcr-ligularol	
12.241	8.034	unknown, m/z = 322	

Table 72. GC-MS result of *L. cymbulifera* (No. 09 43)

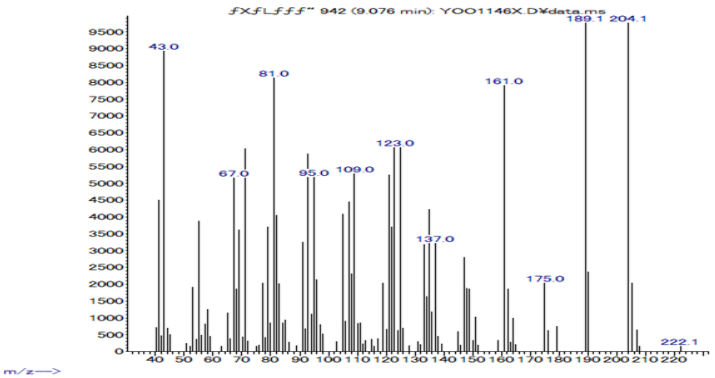

Figure 133. EI mass spectrum of *L. cymbulifera* at RT 9.076 min. (No.09 43)

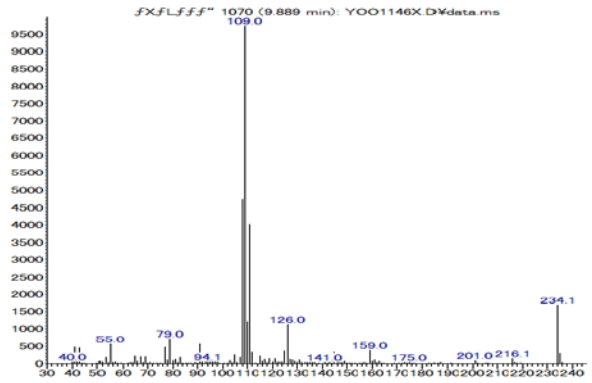

Figure 134. EI mass spectrum of *L. cymbulifera* at RT 9.889 min. (No.09 43)

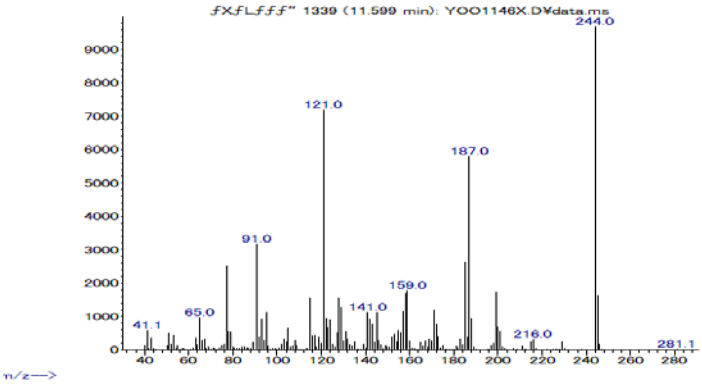

Figure 135. EI mass spectrum of *L. cymbulifera* at RT 11.599 min. (No. 09 43)

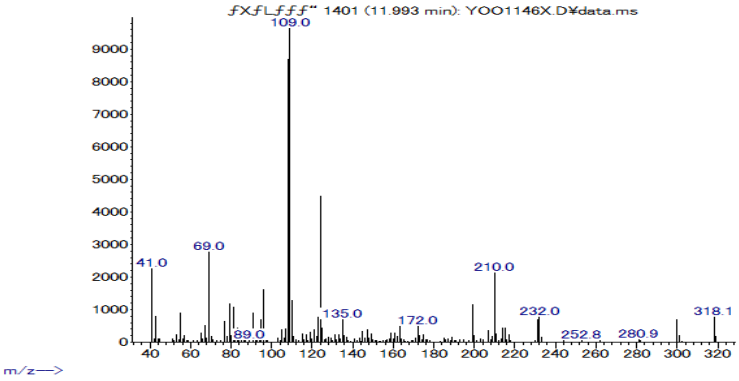

Figure 136. EI mass spectrum of *L. cymbulifera* at RT 11.993 min. (No. 09 43)

6.2.10. L. przewalskii

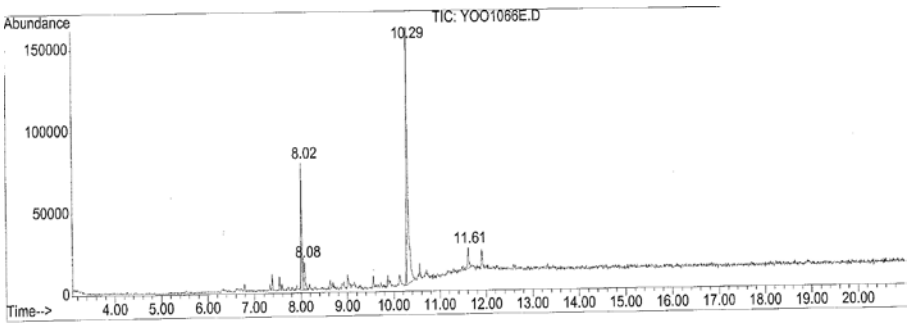

Figure 137. TIC of *L. przewalskii* (Sample 1)

RT (min)	Area %	Compound	Source
8.017	22.448	Eremophila-1(10),11-diene	Wiley
8.081	6.495	β-Bisabolene	Wiley
10.295	**66.571**	Euparin	MassFinder
11.612	4.486	unknown, m/z = 281	

Table 73. GC-MS result of *L. przewalskii* (Sample 1)

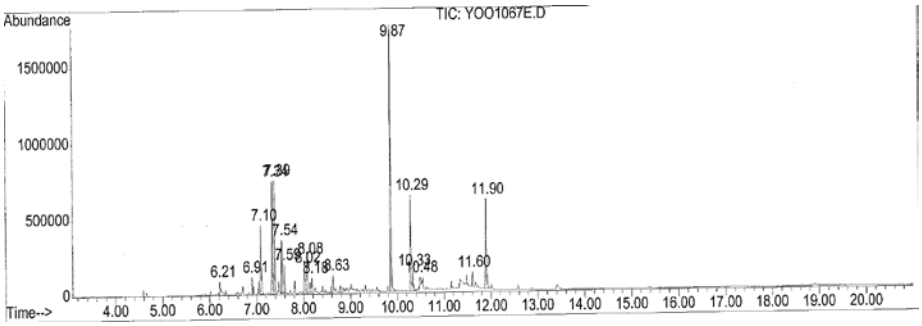

Figure 138. TIC of *L. przewalskii* (Sample 2)

RT (min)	Area %	Compound	Source
6.213	0.880	Thymol methyl ether	Wiley
6.906	1.718	unknown, m/z = 207	
7.095	7.337	unknown, m/z = 204	
7.341	10.539	unknown, m/z = 204	
7.386	9.767	unknown, m/z = 204	
7.539	4.455	unknown, m/z = 204	
7.591	2.633	β-Caryophyllene	Wiley
8.018	3.850	(-)-Alloaromadendrene	Wiley
8.075	3.348	β-Bisabolene	Wiley
8.180	1.275	β-Sesquiphellandrene	Wiley
8.630	1.510	β-Caryophyllene epoxide	Wiley
9.867	**26.037**	5,6-dimethoxy-2-(prop-1-en-2-yl)benzofuran	MassFinder
10.286	10.002	Euparin	MassFinder
10.334	2.708	unknown, m/z = 220	
10.484	0.635	Palmitic acid	Wiley
11.605	1.693	unknown, m/z = 318	
11.898	11.613	Toxol-3-OAng-6-OH	MassFinder

Table 74. GC-MS result of *L. przewalskii* (Sample 2)

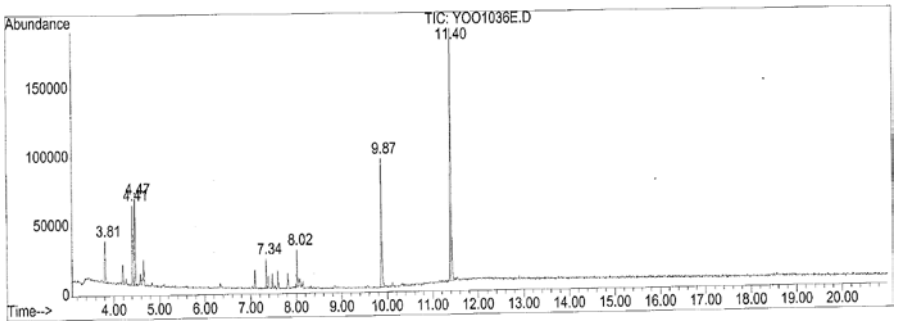

Figure 139. TIC of *L. przewalskii* (Sample 3)

RT (min)	Area %	Compound	Source
3.813	6.408	α-Pinene	MassFinder
4.413	10.205	α-Phellandrene	Wiley
4.466	11.849	3-Carene	MassFinder
7.341	3.463	Selina-4,11-diene	MassFinder
8.017	5.601	Valencene	MassFinder
9.873	21.246	5,6-dimethoxy-2-(prop-1-en-2-yl)benzofuran	MassFinder
11.404	**41.228**	FE-15,6-olide	MassFinder

Table 75. GC-MS result of *L. przewalskii* (Sample 3)

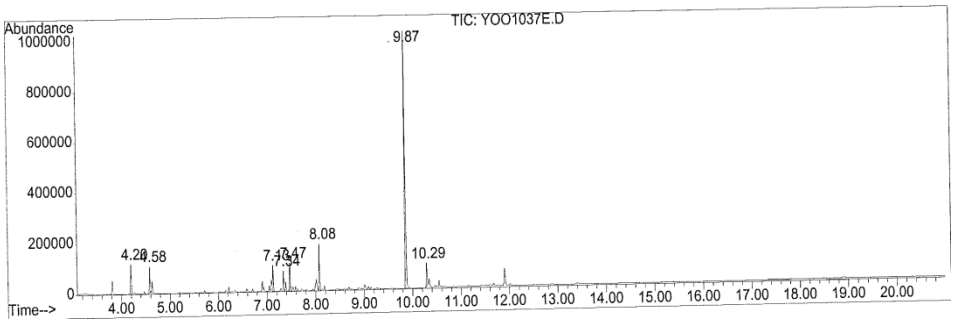

Figure 140. TIC of *L. przewalskii* (Sample 4)

RT (min)	Area %	Compound	Source
4.197	6.946	β-Pinene	MassFinder
4.583	5.219	p-Cymene	MassFinder
7.127	6.139	α-Longipinene	MassFinder
7.341	4.239	Selina-4,11-diene	MassFinder
7.472	6.521	γ-Maaliene	MassFinder
8.077	9.477	β-Bisabolene	MassFinder
9.867	**55.931**	5,6-dimethoxy-2-(prop-1-en-2-yl)benzofuran	MassFinder
10.291	5.528	Euparin	MassFinder

Table 76. GC-MS result of *L. przewalskii* (Sample 4)

6.2.11. L. sagitta

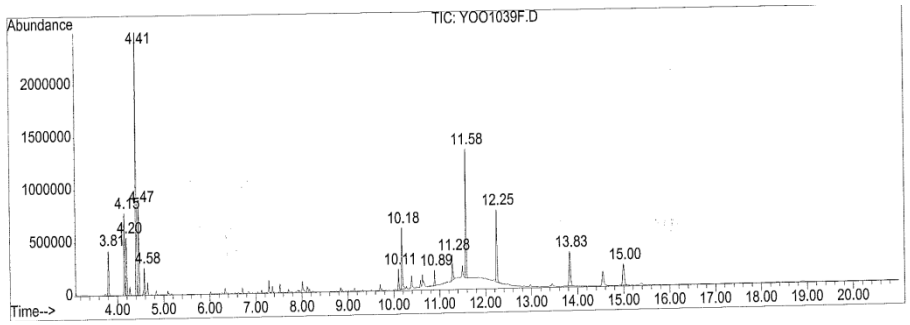

Figure 141. TIC of *L. sagitta* (Sample 2)

RT (min)	Area %	Compound	Source
3.813	4.863	α-Pinene	MassFinder
4.152	7.743	Sabinene	MassFinder
4.195	6.014	β-Pinene	MassFinder
4.415	**23.648**	α-Phellandrene	Wiley
4.467	8.614	3-Carene	MassFinder
4.582	2.476	o-Cymene	Wiley
10.106	2.225	unknown, m/z = 246	
10.183	6.253	unknown, m/z = 230	
10.892	1.453	unknown, m/z = 248	
11.280	2.983	unknown, m/z = 230	
11.581	13.598	*unknown*, m/z = 316	
12.248	9.125	*unknown*, m/z = 248	
13.831	6.237	unknown, m/z = 374	
14.997	4.769	unknown, m/z = 328	

Table 77. GC-MS result of *L. sagitta* (Sample 2)

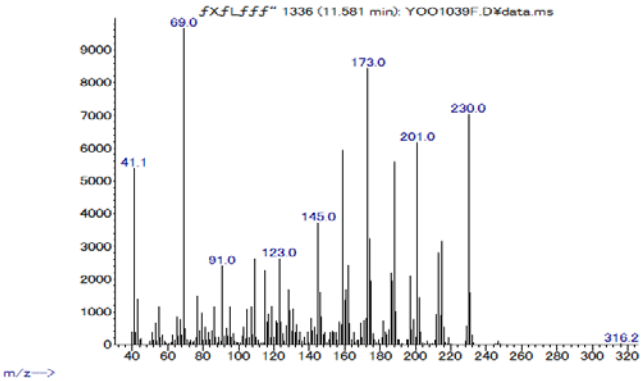

Figure 142. EI mass spectrum of *L. sagitta* at RT 11.581 min. (Sample 2)

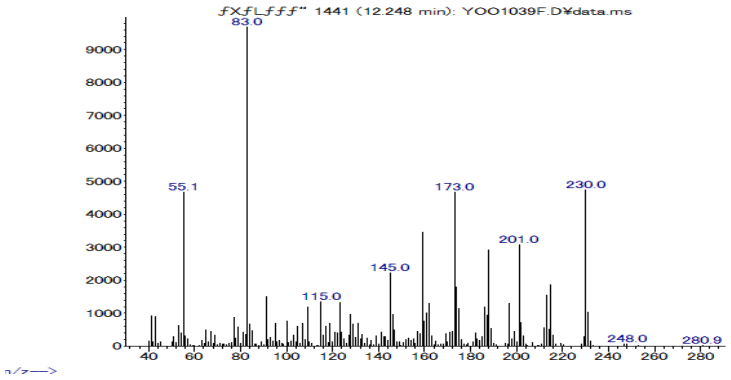

Figure 143. EI mass spectrum of *L. sagitta* at RT 12.248 min. (Sample 2)

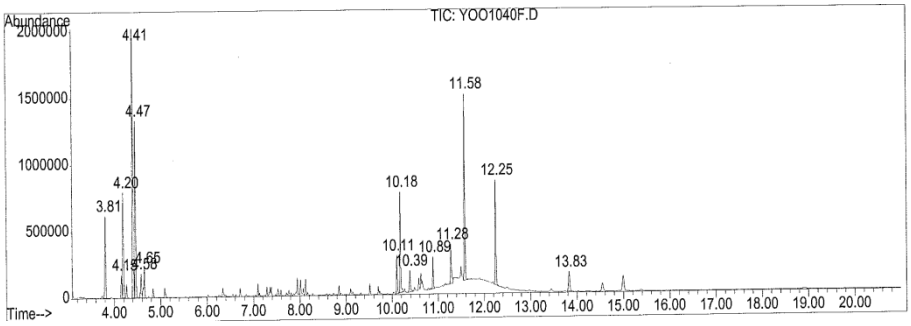

Figure 144. TIC of L. sagitta (Sample 3)

RT (min)	Area %	Compound	Source
3.814	6.970	α-Pinene	Wiley
4.152	1.806	Sabinene	Wiley
4.196	8.319	β-Pinene	Wiley
4.414	**20.915**	α-Phellandrene	Wiley
4.467	13.933	3-Carene	Wiley
4.582	2.090	o-Cymene	Wiley
4.655	3.054	cis-Ocimene	Wiley
10.105	2.620	unknown, m/z = 246	
10.183	6.810	unknown, m/z = 230	
10.388	2.004	unknown, m/z = 230	
10.891	2.428	unknown, m/z = 248	
11.278	3.755	unknown, m/z = 230	
11.581	13.573	unknown, m/z = 316	
12.247	9.180	unknown, m/z = 248	
13.832	2.543	unknown, m/z = 332	

Table 78. GC-MS result of *L. sagitta* (Sample 3)

6.3. MassFinder Library

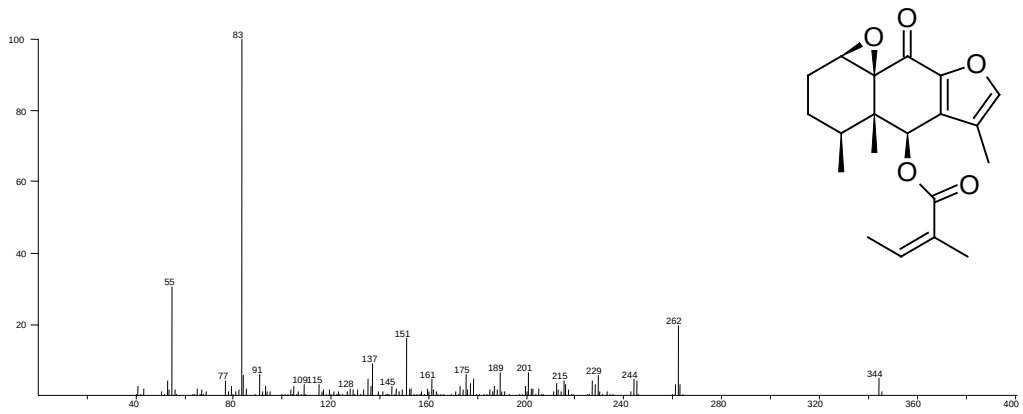

Figure 145. EI mass spectrum of compound **34** at RT 16.54 min.

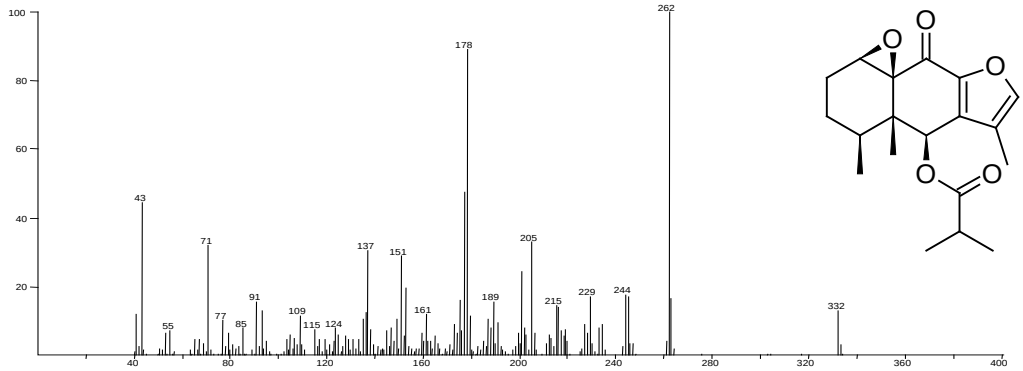

Figure 146. EI mass spectrum of compound **35** at RT 14.90 min.

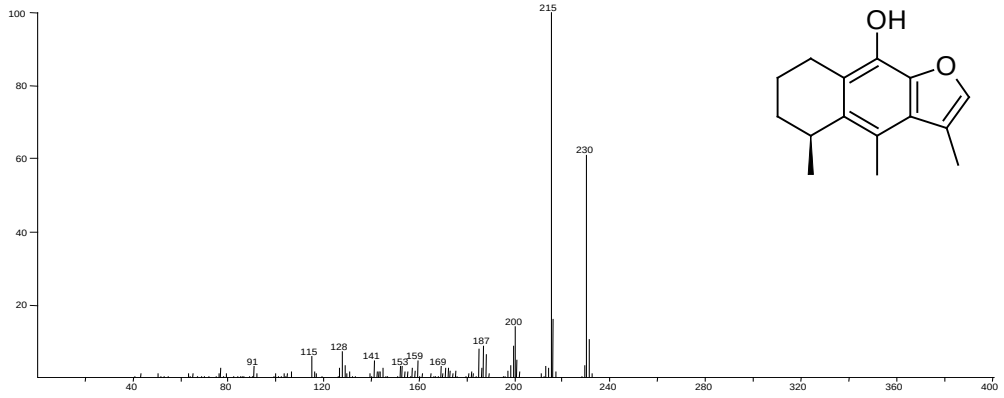

Figure 147. EI mass spectrum of cacalol (**15**) at RT 11.31 min.

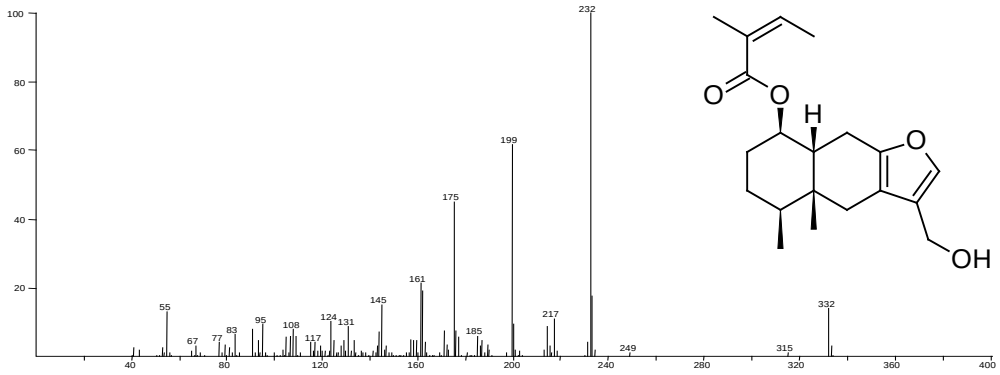

Figure 148. EI mass spectrum of subspicatin A (**27**) at RT 13.98 min.

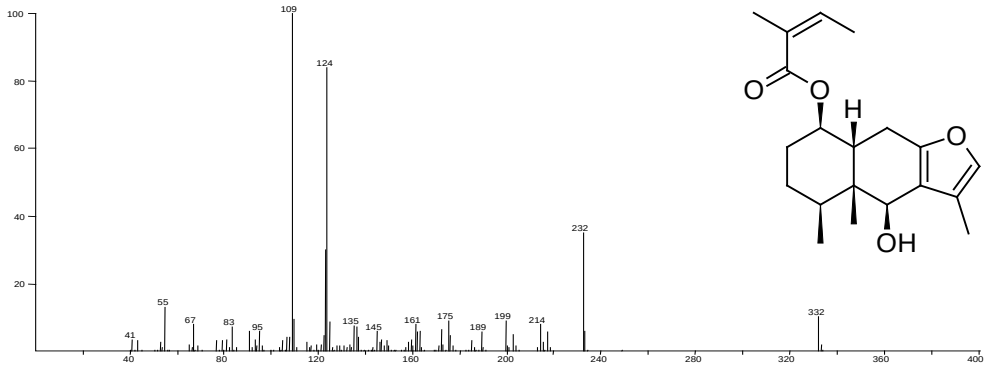

Figure 149. EI mass spectrum of subspicatin B (**28**) at RT 13.21 min.

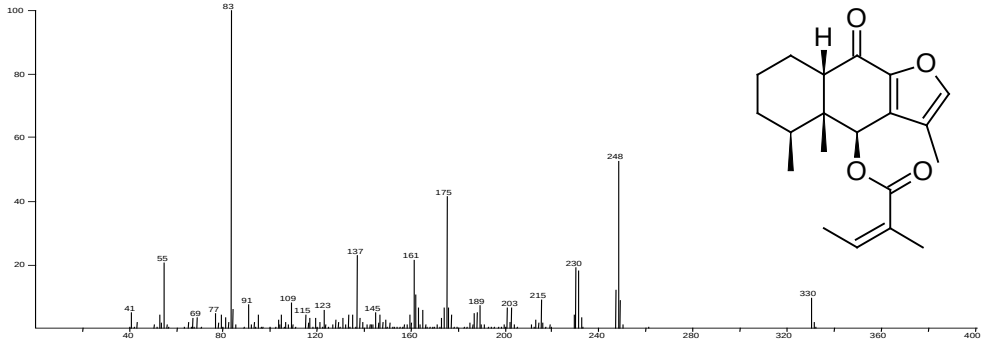

Figure 150. EI mass spectrum of compound **30** at RT 13.17 min.

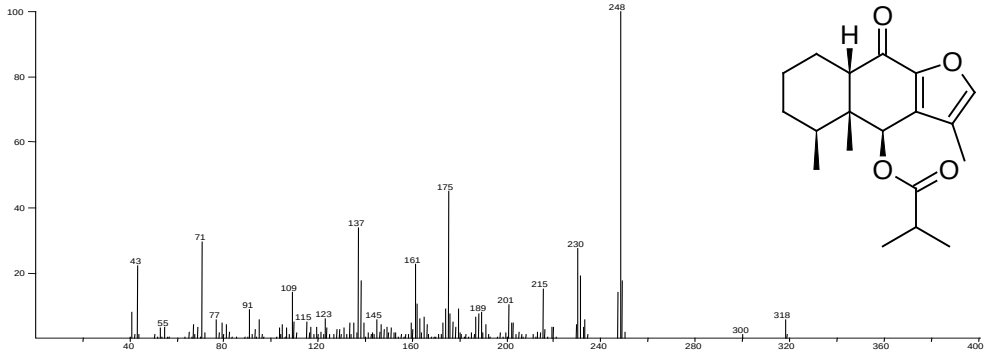

Figure 151. EI mass spectrum of compound **31** at RT 12.20 min.

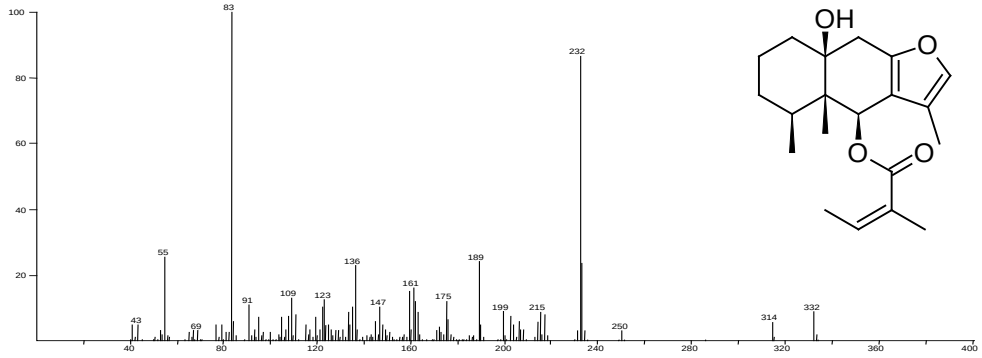

Figure 152. EI mass spectrum of compound **24** at RT 12.16 min.

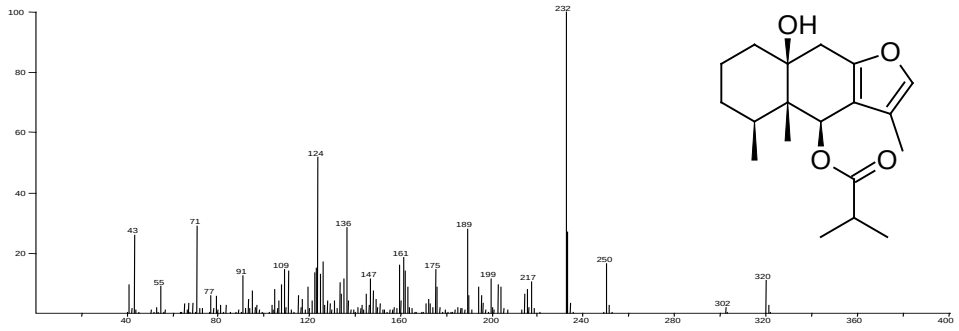

Figure 153. EI mass spectrum of compound **26** at RT 11.41 min.

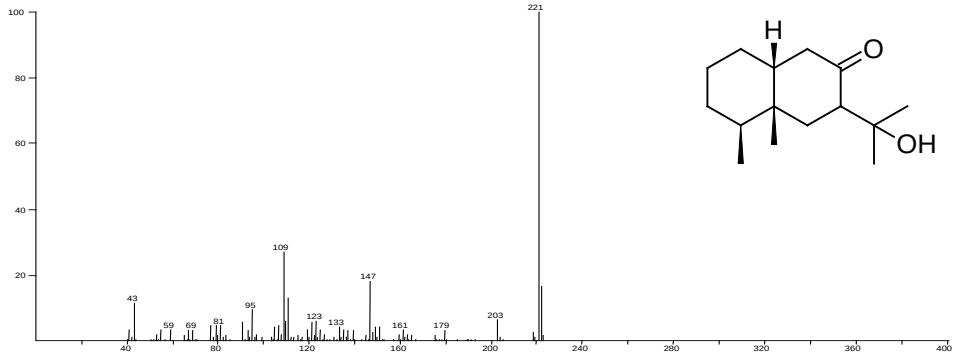

Figure 154. EI mass spectrum of compound **68** (MW = 238, m/z = 221 $[M\text{-}H_2O]^+$) at RT 9.57 min.

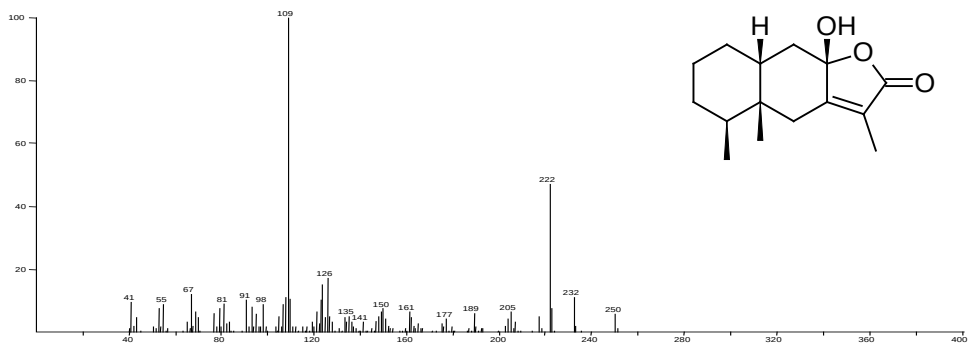

Figure 155. EI mass spectrum of compound **60** at RT 11.46 min.

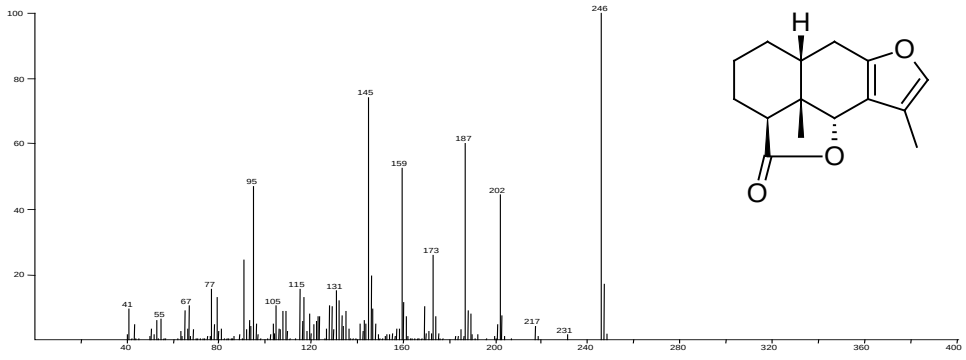

Figure 156. EI mass spectrum of compound **43** at RT 11.42 min.

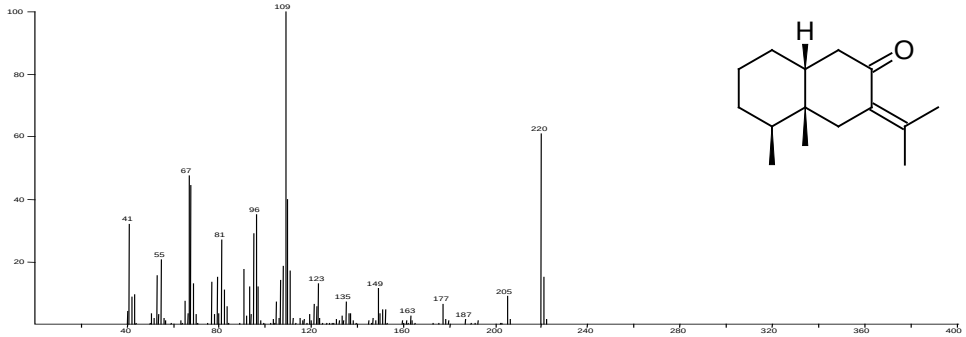

Figure 157. EI mass spectrum of fukinone (**69**) at RT 11.42 min.

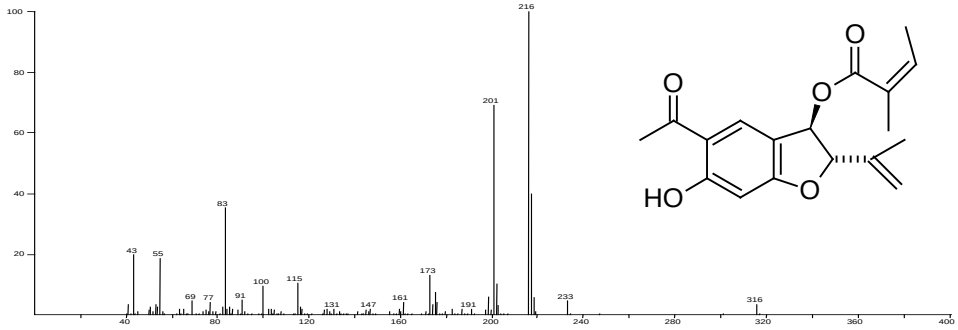

Figure 158. EI mass spectrum of compound **91** at RT 11.92 min.

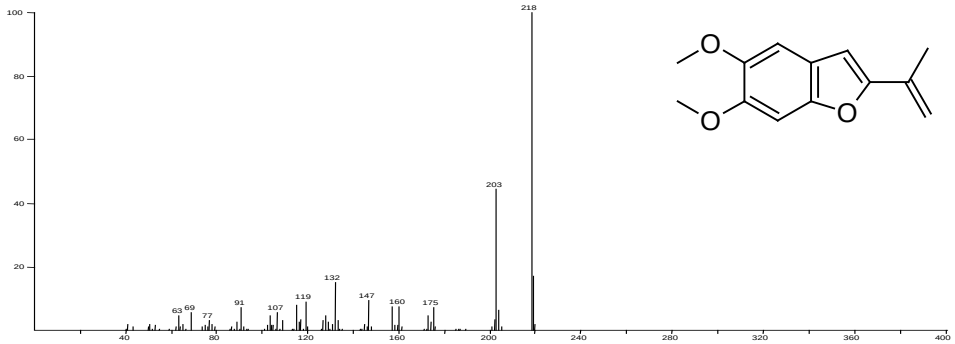

Figure 159. EI mass spectrum of compound **92** at RT 9.93 min.

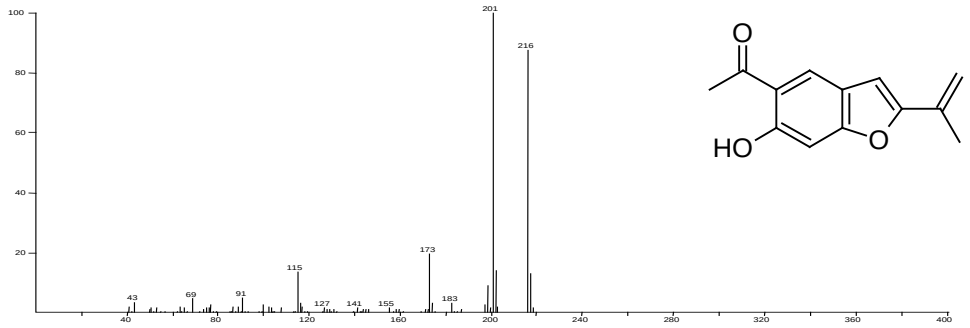

Figure 160. EI mass spectrum of euparin (**93**) at RT 10.30 min.

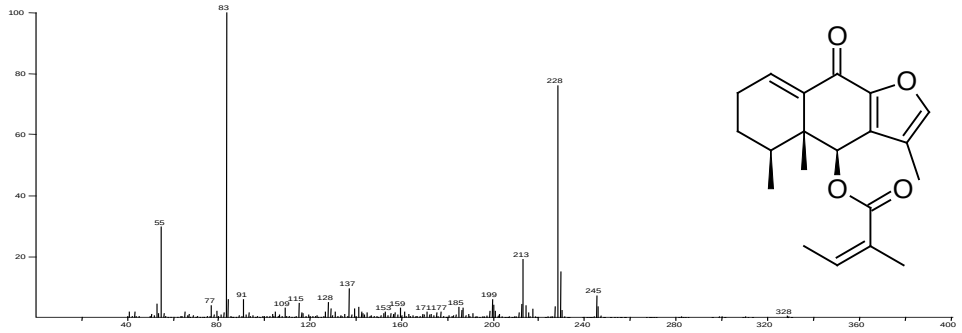

Figure 161. EI mass spectrum of compound **32** at RT 15.59 min.

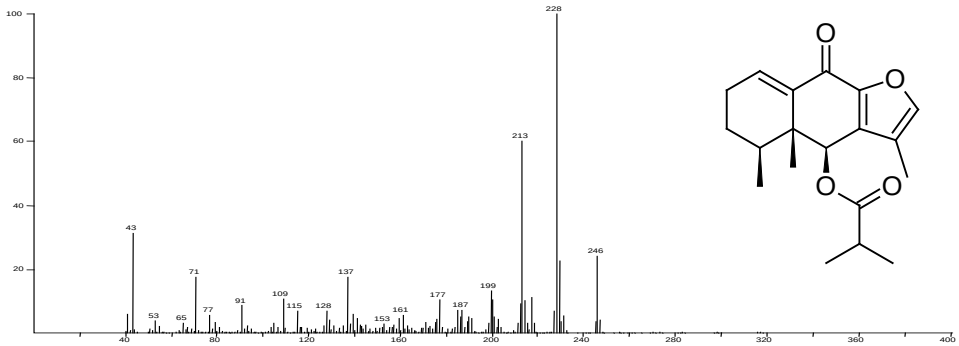

Figure 162. EI mass spectrum of compound **33** at RT 14.23 min.

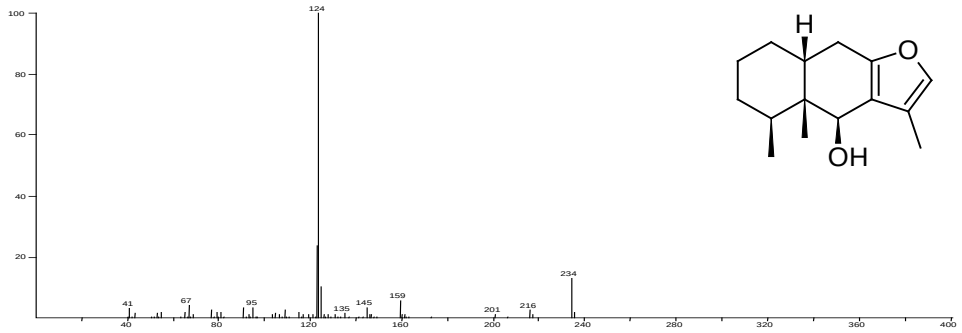

Figure 163. EI mass spectrum of ligularol (**16**) at RT 10.02 min.

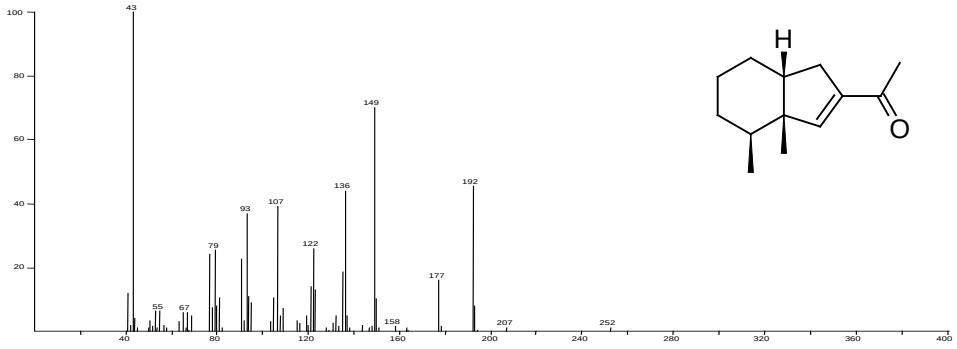

Figure 164. EI mass spectrum of compound **89** at RT 8.09 min.

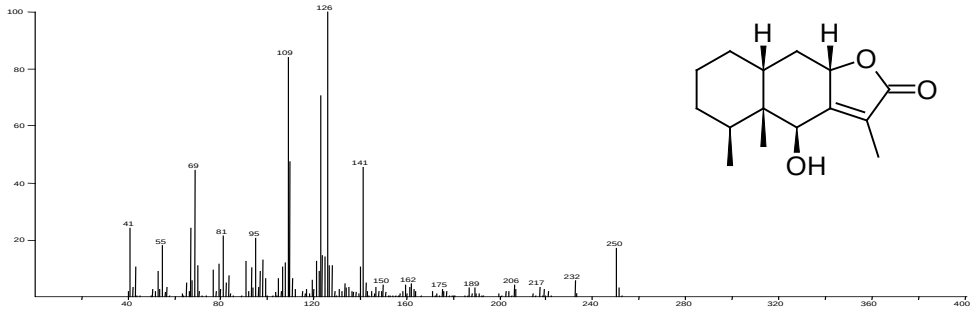

Figure 165. EI mass spectrum of compound **61** at RT 12.35 min.

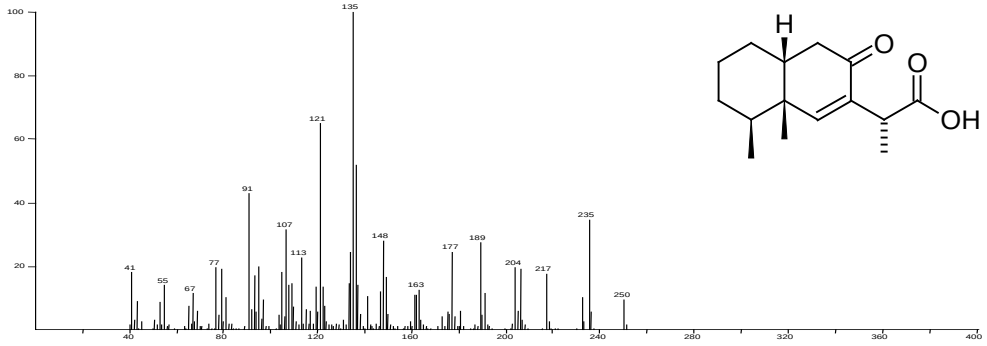

Figure 166. EI mass spectrum of compound **79** at RT 10.88 min.

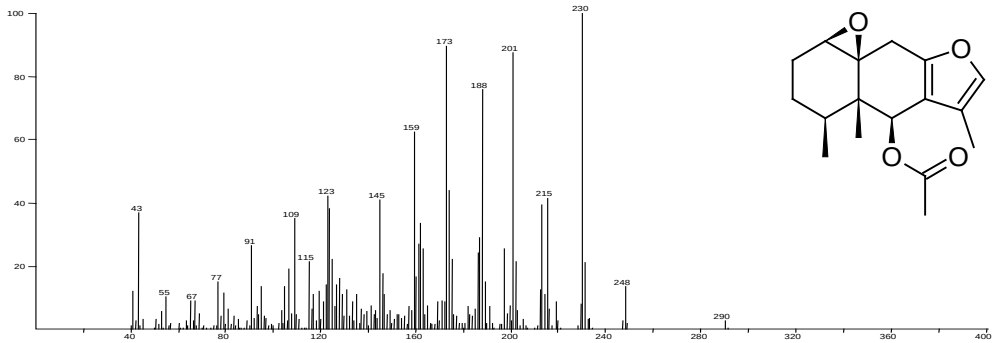

Figure 167. EI mass spectrum of compound **37** at RT 10.90 min.

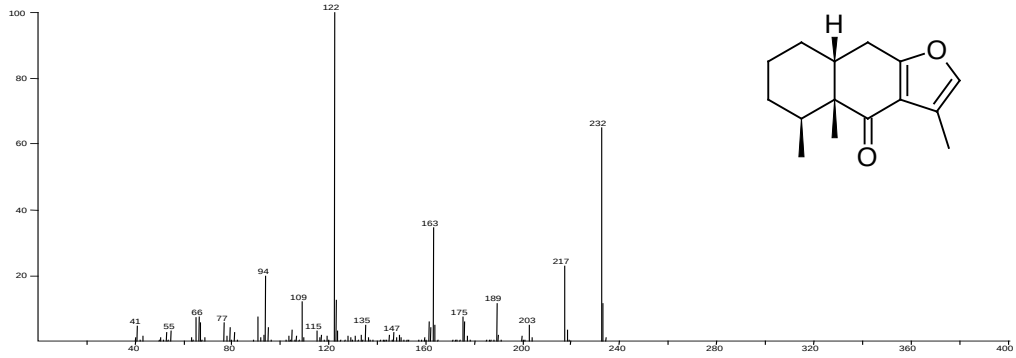

Figure 168. EI mass spectrum of ligularone (**39**) at RT 9.75 min.

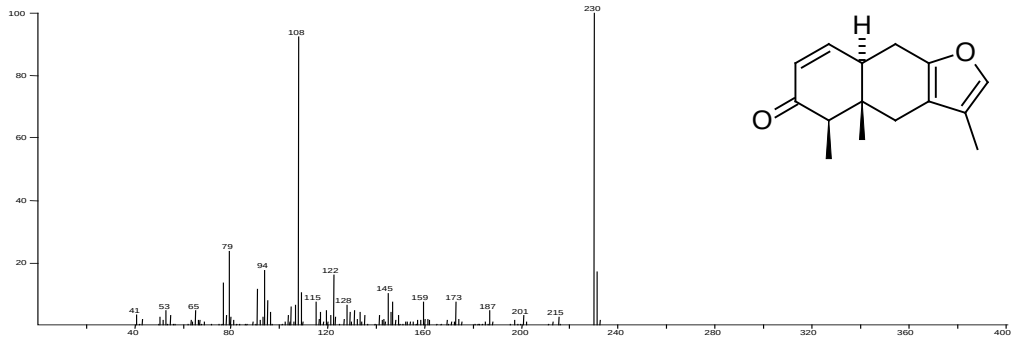

Figure 169. EI mass spectrum of furanoligularenone (**40**) at RT 10.24 min.

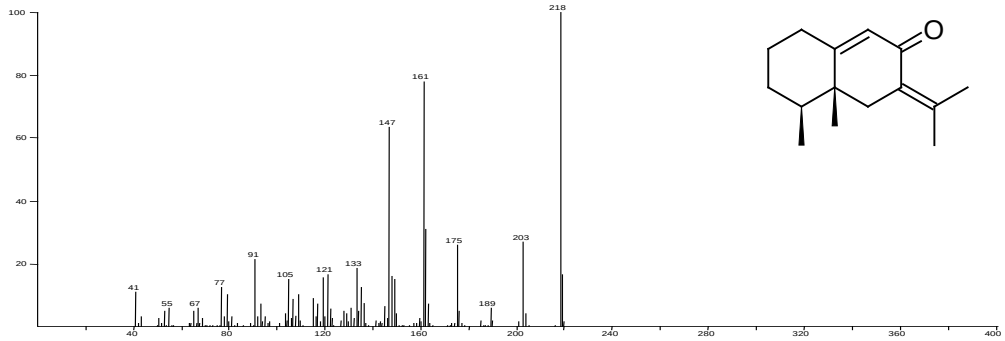

Figure 170. EI mass spectrum of dehydrofukinone (**70**) at RT 9.90 min.

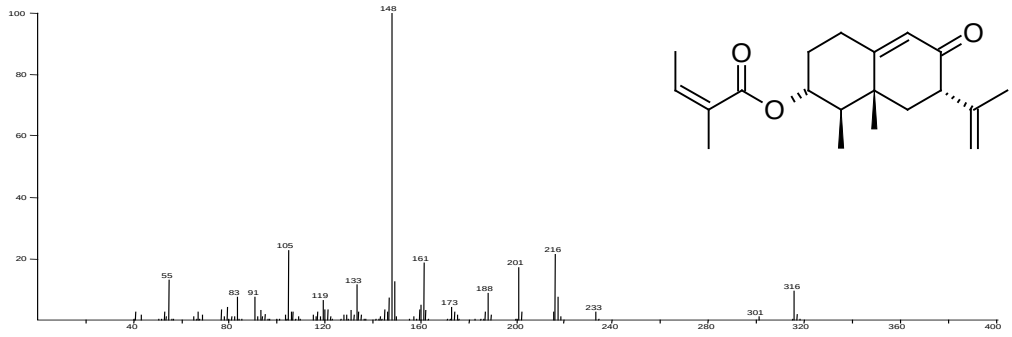

Figure 171. EI mass spectrum of petasin (**74**) at RT 13.02 min.

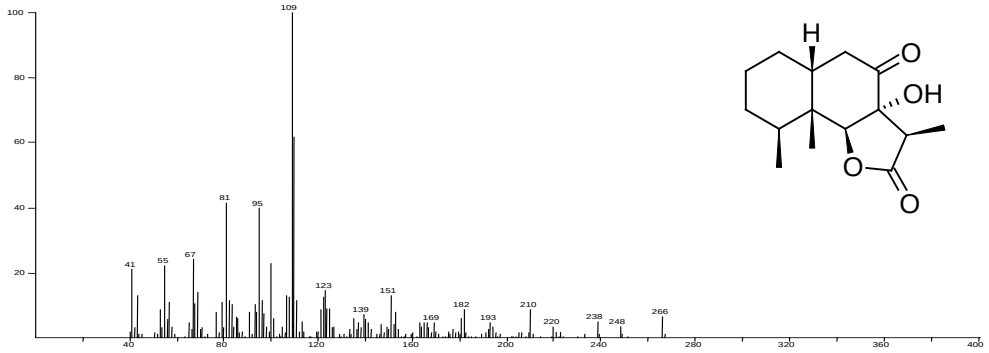

Figure 172. EI mass spectrum of subspicatolide (**5**) at RT 10.74 min.

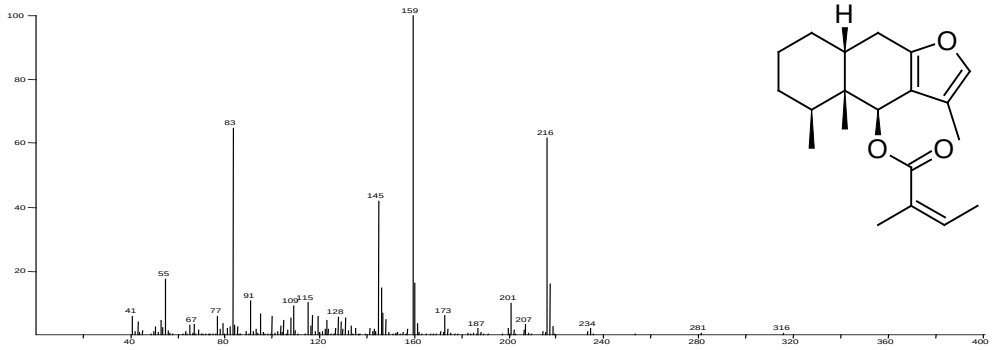

Figure 173. EI mass spectrum of compound **19** at RT 11.54 min.

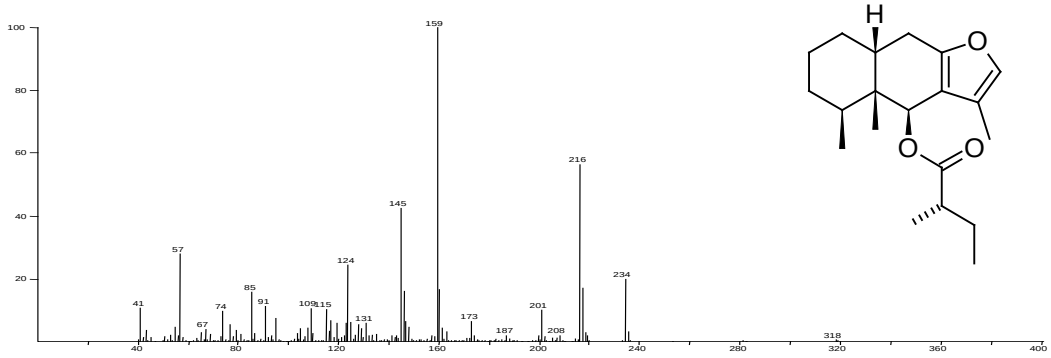

Figure 174. EI mass spectrum of compound **20** at RT 11.36 min.

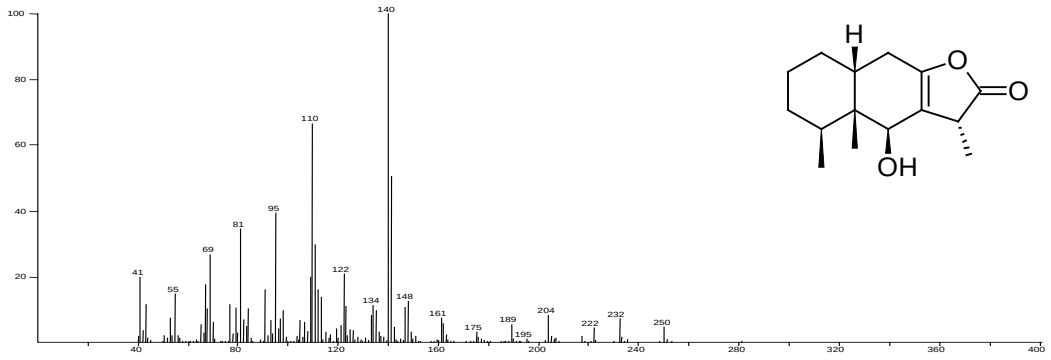

Figure 175. EI mass spectrum of eremofarfugin C (**58**) at RT 11.12 min.

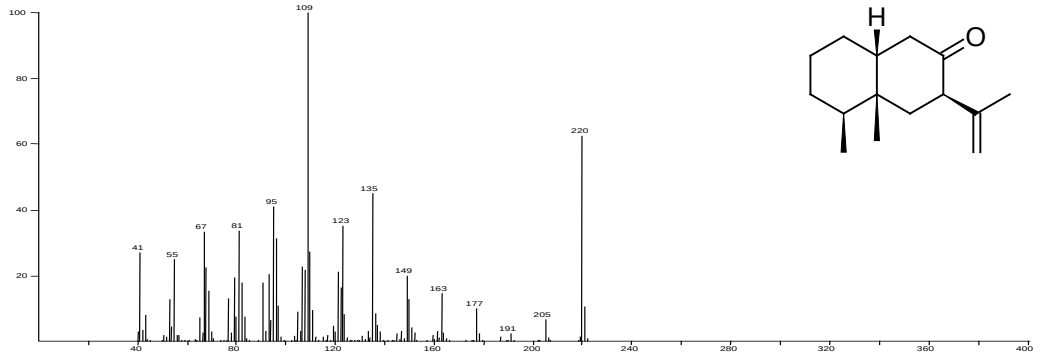

Figure 176. EI mass spectrum of compound **73** at RT 9.25 min.

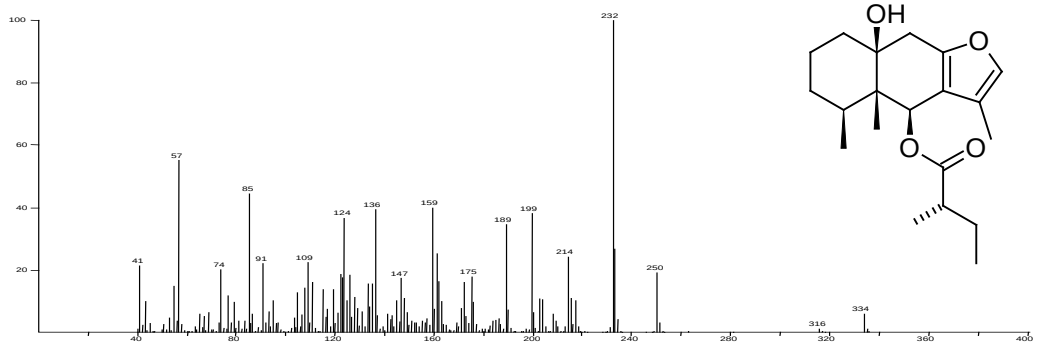

Figure 177. EI mass spectrum of compound **25** at RT 11.90 min.

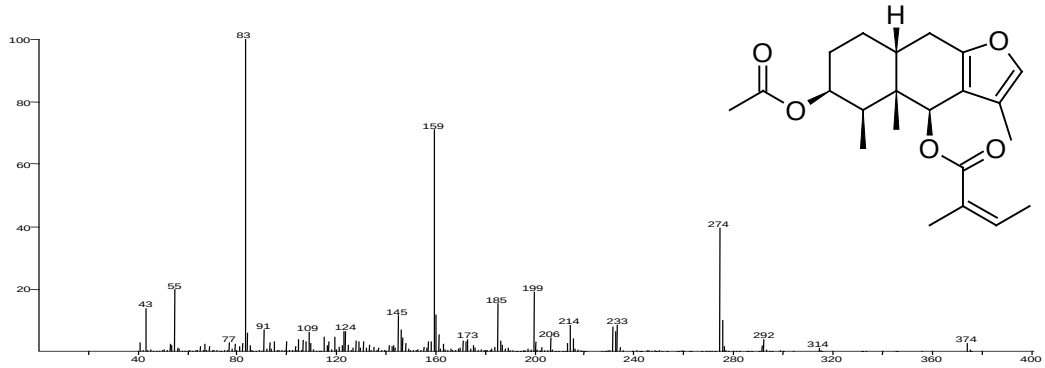

Figure 178. EI mass spectrum of compound **47** at RT 13.77 min.

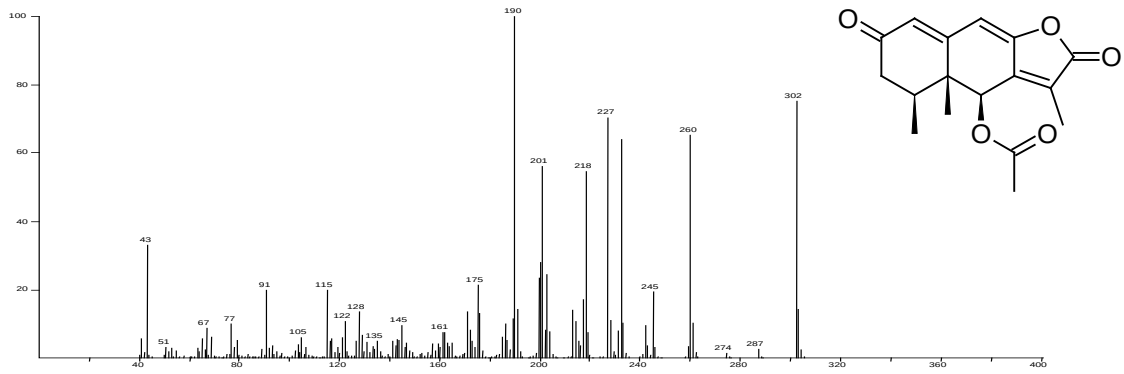

Figure 179. EI mass spectrum of virgaurenolide B (**14**) at RT 14.76 min.

6.4. Mass spectral data (APCI)

6.4.1. L. virgaurea

6.4.1.1. MS direct measurement

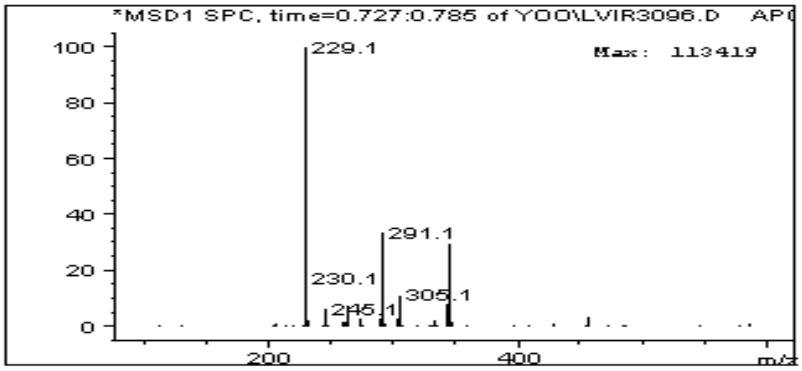

Figure 180. APCI mass spectrum of *L. virgaurea* type 1 (Sample 13)

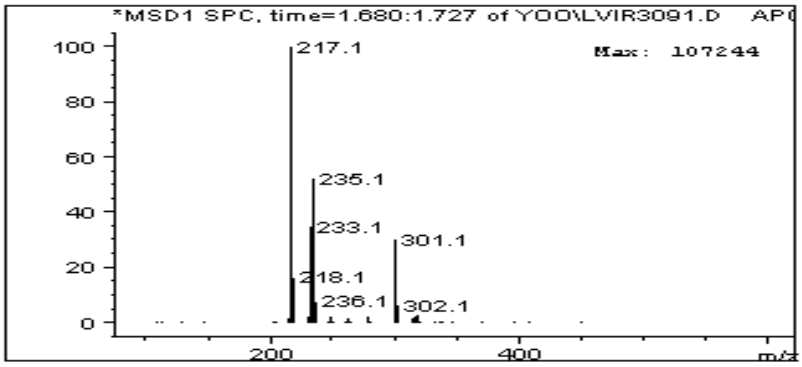

Figure 181. APCI mass spectrum of *L. virgaurea* type 2 (Sample 8)

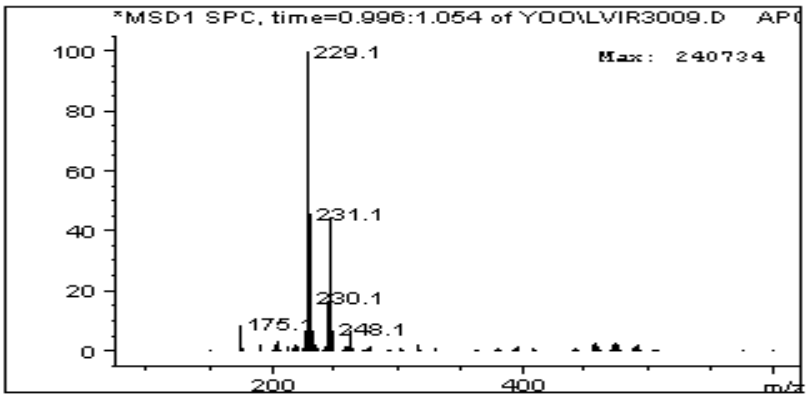

Figure 182. APCI mass spectrum of *L. virgaurea* type 3 (Sample 1)

6.4.1.2. LC-MS results

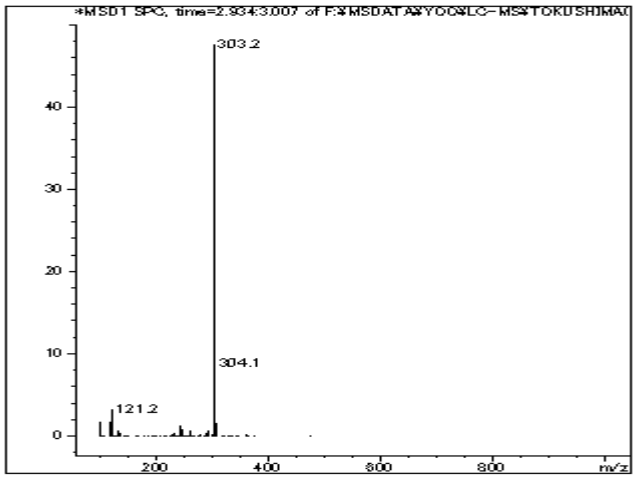

Figure 183. APCI mass spectrum of L. virgaurea type 1 at RT = 2.972 min. (Sample 13)

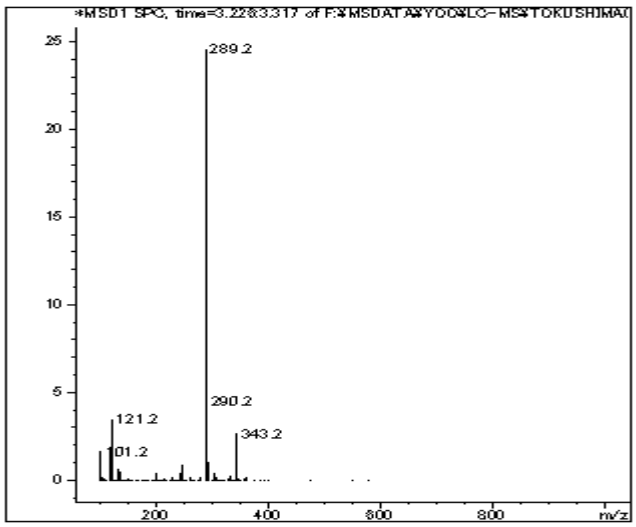

Figure 184. APCI mass spectrum of L. virgaurea type 1 at RT 3.272 min. (Sample 13)

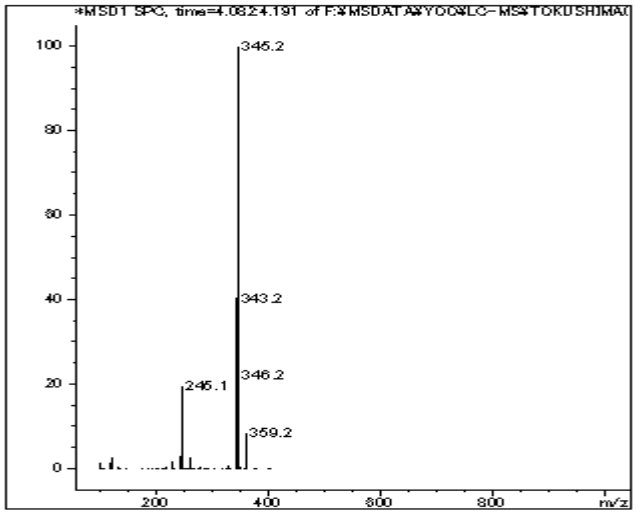

Figure 185. APCI mass spectrum of L. virgaurea type 1 at RT 4.137min. (Sample 13)

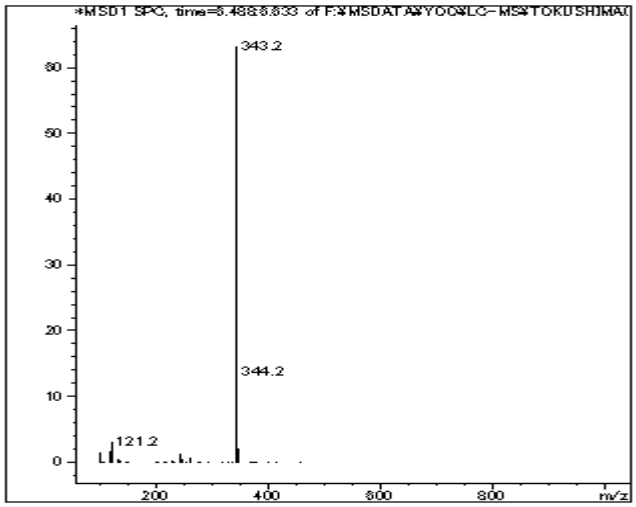

Figure 186. APCI mass spectrum of L. virgaurea type 1 at RT 6.564 min. (Sample 13)

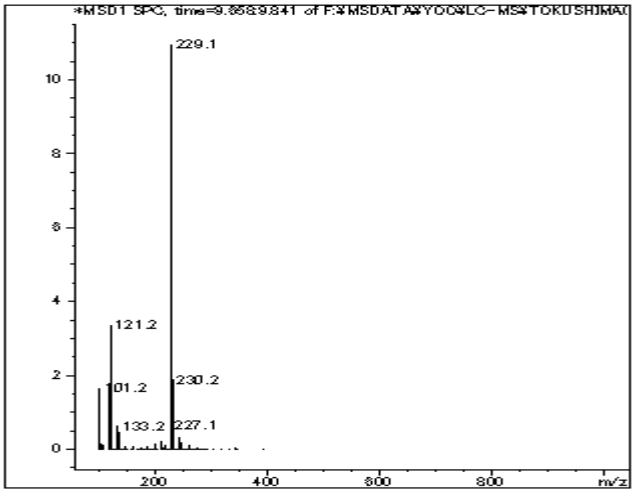

Figure 187. APCI mass spectrum of L. virgaurea type 1 at RT 9.750 min. (Sample 13)

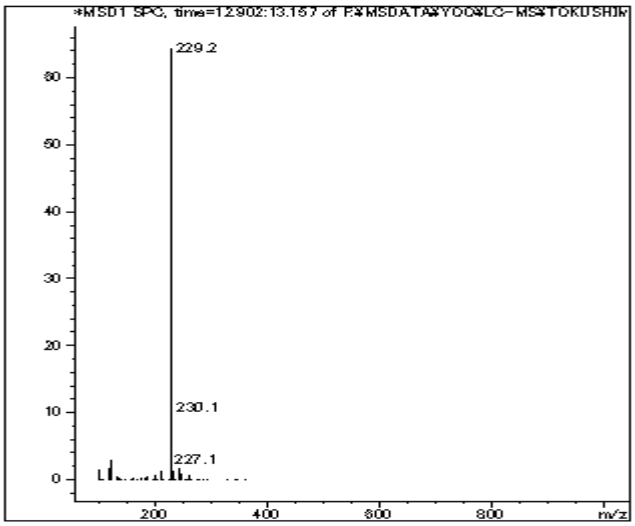

Figure 188. APCI mass spectrum of L. virgaurea type 1 at RT 13.032 min. (Sample 13)

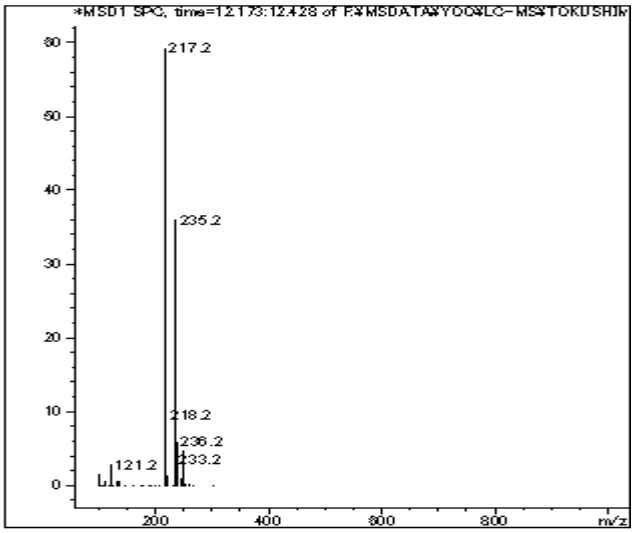

Figure 189. APCI mass spectrum of *L. virgaurea* type 2 at RT 12.293 min. (Sample 27)

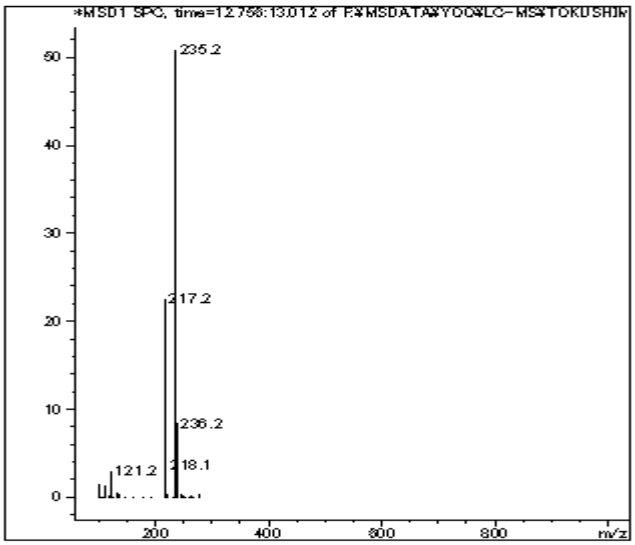

Figure 190. APCI mass spectrum of *L. virgaurea* type 2 at RT 12.880 min. (Sample 27)

Curriculum vitae

Personal information

Name:	Sin-Yeung, Yoo
Date of birth:	January 22nd 1982 in Seoul, South Korea
Nationality:	Austria
Marital status:	single
Sex:	female

Education

March 2010 – May 2010:	Work on master thesis, Bunri University, Tokushima, Japan
October 2003 - present:	Master of Pharmacy, University of Vienna, Austria
October 2000 - present:	Master of International Business Administration, University of Vienna, Austria
1992 - 2000:	Secondary school, Vienna, Austria
1987-1996:	Korean studies, Vienna, Austria *(Subjects: Korean language and culture)*

Work experience

May 2009 – present:	Allerheiligen Apotheke, 1200 Vienna, Austria *(Pharmaceutical assistant)*
Oct. 2008 – Feb. 2009:	Mohren Apotheke, 1010 Vienna, Austria *(Pharmaceutical assistant)*
Oct. 2005 - June 2008:	Faculty of Business and Economics, Chair of production and operations management, University of Vienna, Austria *(Research and teaching assistant)*
June 2005 – March 2006:	Sternwarte Apotheke, 1180 Vienna, Austria *(Pharmaceutical assistant)*
2001 – July 2003:	Merkur Handelswaren AG, 1130 Vienna, Austria (*Part time)*

Foreign languages

Korean *(mother tongue),* German *(fluently),* English *(fluently)*

Computer skills

Microsoft Office